Supporting Information

Exploiting Reduced-Symmetry Ligands with Pyridyl and Imidazole Donors to Construct a Second-Generation Stimuli-Responsive Heterobimetallic $[PdPtL_4]^{4+}$ Cage

Aston C. Pearcy,[a] Lynn S. Lisboa,[a] Dan Preston,[b] Nick B. Page,[a] Tristan Lawrence,[a] L. James Wright,[c] Christian G. Hartinger,[c] and James D. Crowley*[a]

[a] Department of Chemistry, University of Otago, PO Box 56, Dunedin 9054, New Zealand

[b] Research School of Chemistry, Australian National University, Canberra ACT 0200, Australia

[c] School of Chemistry, University of Auckland, Private Bag 92019, Auckland 1142, New Zealand

***jcrowley@chemistry.otago.ac.nz**

Contents

1 Experimental Procedures

1.1 General

Unless otherwise stated, all reagents were purchased from commercial sources and used without further purification. $[Pd(DMAP)_4](BF_4)_2$ was synthesised using methods described by Crowley et al.[1] 3-[1-(phenylmethyl)-1*H*-1,2,3-triazol-4-yl]pyridine (**pytri**) was synthesised using methods described by Fokin et al.[2] TLC plates (200 μm thickness) and silica gel (40 – 63 μm) were purchased from Silicycle. The solvents used were laboratory reagent grade unless specified otherwise. Petroleum ether refers to the fraction of petrol boiling in the range of 40-60 °C. Abbreviated solvents and reagents include acetonitrile (CH_3CN), dichloromethane (DCM), dimethylformamide (DMF), dimethylsulfoxide (DMSO), and ethylenediaminetetraacetate (EDTA). 0.1 M Ammonium hydroxide/ethylenediaminetetraacetic acid (NH_4OH/EDTA) solution was made up by mixing 30 g EDTA with 900 mL water and 100 mL NH_4OH. ^1H and $^{13}C\{^1H\}$ NMR spectra were recorded on either a 400 MHz Varian/Agilent 400-MR or Varian 500 MHz AR spectrometer. ^1H DOSY NMR spectra were obtained on a Bruker Avance 400 MHz NMR spectrometer and processed on MestReNova 14.2.2 using the peak fit method. Chemical shifts are reported in parts per million and referenced to residual solvent peaks ([D_6]DMSO: ^1H δ 2.50 ppm; ^{13}C δ 39.52 ppm, [D_3]acetonitrile: ^1H δ 1.94 ppm; ^{13}C δ 1.32 ppm, [D]chloroform: : ^1H δ 7.26 ppm ^{13}C δ 77.16 ppm). Coupling constants (J) are reported in Hertz (Hz). Standard abbreviations indicating multiplicity were used as follows: m = multiplet, sex = sextet, quin = quintet, q = quartet, t = triplet, dt = doublet of triplets, d = doublet, dd = doublet of doublets, dq = doublet of quartets. Signals in ^1H NMR spectra of compounds were assigned using a combination of 2D NMR techniques. Deuterated solvents labelled in NMR spectra refer to the residual protio solvent in the deuterated solvent specified. IR spectra were recorded on a Bruker ALPHA FT-IR spectrometer with an attached ALPHA-P measurement module. Microanalyses were performed at the Campbell Microanalytical Laboratory at the University of Otago. Electrospray ionisation mass spectra (ESIMS) were collected on a Shimadzu LCMS-9030 spectrometer and Bruker micro-TOF-Q spectrometer; spectra for the cage **C**, and $[Pt(\mathbf{L})_4](BF_4)_2$ were obtained using pseudo-coldspray conditions (nebuliser (3.0 L/min) and heating gases (10.0 L/min) at room temperature, interface voltage = 3.50 kV, interface temperature = 373 K); spectra for the G⊂C host-guest adducts were obtained using coldspray conditions (nebuliser (1.0 L/min) cooled to 223 K and heating gases off, interface voltage = 3.50 kV). UV-visible absorption spectra were acquired with a Shimadzu UV-2600 spectrophotometer.

Synthetic scheme showing the synthesis of **2**, **3**, **L**, $[Pt(\mathbf{L})_4](BF_4)_2$, and **C**.

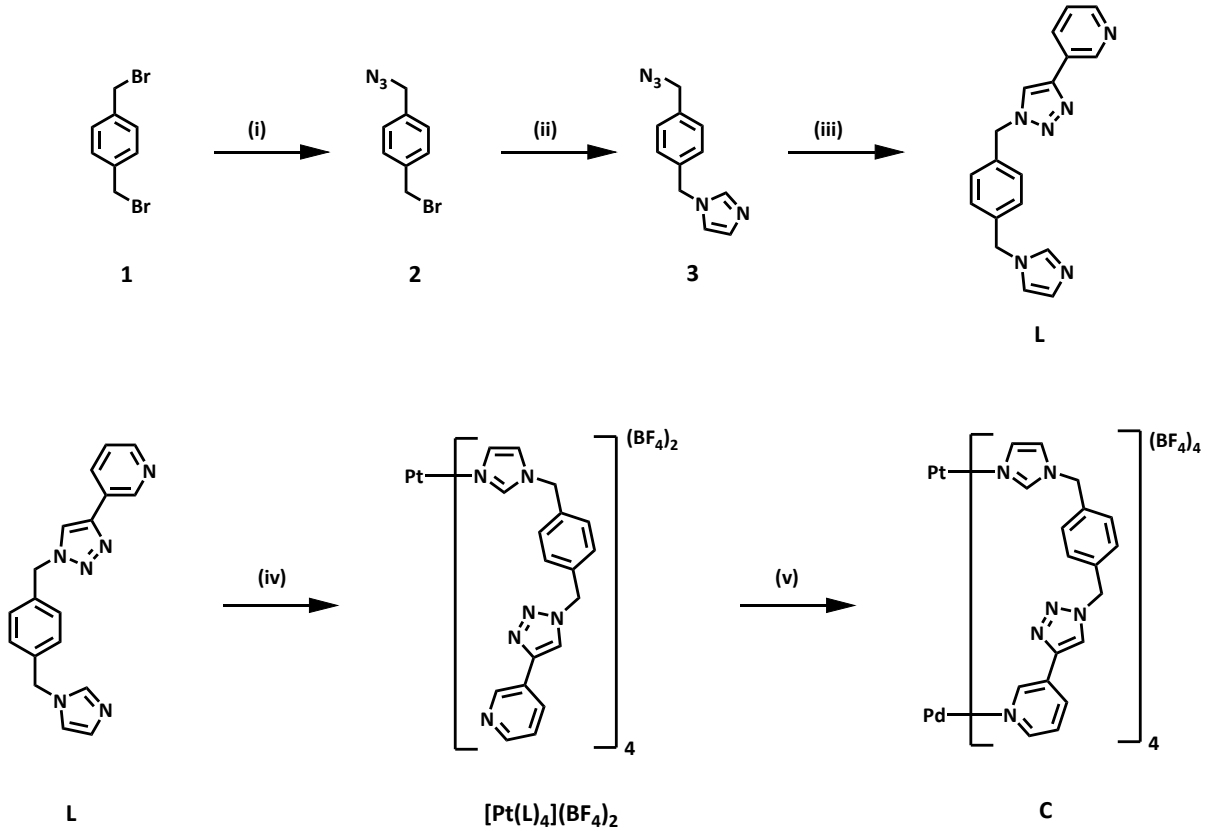

Scheme S1 Synthesis of $[PdPt(\mathbf{L})_4](BF_4)_4$ (**C**): (i) NaN_3, CH_3CN, 60 °C, 24 h (27%), (ii) imidazole, KOH, CH_3CN, RT, 6 h (77%), (iii) $CuSO_4{\cdot}5H_2O$, sodium ascorbate, 3-ethynylpyridine, DMF/H_2O (4:1), RT, 24 h (91%), (iv) $[Pt(DMSO)_2Cl_2]$, $AgBF_4$, DMSO, 60 °C, 7 days in the absence of light (68%), (v) $[Pd(CH_3CN)_4](BF_4)_2$, CH_3CN, RT, 24 h (87%).

1.2 Synthesis of 2

1-(Azidomethyl)-4-(bromomethyl)benzene **2** was synthesised following a modified literature procedure.[3]

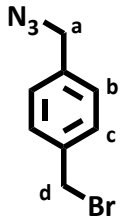

2

Sodium azide (1.478 g, 22.73 mM, 1 eq.) was added to a solution of 1,4-bis(bromomethyl)benzene (6.000 g, 22.73 mM, 1 eq.) in CH_3CN (120 mL) and heated under reflux for 24 h. The reaction was monitored via TLC, and when complete (ca. 24 h) water (300 mL) was added to quench the reaction. The reaction mixture was then extracted with chloroform (200 mL), the organic extracts washed with water (4 x 50 mL) and brine (2 x 50 mL). The organic layer was dried over anhydrous sodium sulfate and after removal of the drying agent by filtration, the solvent was removed from the filtrate under reduced pressure.

The crude product was purified via column chromatography using silica gel as the solid support and 0-2% dichloromethane in petroleum ether as eluent to give a yellow/brown oil. (Yield: 1.379 g, 6.099 mM, 27%). ^{1}H NMR (400 MHz, [D_3]acetonitrile) δ: 7.46 (d, *J* = 2.0 Hz, 2H, H_b), 7.35 (d, *J* = 2.0 Hz, 2H, H_c), 4.61 (s, 2H, H_d), 4.39 (s, 2H, H_a). ^{13}C{^{1}H} NMR (125 MHz, [D]chloroform) δ: 137.9, 135.7, 129.6, 128.6, 54.4, 33.0. I.R. (cm^{-1}) 2090 (azide stretch), 605 (C-Br stretch). N.B. The yield of this reaction proved variable with a range (27-45%) of isolated yields obtained.

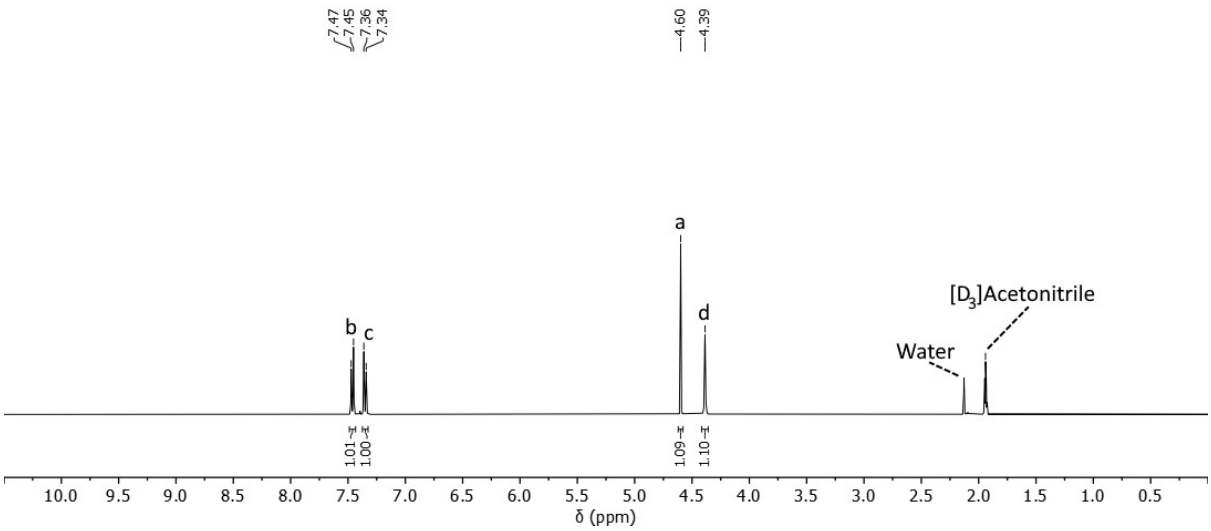

Figure S1 ^{1}H NMR spectrum (400 MHz, [D_3]acetonitrile, 298 K) of **2**.

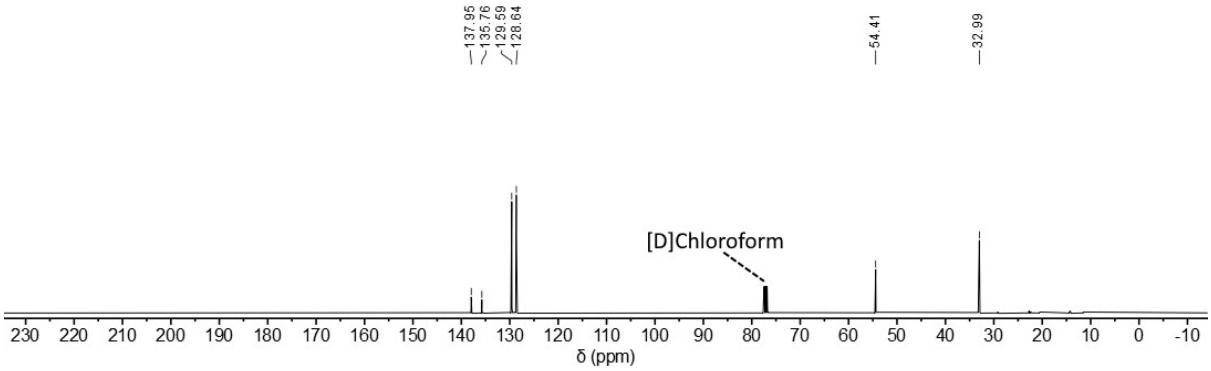

Figure S2 ^{13}C{^{1}H} NMR spectrum (125 MHz, [D]chloroform, 298 K) of **2**.

1.3 Synthesis of 3

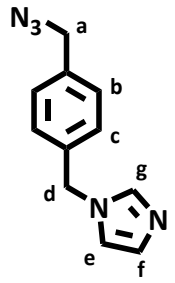

3

Imidazole (0.4570 g, 6.709 mM, 1.1 eq.) and potassium hydroxide (0.6840 g, 12.20 mM, 2 eq.) were stirred in CH_3CN (250 mL) for 2 h at RT. 1-(Azidomethyl)-4-(bromomethyl)benzene (1.379 g, 6.099 mM, 1 eq.) was added to the solution and the reaction mixture was stirred for a further 4 h at RT. The solution was filtered through Celite and then the solvent was removed under reduced pressure. The crude product was dissolved in chloroform (100 mL) and then washed with water (3 x 50 mL), the organic layer dried over sodium sulfate, then the solvent was removed under reduced pressure. The residue was purified via silica gel chromatography (100% acetone), to afford a yellow oil. (Yield: 1.001 g, 4.696 mM, 77%). ^{1}H NMR (400 MHz, [D_3]acetonitrile) δ: 7.57 (s, 1H, H_g), 7.35 (d, J = 2.0 Hz, 2H, H_b), 7.25 (d, J = 2.0 Hz, 2H, H_c), 7.02 (s, 1H, H_e), 6.94 (s, 1H, H_f), 5.16 (s, 2H, H_d), 4.37 (s, 2H, H_a). ^{13}C{^{1}H} NMR (125 MHz, [D_3]acetonitrile) δ: 138.7, 138.4, 136.6, 130.1, 129.8, 128.8, 120.3, 54.7, 50.6. I.R. ν (cm^{-1}) 2094 (Azide stretch). Anal. calc. for $C_{18}H_{16}N_6$•(CH_3CN)•0.5(H_2O): C, 59.30%; H, 5.74%; N, 31.92%. Found: C, 59.09%; H, 5.39%; N, 32.13%. HRESI-MS: ($CH_3CN/CHCl_3$) *m/z* = 214.1075 (calc. for [**3** + H]$^+$ = 214.1087).

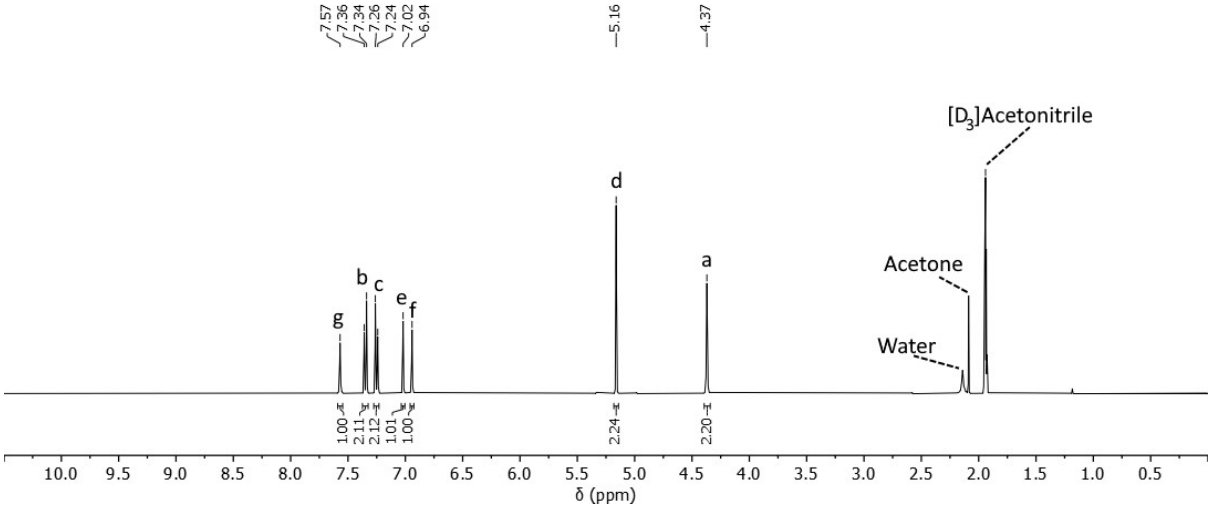

Figure S3 ^{1}H NMR spectrum (400 MHz, [D_3]acetonitrile, 298 K) of **3**.

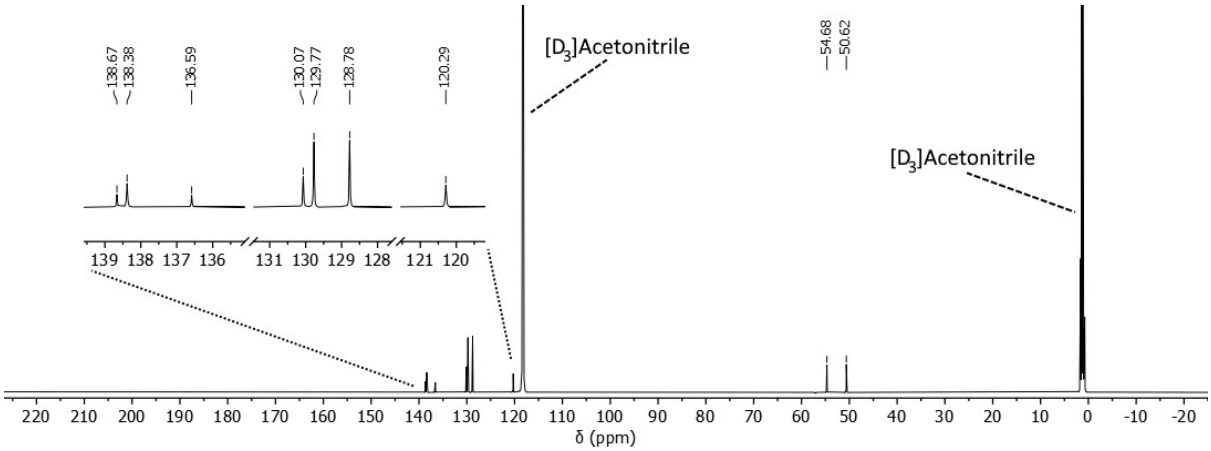

Figure S4 ^{13}C{^{1}H} NMR spectrum (125 MHz, [D_3]acetonitrile, 298 K) of **3**.

1.4 Synthesis of L

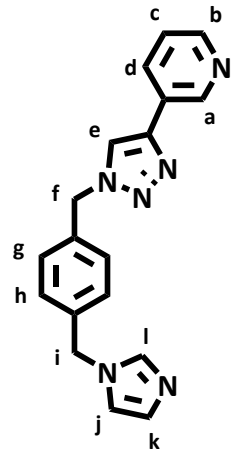

L

Copper(II) sulfate pentahydrate (0.6830 g, 2.735 mM, 0.68 eq.), sodium ascorbate (0.7170 g, 3.620 mM, 0.9 eq.) and 3-ethynylpyridine (0.6760 g, 6.556 mM, 1.63 eq.) were added to a solution of 1-(4-(azidomethyl)benzyl)-1H-imidazole in 4:1 DMF:water (15 mL) and the mixture was stirred for 24 h at RT in a sealed vessel. NH_4OH/EDTA (50 mL) and DCM (50 mL) were added and the solution was stirred vigorously for another 3 hours at RT. The mixture was extracted with DCM (2 x 50 mL), and the combined organic layers washed with water (4 x 50 mL), brine (2 x 50 mL), dried over sodium sulfate and then the solvent removed under reduced pressure to afford a pale-yellow powder. Slow evaporation of a concentrated diethyl ether solution of **L** gave colourless needle-like crystals suitable for single crystal X-ray diffraction. (Yield: 1.194 g, 3.774 mM, 91%). ^{1}H NMR (400 MHz, [D_3]acetonitrile) δ: 9.00 (s, 1H, H_a), 8.52 (dd, *J* = 4.7, 1.5 Hz, 1H, H_b), 8.19 (s, 1H, H_e), 8.15 (dt, *J* = 7.9, 2.0 Hz, 1H, H_d), 7.55 (s, 1H, H_l), 7.39 (dd, *J* = 7.6, 5.3 Hz, 1H, H_c), 7.35 (d, *J* = 8.1 Hz, 2H, H_g), 7.24 (d, *J* = 8.0 Hz, 2H, H_h), 7.00 (s, 1H, H_j), 6.93 (s, 1H, H_k), 5.59 (s, 2H, H_f), 5.15 (s, 2H, H_i). ^{13}C{^{1}H} NMR (125 MHz, [D_6]DMSO) δ: 148.9 (C_b), 146.4 (C_a), 143.9, 137.9, 137.4 (C_l), 135.3, 132.4 (C_d), 128.7 (C_j), 128.3 (C_g), 127.9 (C_h), 126.6, 124.0 (C_c), 122.2 (C_e), 119.5 (C_k), 52.8 (C_f), 49.0 (C_i). Anal. calc. for $C_{18}H_{16}N_6$•0.5(H_2O): C, 66.45%; H, 5.27%; N, 25.83%. Found: C, 66.22%; H, 5.03%; N, 25.59%. HRESI-MS: (CH_3CN) *m/z* = 317.1521 (calc. for [**L** + H]$^+$ = 317.1509).

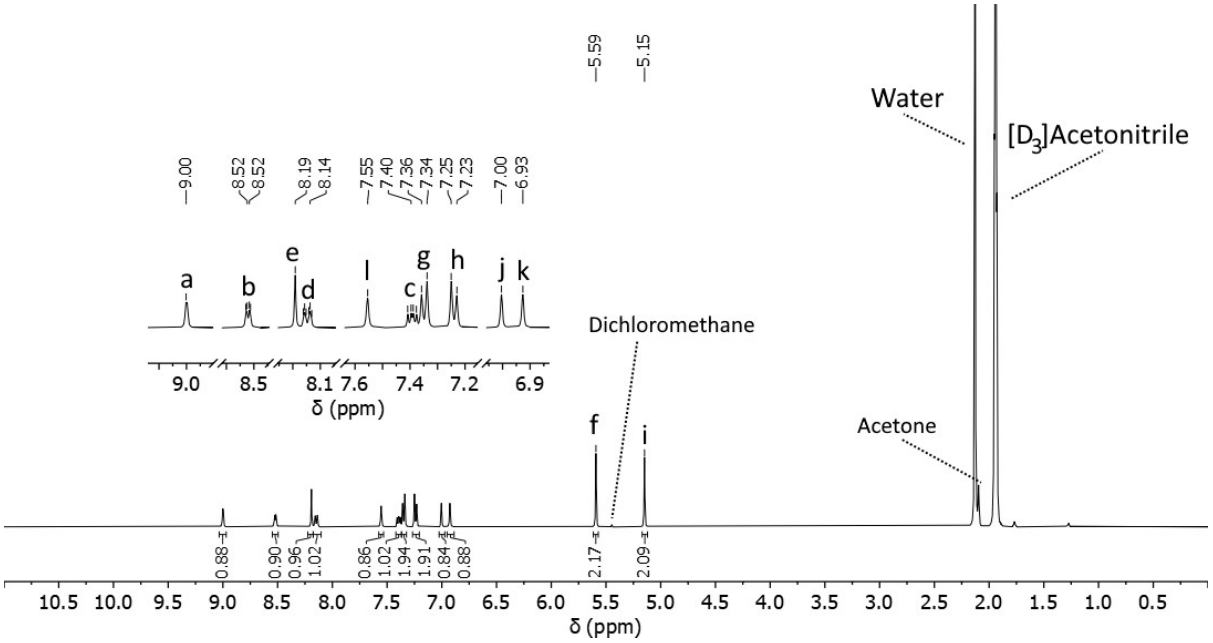

Figure S5 ^{1}H NMR spectrum (400 MHz, [D_3]acetonitrile, 298 K) of **L**.

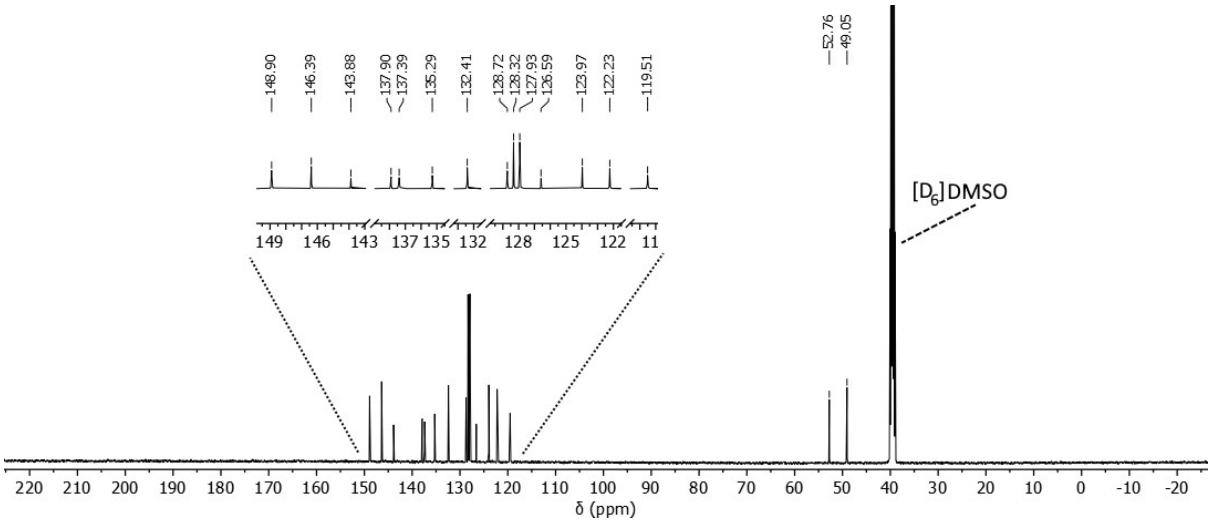

Figure S6 ^{13}C{^{1}H} NMR spectrum (125 MHz, [D_6]DMSO, 298 K) of **L**.

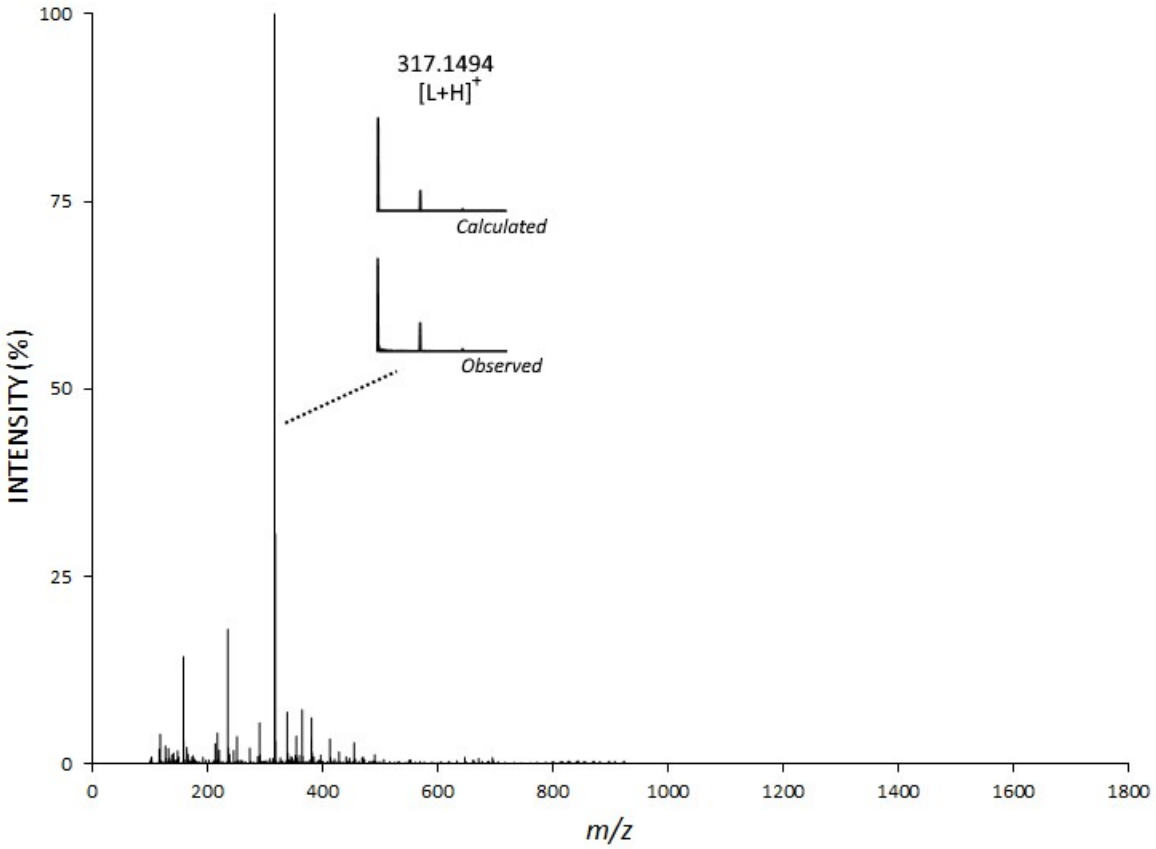

Figure S7 High resolution electrospray ionisation mass spectrum (CH_3CN) of **L**.

1.5 Synthesis of $[Pt(L)_4](BF_4)_2$

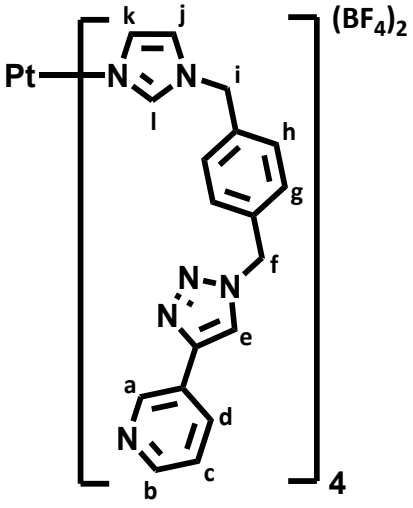

L (25.65 mg, 0.08110 mM, 4.1 eq.) and $[Pt(DMSO)_2Cl_2]$ (8.350 mg, 0.01980 mM, 1 eq.) were added to a foil-covered, sealed tube. DMSO (0.6 mL) was added, followed by the addition of $AgBF_4$ (8.469 mg, 0.04350 mM, 2.2 eq.). The solution was heated at 60 °C and stirred in the absence of light for 7 days. The colourless insoluble silver chloride precipitate was removed by centrifuging the mixture (6000 rpm, 5 min), and the supernatant decanted. Ice cold EtOAc was added to this, and the white precipitate that formed isolated by centrifuging the mixture

(6000 rpm, 5 min) and removing the supernatant by decantation. The precipitate was washed with EtOAc (1 x 10 mL), diethyl ether (1 x 10 mL), dichloromethane (2 x 5 mL). After each addition of solvent the mixture was sonicated for 1 min, centrifuged (6000 rpm, 5 min), and the supernatant decanted. The precipitate remaining in the centrifuge tubes was dried *in vacuo* to afford a colourless crystalline solid. (Yield: 0.02192 g, 0.01346 mM, 68%). ^{1}H NMR (400 MHz, [D_6]DMSO) δ 9.01 (s, 1H, H_a), 8.74 (s, 1H, H_e), 8.53 (dd, *J* = 4.8, 1.7 Hz, 1H, H_b), 8.29 (s, 1H, H_l), 8.16 (dt, *J* = 8.0, 3.8 Hz, 1H, H_d), 7.47-7.43 (m, 2H, H_c, H_j), 7.31 (d, *J* = 8.1 Hz, 2H, H_g), 7.17 (d, *J* = 8.1 Hz, 2H, H_h), 6.92 (s, 1H, H_k), 5.65 (s, 2H, H_f), 5.21 (s, 2H, H_i). ^{13}C{^{1}H} NMR (125 MHz, [D_6]DMSO) δ: 149.5, 146.9, 144.4, 140.0, 136.6, 136.4, 132.9, 129.1, 129.0, 128.5, 127.0, 124.6, 122.9, 122.3, 53.2, 51.0. Anal. calc. for $C_{72}H_{64}N_{24}PtB_2F_8$•1.7(DCM): C, 49.77%; H, 3.82%; N, 18.90%. Found: C, 49.45%; H, 3.96%; N, 19.20%. HRESI MS: (CH_3CN) *m/z* = 1546.5385 [**M** – BF_4]$^{+}$ (calc. for [$C_{72}H_{64}N_{24}PtBF_4$]$^{+}$, 1546.5431), 730.2721 [**M** – 2BF_4]$^{2+}$ (calc. for [$C_{72}H_{64}N_{24}Pt$]$^{2+}$, 730.2701), 317.1510 [**L** + H]$^{+}$ (calc. for [$C_{18}H_{16}N_6$]$^{+}$, 317.1509).

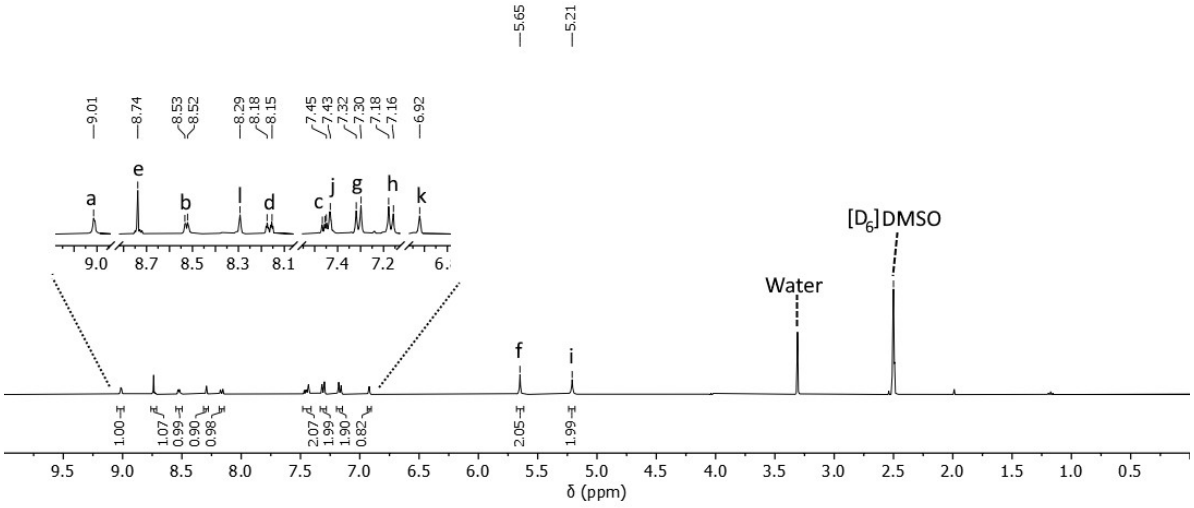

Figure S8 ^{1}H NMR spectrum (400 MHz, [D_6]DMSO, 298 K) of [Pt(**L**)$_4$](BF_4)$_2$.

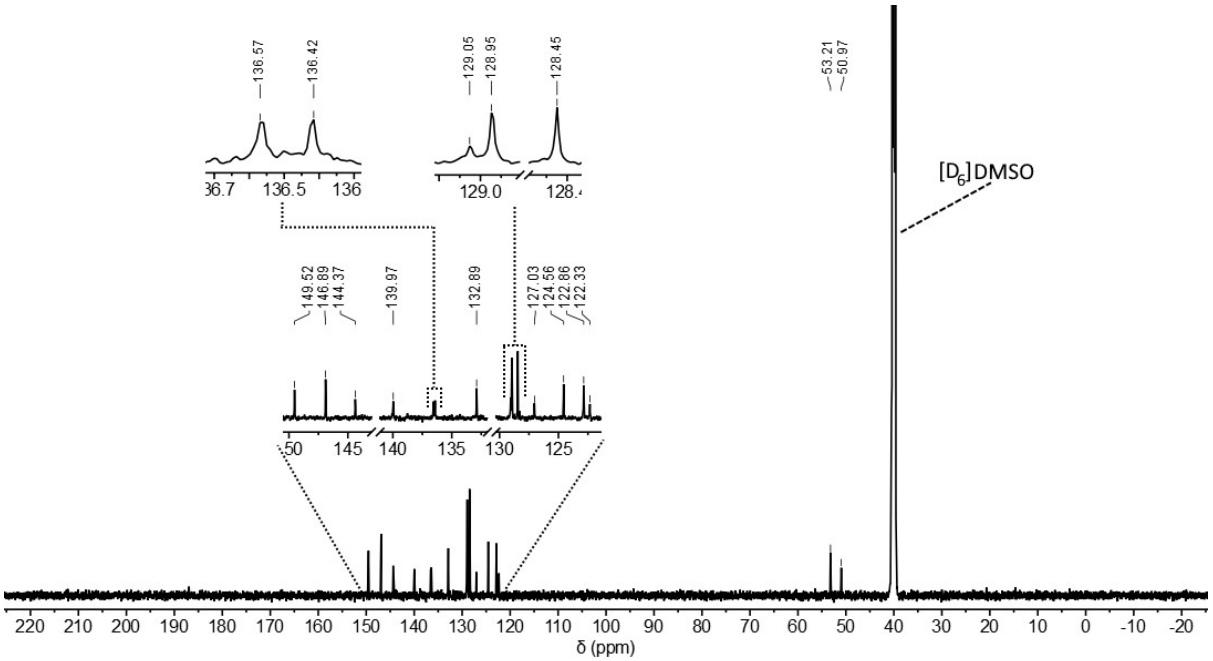

Figure S9 ^{13}C{^{1}H} NMR spectrum (125 MHz, [D_6]DMSO, 298 K) of [Pt(**L**)$_4$](BF_4)$_2$.

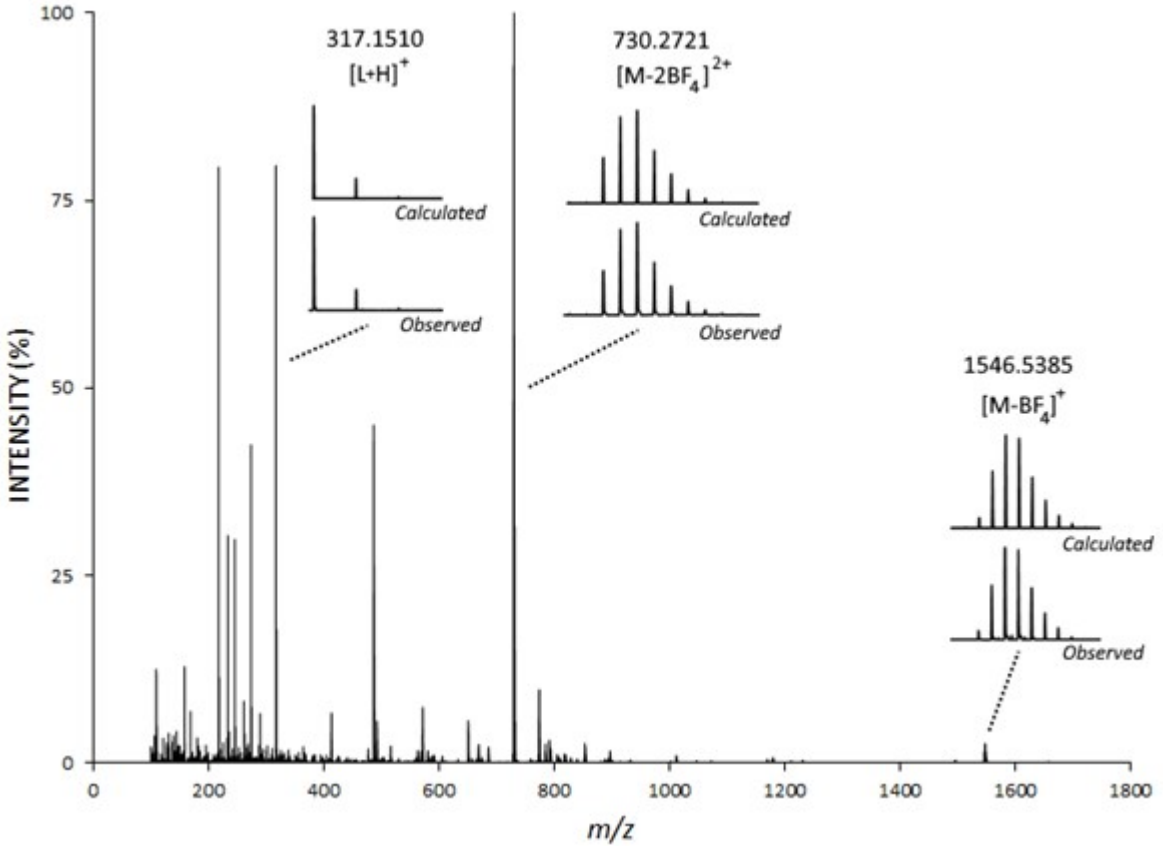

Figure S10 High resolution electrospray ionisation mass spectrum (CH_3CN) of $[Pt(\mathbf{L})_4](BF_4)_2$, performed under pseudo-coldspray conditions.

1.6 Synthesis of C

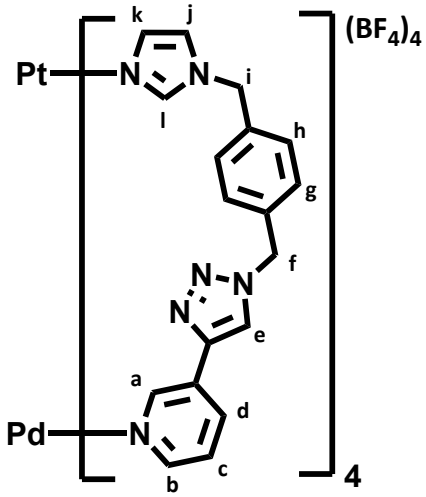

$[Pd(CH_3CN)_4](BF_4)_2$ (21.75 mg, 0.04900 mM, 1 eq.) was added to a stirring solution of $[Pt(\mathbf{L})_4](BF_4)_2$ (80.00 mg, 0.04900 mM, 1 eq.) in CH_3CN (25 mL) in a round bottom flask. The solution was stirred for 24 h at RT, then the cage was precipitated with diethyl ether and the solution filtered. The precipitate was washed with diethyl ether (2 x 15 mL), dichloromethane (2 x 10 mL), and dried *in vacuo* to give a tan powder. (Yield: 0.08171 g, 0.04263 mM, 87%). Slow diffusion of diethyl ether into a concentrated CH_3CN solution of **C** gave colourless rectangular crystals suitable for single crystal X-ray diffraction. ^{1}H NMR (400 MHz, [D_6]DMSO) δ 9.65 (s, 1H, H_a), 9.05 (d, J = 5.7 Hz, 1H, H_b), 8.93 (s, 1H, H_e), 8.29 (d, J = 8.0 Hz, 1H, H_d), 8.19 (s, 1H, H_l), 7.75 (dd, J = 8.0, 5.7 Hz, 1H, H_c), 7.54 (d, J = 7.9 Hz, 2H, H_g), 7.38 (s, 1H,

H_k), 7.30 (d, *J* = 7.9 Hz, 2H, H_h), 6.50 (s, 1H, H_j), 5.69 (s, 2H, H_f), 5.25 (s, 2H, H_i). $^{13}C\{^1H\}$ NMR (125 MHz, [D_6]DMSO) δ: 150.0, 146.8, 141.4, 138.5, 137.0, 136.5, 136.0, 129.6, 129.6, 128.8, 127.7, 127.6, 124.1, 122.0, 53.1, 50.9. Anal. calc. for $C_{72}H_{64}N_{24}PtPdB_4F_{16}$•1.8(DCM): C, 42.88%; H, 3.30%; N, 16.26%. Found: C, 42.60%; H, 3.25%; N, 16.54%. HRESI-MS: (CH_3CN) *m/z* = 869.7324 [**M** – $2BF_4$]$^{2+}$ (calc. for [$C_{72}H_{64}N_{24}PtPdB_2F_8$]$^{2+}$, 869.7256), 551.1533 [**M** – $3BF_4$]$^{3+}$ (calc. for [$C_{72}H_{64}N_{24}PtPdBF_4$]$^{3+}$, 551.1490), 391.6139 [**M** – $4BF_4$]$^{4+}$ (calc. for [$C_{72}H_{64}N_{24}PtPd$]$^{4+}$, 391.6107).

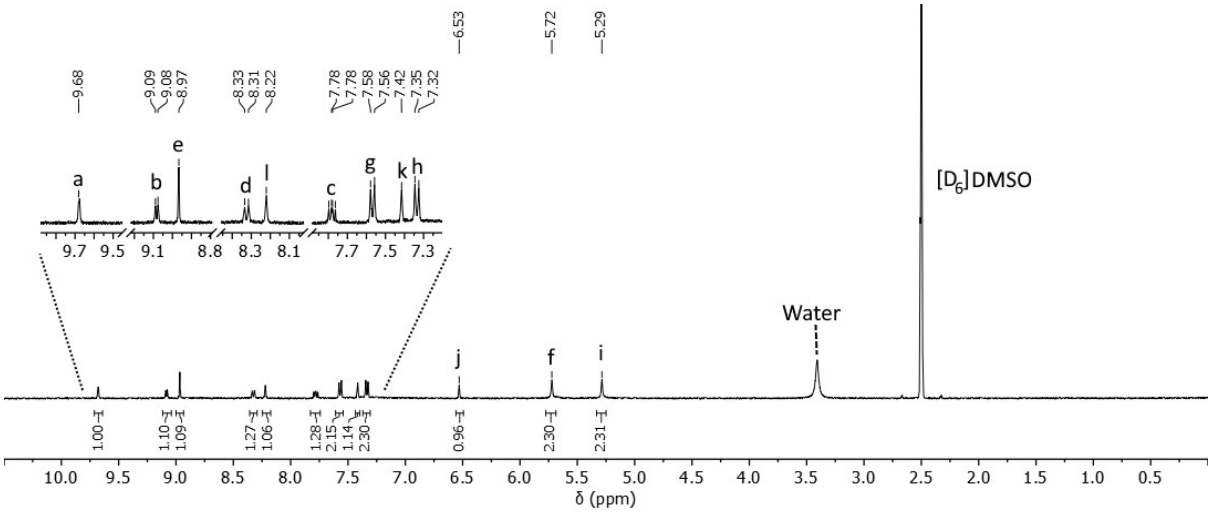

Figure S11 ^1H NMR spectrum (400 MHz, [D_6]DMSO, 298 K) of **C**.

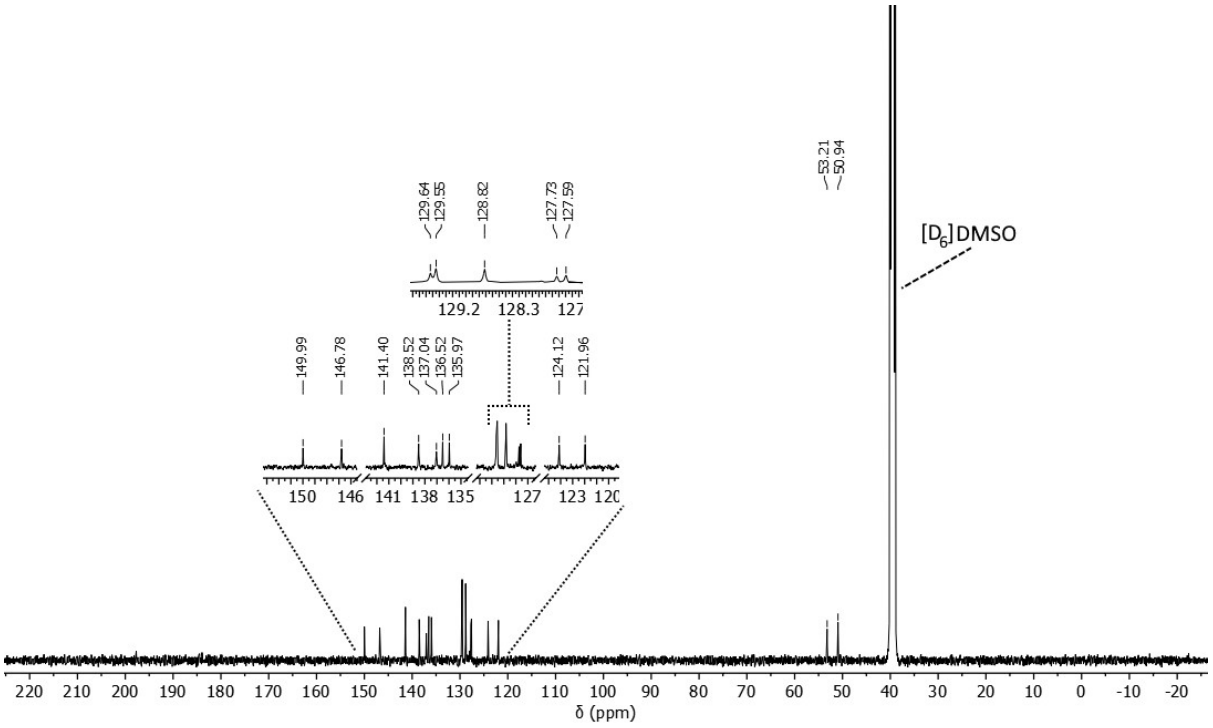

Figure S12 $^{13}C\{^1H\}$ NMR spectrum (125 MHz, [D_6]DMSO, 298 K) of **C**.

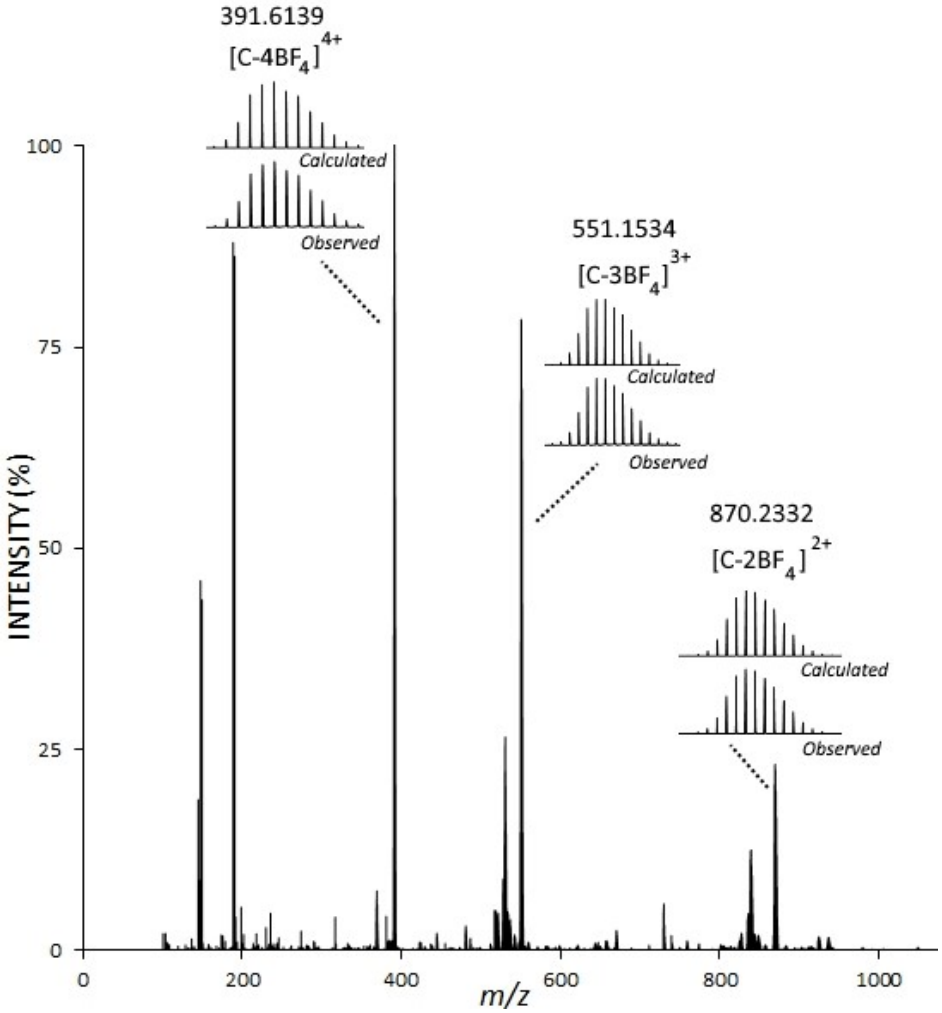

Figure S13 High resolution electrospray ionisation mass spectrum (CH_3CN) of **C**, performed under pseudo-coldspray conditions.

1.7 Synthesis of $[Pd(pytri)_4](BF_4)_2$

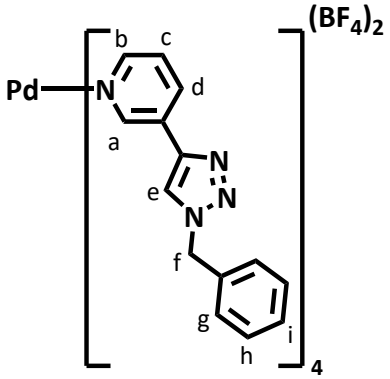

Pytri[2] (98.00 mg, 0.4080 mM) and $[Pd(CH_3CN)_4](BF_4)_2$ (0.04480 mg, 0.1000 mM) were added to acetonitrile (2.250 mL) and the solution was stirred at RT for 1 h. Diethyl ether (5 mL) was added and the solution was filtered to obtain $[Pd(\mathbf{pytri})_4](BF_4)_2$ as a pale yellow solid. (114.0 mg, 0.9344 mM, 93%). Slow diffusion of diethyl ether into an acetonitrile solution of [Pd(**pytri**)-

$_4](BF_4)_2$ gave colourless needles suitable for single crystal X-ray diffraction. ^{1}H NMR (400 MHz, [D_3]acetonitrile): δ 9.56 (s, 1H, H_a), 8.85 (d, *J* = 5.1 Hz, 1H, H_b), 8.27 (s, 1H, H_e), 8.21 (d, *J* = 8.7 Hz, 1H, H_d), 7.55 (dd, *J* = 8.5, 5.3 Hz, 1H, H_d), 7.38 (m, 5H, $H_{g,h,i}$), 5.60 (s, 2H, H_f). ^{13}C{^{1}H} NMR (125 MHz, [D_3]acetonitrile): δ 149.6, 147.4, 142.0, 137.0, 135.3, 130.8, 129.0, 128.7, 128.2, 127.6, 122.9, 53.9.

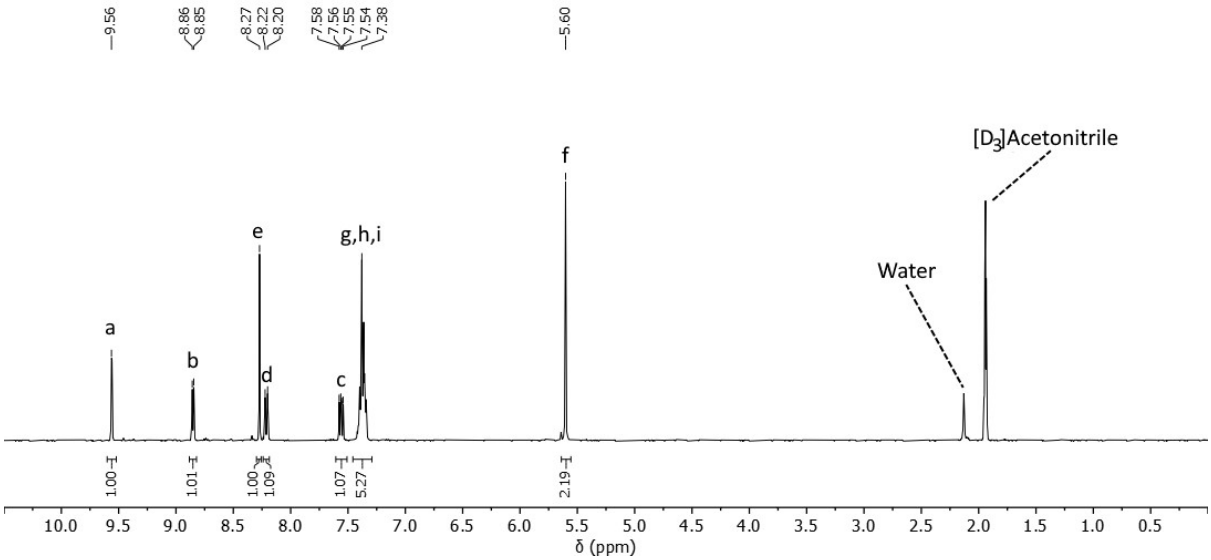

Figure S14 ^{1}H NMR spectrum (400 MHz, [D_3]Acetonitrile, 298 K) of [Pd(**pytri**)$_4$](BF$_4$)$_2$.

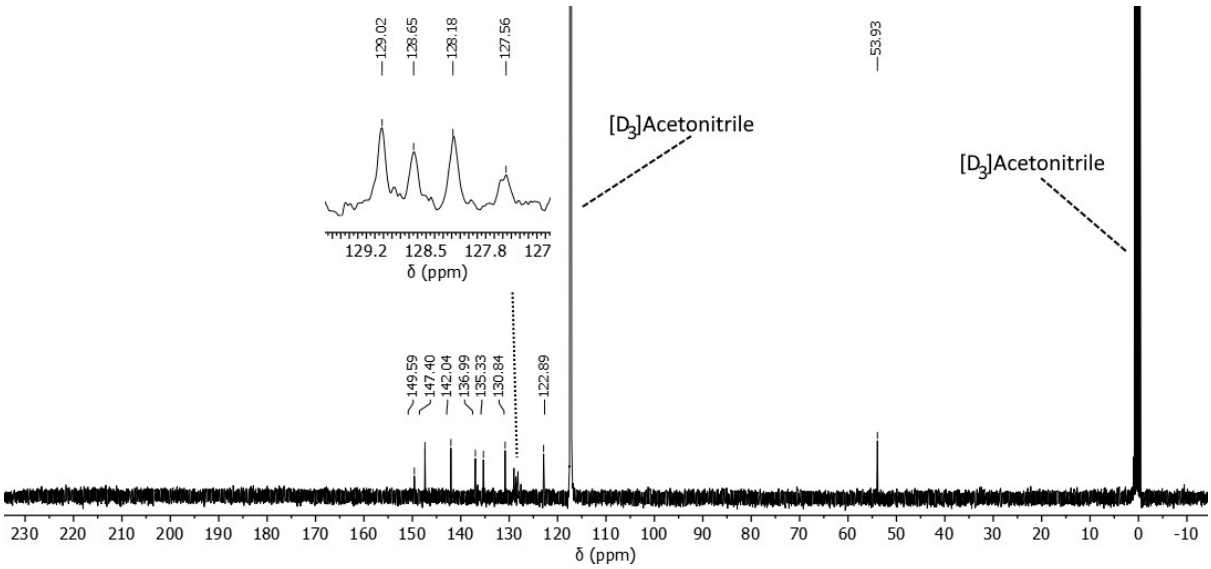

Figure S15 ^{13}C{^{1}H} NMR spectrum (125 MHz, [D_3]Acetonitrile, 298 K) of [Pd(**pytri**)$_4$](BF$_4$)$_2$.

1.8 Synthesis of [Pd(meim)$_4$](BF$_4$)$_2$

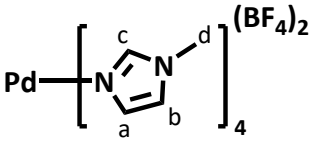

To a stirring solution of N-methylimdazole (10.50 mg, 0.1220 mM) in acetonitrile (500.0 µL) was added a solution of [Pd(CH$_3$CN)$_4$](BF$_4$)$_2$ (13.50 mg, 0.03000 mM) in acetonitrile (500.0 µL). The resulting solution was stirred at RT for 30 min, then diethyl ether (5 mL) was added and the precipitate isolated by centrifuging (6000 rpm, 5 min), then washed with diethyl ether

(2 x 3 mL) to afford [Pd(**meim**)$_4$](BF$_4$)$_2$ as a pale yellow solid. (16.80 mg, 0.02730 mM, 91%). Slow diffusion of diethyl ether into a concentrated acetonitrile solution of [Pd(**meim**)$_4$](BF$_4$)$_2$ gave colourless rectangular crystals suitable for single crystal X-ray diffraction. ^{1}H NMR (400 MHz, [D$_3$]acetonitrile): δ 7.63 (s, 1H, H$_c$), 7.06 (t, J = 1.6 Hz, 1H, H$_a$), 6.82 (t, J = 1.5 Hz, 1H, H$_b$), 3.67 (s, 3H, H$_d$). ^{13}C{^{1}H} NMR (100 MHz, [D$_3$]acetonitrile): δ 139.0, 127.9, 122.4, 34.5. Anal. calc. for C$_{16}$H$_{24}$N$_8$B$_2$F$_8$Pd: C, 31.58%; H, 3.98%; N, 18.42%. Found: C, 31.79%; H, 3.52%; N, 18.45%. HRESI-MS: m/z = 371.0648 [**M** - L + F]$^+$ (calc. for [C$_{12}$H$_{18}$N$_6$PdF]$^+$, 371.0632). I.R. ν (cm^{-1}) 3139, 1543, 1526, 1289, 1245, 1113, 1036, 847, 779, 758, 680, 655.

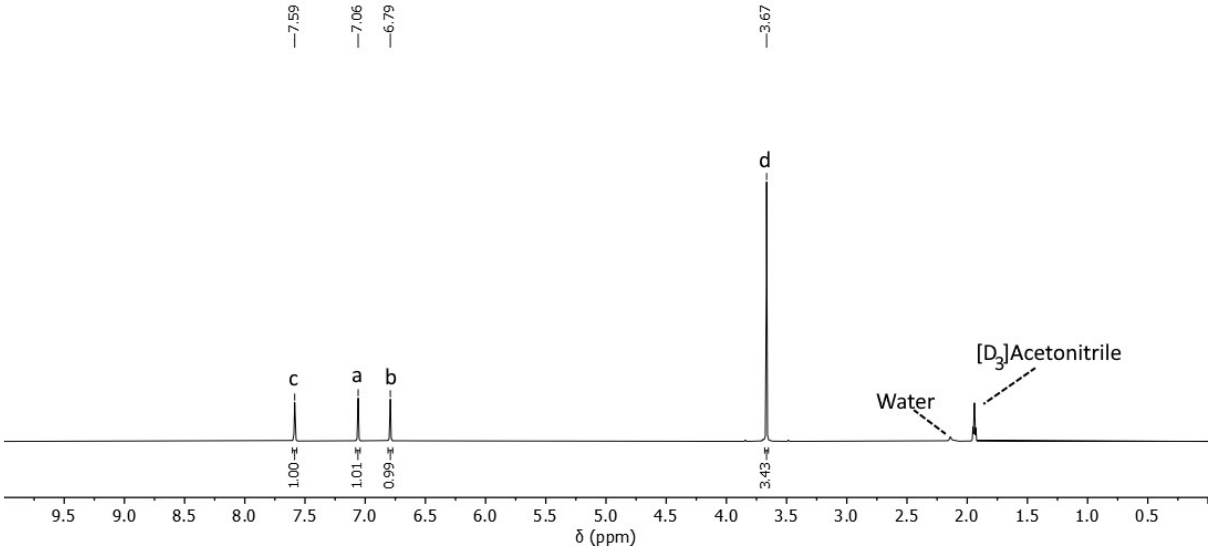

Figure S16 ^{1}H NMR spectrum (400 MHz, [D$_3$]Acetonitrile, 298 K) of [Pd(**meim**)$_4$](BF$_4$)$_2$.

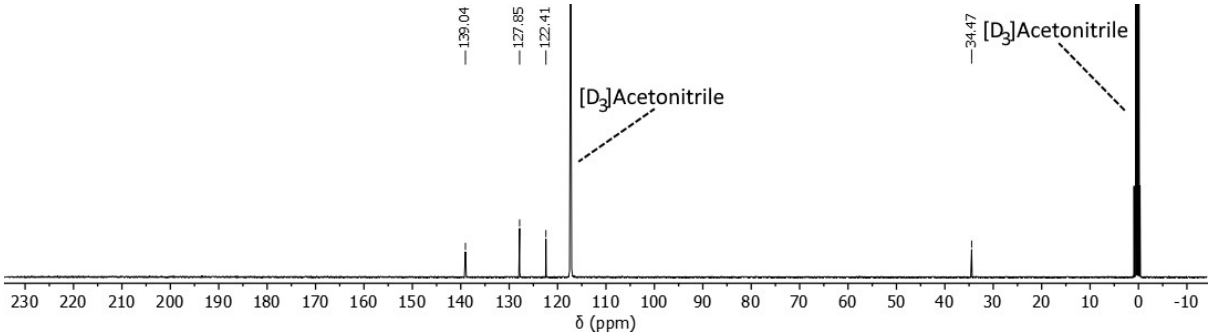

Figure S17 ^{13}C{^{1}H} NMR spectrum (125 MHz, [D$_3$]Acetonitrile, 298 K) of [Pd(**meim**)$_4$](BF$_4$)$_2$.

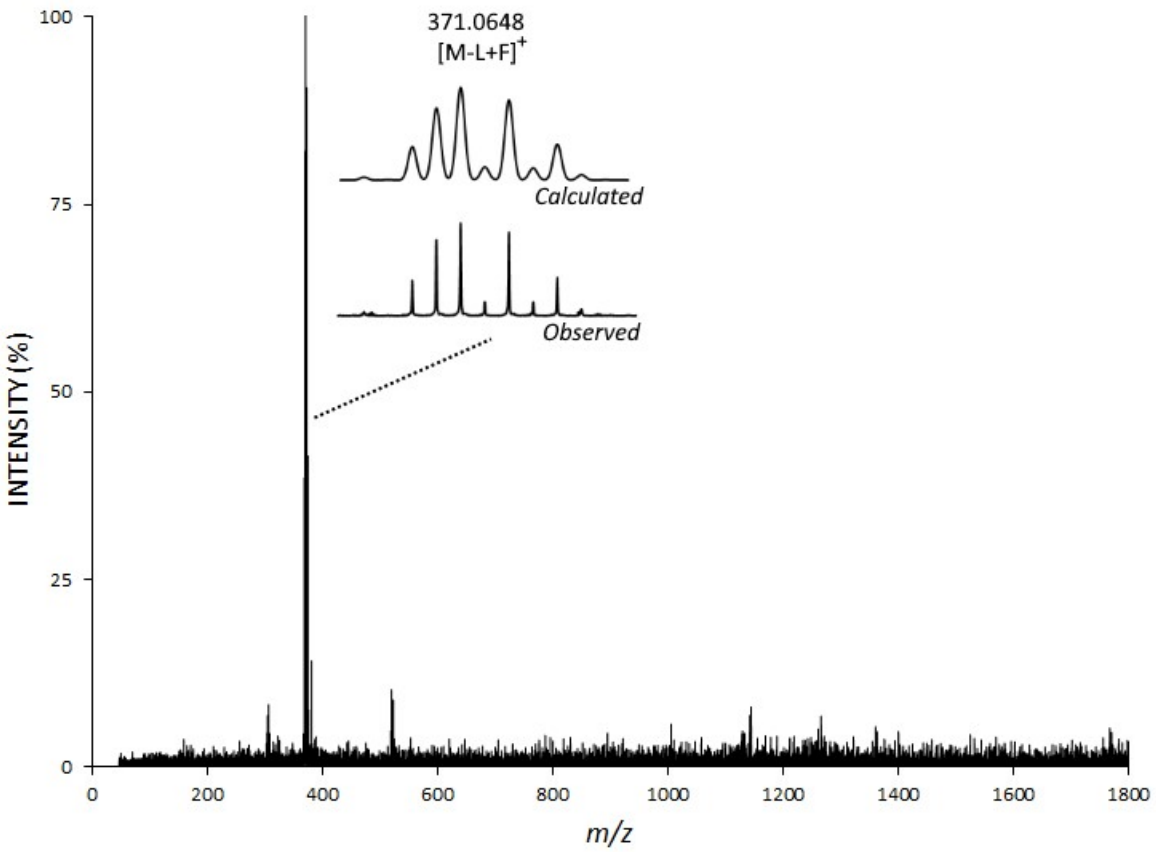

Figure S18 High resolution electrospray ionisation mass spectrum (CH_3CN) of [Pd(**meim**)$_4$](BF_4)$_2$.

2 Model Studies

2.1 Model System

Before undertaking the synthesis of **L**, a model system was prepared to provide confidence that in using **L** we would feasibly be able to form a heterometallic cage through selective metal coordination at specific donor sites. The model system consisted of a pyridyl-triazole model ligand (**pytri**, Figure S19a), methyl imidazole (**meim**, Figure S19c), and the palladium(II) complexes of these ligands (Figure S19b, Figure S19d).

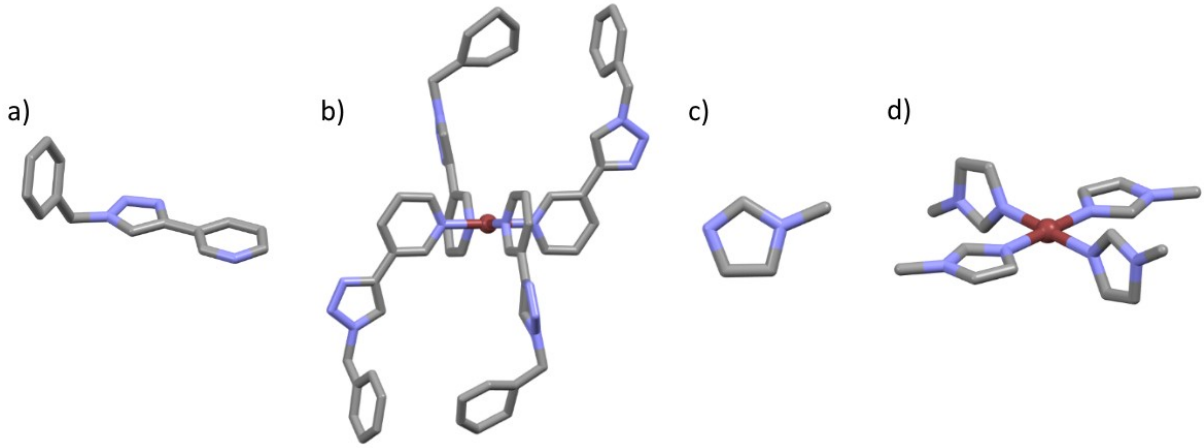

Figure S19 Model ligands and complexes: a) **pytri**, b) [Pd(**pytri**)$_4$](BF$_4$)$_2$, c) **meim**, d) [Pd(**meim**)$_4$](BF$_4$)$_2$. Stick models of ligands are SPARTAN'16 models, whereas stick models of complexes are the molecular structures that were determined by X-ray diffraction analysis. Colour scheme: carbon = grey, nitrogen = periwinkle, palladium = brown. Solvent molecules, hydrogen atoms and counterions omitted for clarity.

2.2 Competition Experiments

5 eq. of **meim** were added to an [D_3]acetonitrile solution of [Pd(**pytri**)$_4$](BF_4)$_2$. This was monitored via ^{1}H NMR spectroscopy (400 MHz, 298 K, Figure S20) at various time points after the addition. Signals due to [Pd(**pytri**)$_4$](BF_4)$_2$ disappeared immediately after the addition, and were replaced by a new set of resonances corresponding to the complex [Pd(**meim**)$_4$](BF_4)$_2$.

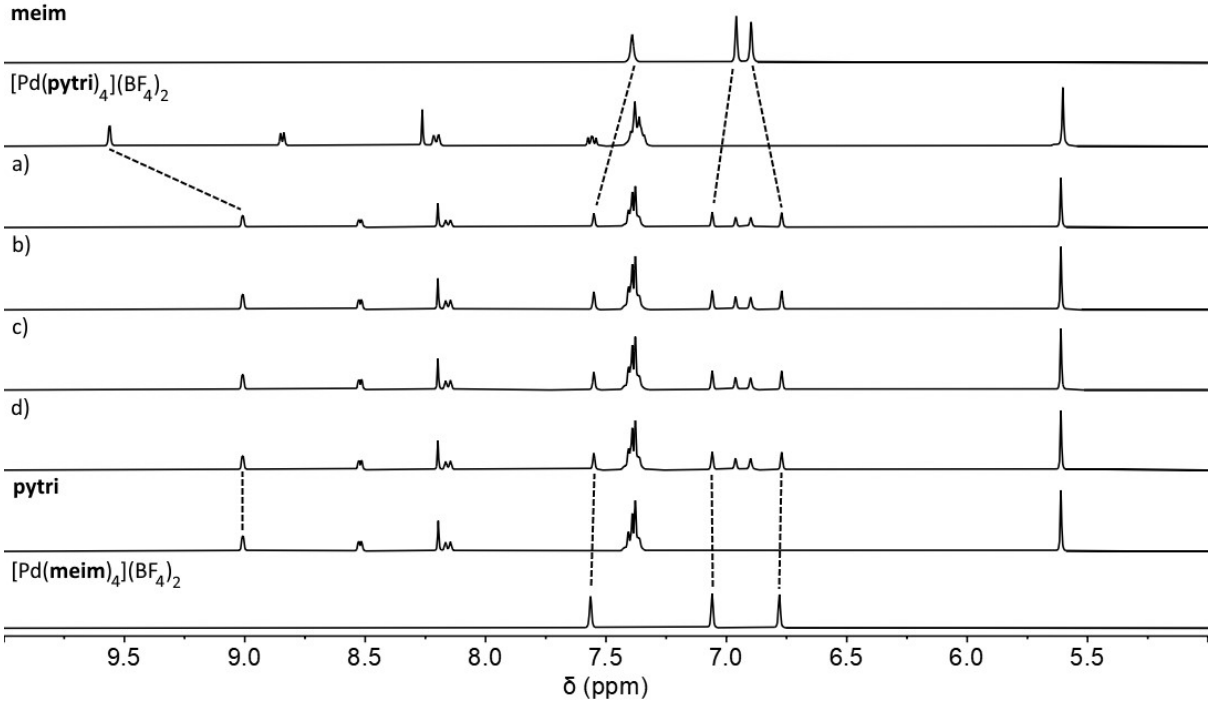

Figure S20 Stacked partial ^{1}H NMR spectra (400 MHz, [D_3]acetonitrile, 298 K) of **meim**:[Pd(**pytri**)$_4$](BF_4)$_2$ competition experiment a) immediately, b) 1 h, c) 4 h, d) 9 h after the addition.

5 eq. of **pytri** were then added to an [D_3]acetonitrile solution of [Pd(**meim**)$_4$](BF_4)$_2$ and the reaction monitored via ^{1}H NMR spectroscopy (400 MHz, 298 K, Figure S21) at various time points after the addition. No change in resonances of [Pd(**meim**)$_4$](BF_4)$_2$ was seen. The final ^{1}H NMR spectrum recorded 1 week after the addition contained only resonances due to that of [Pd(**meim**)$_4$](BF_4)$_2$ and free **pytri**.

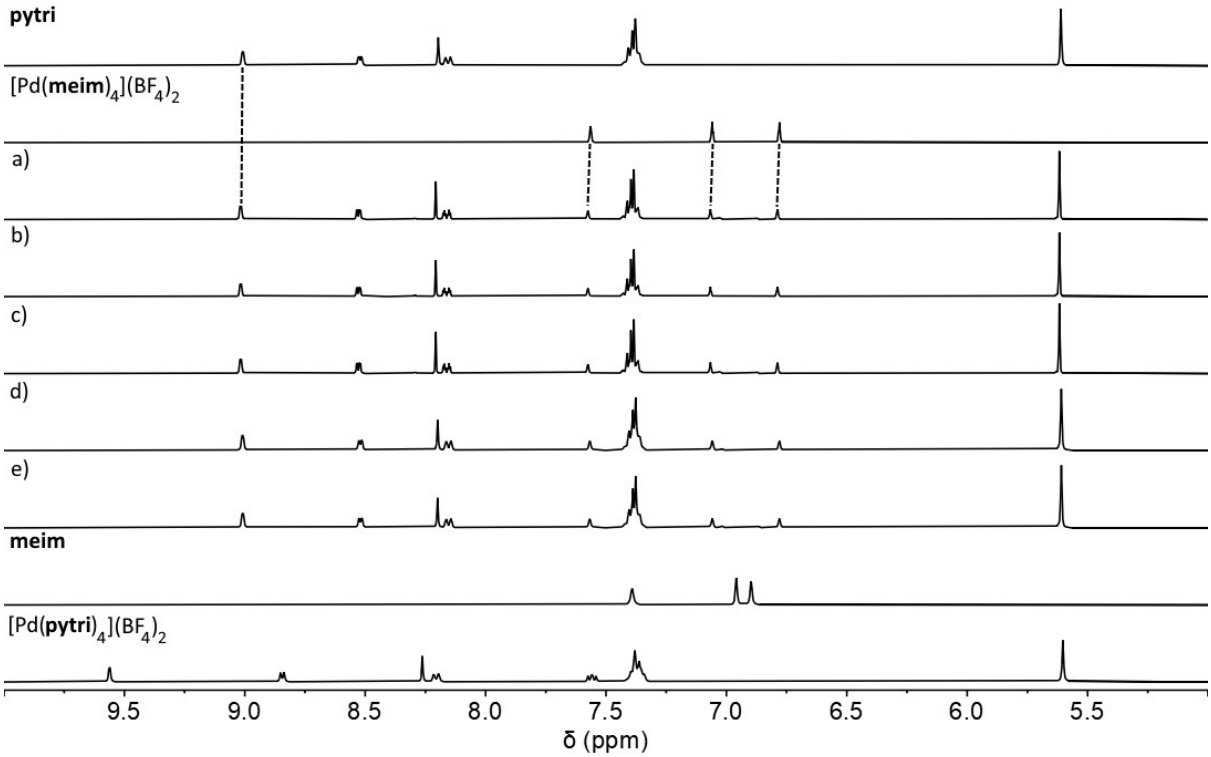

Figure S21 Stacked partial ^{1}H NMR spectra (400 MHz, [D_3]acetonitrile, 298 K) of **Pytri**:[Pd(**Meim**)$_4$](BF$_4$)$_2$ competition experiment a) immediately, b) 1 h, c) 2 h, d) 3 h, e) 1 week after the addition.

3 $[Pt(L)_4](BF_4)_2$ Formation in Different Solvents

Generation of the complex $[Pt(\mathbf{L})_4](BF_4)_2$ was investigated in both $[D_3]$acetonitrile and $[D_6]$DMSO. Standard conditions were used for these experiments, as detailed in the experimental section. In both $[D_6]$DMSO and $[D_3]$acetonitrile, over the course of one week at 60 °C, a number of initial products funnel into the final thermodynamically favourable imidazole ligated Pt(II) complex (Figure S22 and S18). After one week, other (single or multiple) products can be detected via ^{1}H NMR spectroscopy, and are likely similar but subtly different coordination isomers of the formula $[Pt(\mathbf{L})_4](BF_4)_2$ (Figure S22g and Figure S23g). The resonances in the spectra recorded in $[D_3]$acetonitrile appear broader than those in the related $[D_6]$DMSO experiment. Additionally, a greater number of methyl peaks are seen.

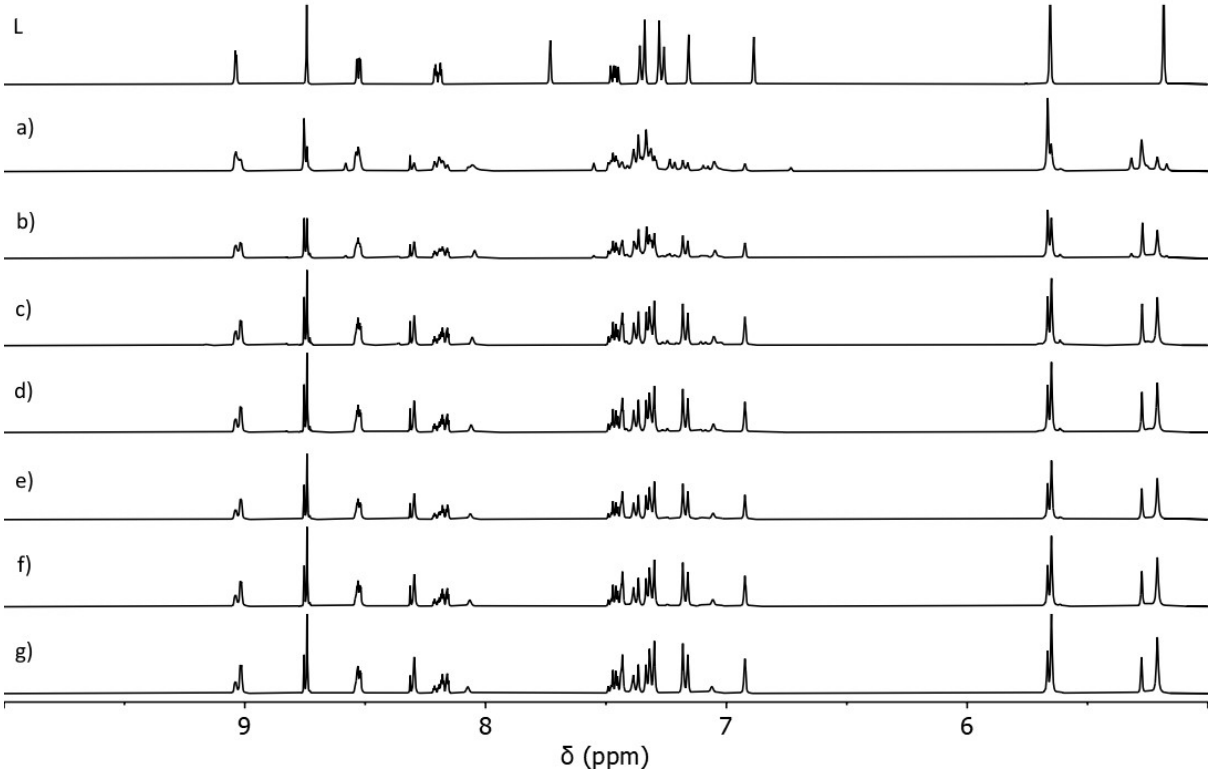

Figure S22 Stacked partial ^{1}H NMR spectra (400 MHz, $[D_6]$DMSO, 298 K) of: L = ligand, $[Pt(\mathbf{L})_4](BF_4)_2$ formation after a) 1 h, b) 3 h, c) 1 day, d) 2 days, e) 3 days, f) 4 days, g) 7 days.

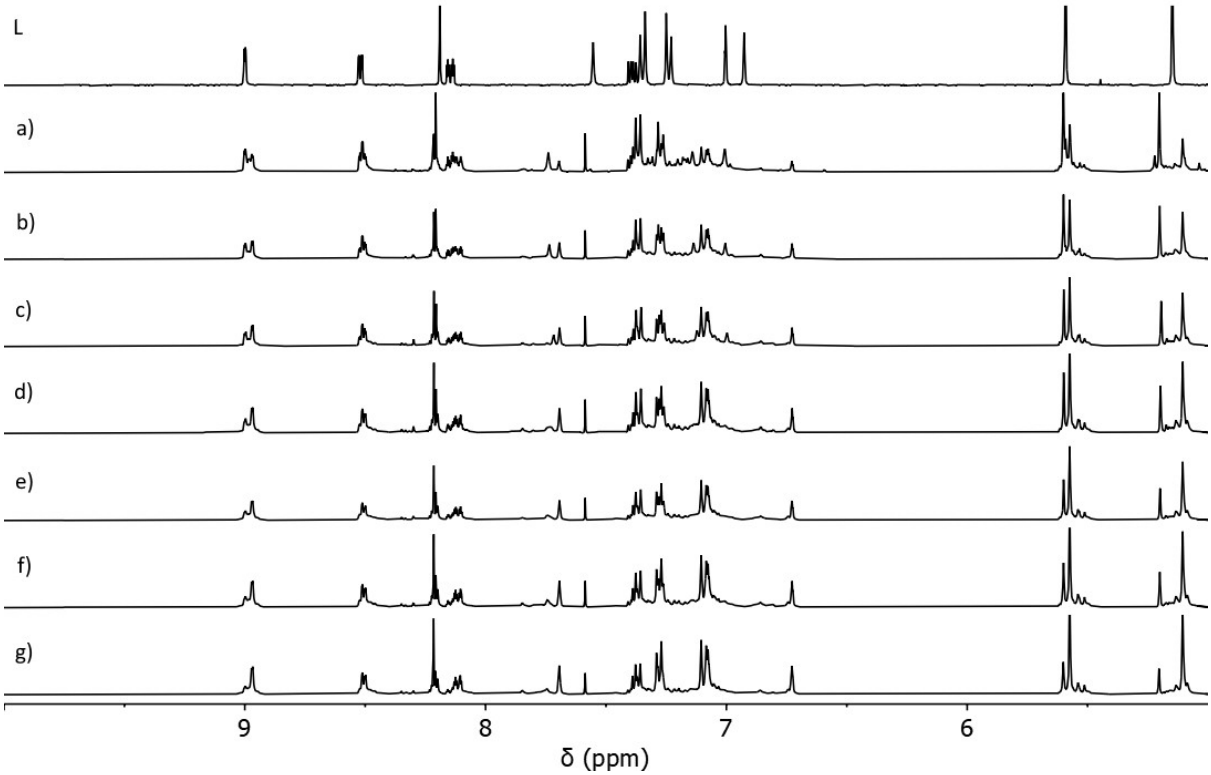

Figure S23 Stacked partial ^{1}H NMR spectra (400 MHz, [D_3]acetonitrile, 298 K) of: L = ligand, [Pt(**L**)$_4$](BF$_4$)$_2$ formation after a) 1 h, b) 3 h, c) 1 day, d) 2 days, e) 3 days, f) 4 days, g) 7 days.

The imidazole ligated complex, [Pt(**L**)$_4$](BF$_4$)$_2$, was isolated from [D_6]DMSO by precipitation with EtOAc after 7 days of heating at 60 °C. It is soluble in CH_3CN and is pure according to ^{1}H NMR spectroscopy. After 7 days of heating at 60 °C in [D_3]acetonitrile imidazole ligated [Pt(**L**)$_4$](BF$_4$)$_2$ can clearly be observed as the major product in the ^{1}H NMR spectrum. However, this spectrum also shows the formation of unidentified by-products (Figure S24).

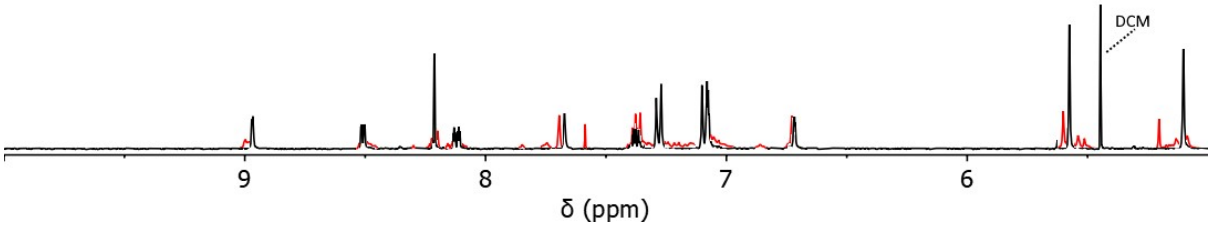

Figure S24 Overlaid ^{1}H NMR spectra (400 MHz, [D_3]acetonitrile, 298 K) of [Pt(**L**)$_4$](BF$_4$)$_2$ complex. Black trace: [Pt(**L**)$_4$](BF$_4$)$_2$ complex formed in DMSO after isolation, red trace: [Pt(**L**)$_4$](BF$_4$)$_2$ formation in [D_3]acetonitrile after 7 days (Figure S23g).

4 ^{1}H DOSY Data

All ^{1}H DOSY NMR spectra were obtained using the convection compensated dstebpgp3s[4] pulse sequence within Topshim.

The spectra in [D_6]DMSO were obtained with δ = 2.6 ms, Δ = 100 ms, and g = 2% – 45%. For [D_3]acetonitrile, they were obtained with δ = 2 ms, Δ = 100 ms, and g = 2% – 95%.

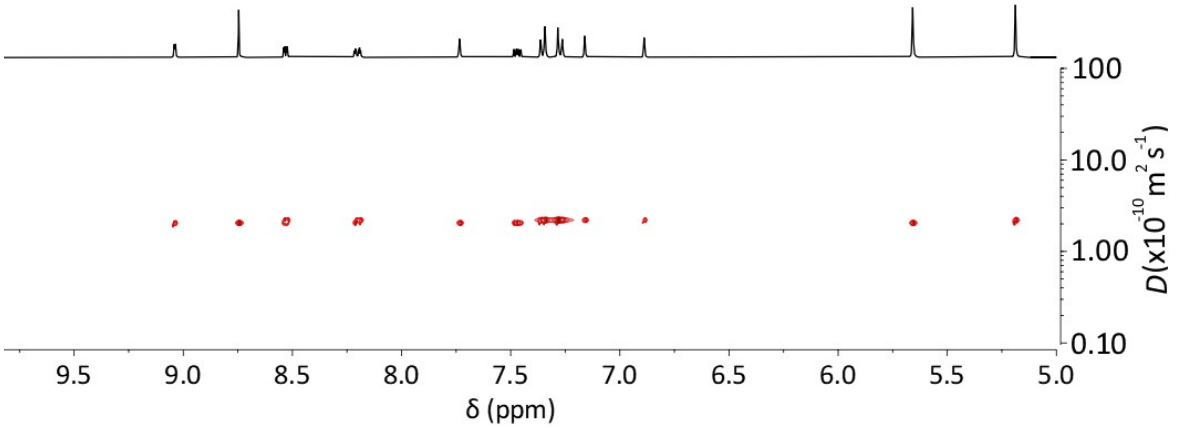

Figure S25 Partial ^{1}H NMR and corresponding DOSY NMR spectra for **L** (400 MHz, [D_6]DMSO, 298 K).

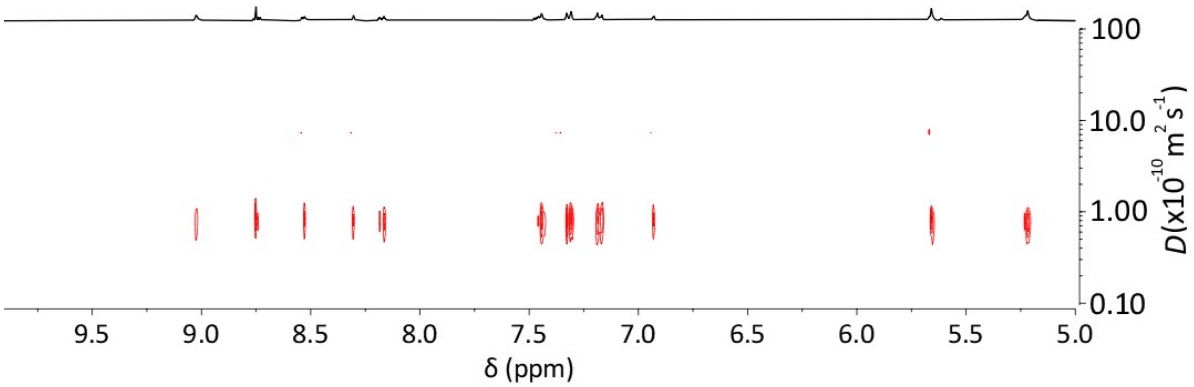

Figure S26 Partial ^{1}H NMR and corresponding DOSY NMR spectra for [Pt(**L**)$_4$](BF$_4$)$_2$ (400 MHz, [D_6]DMSO, 298 K).

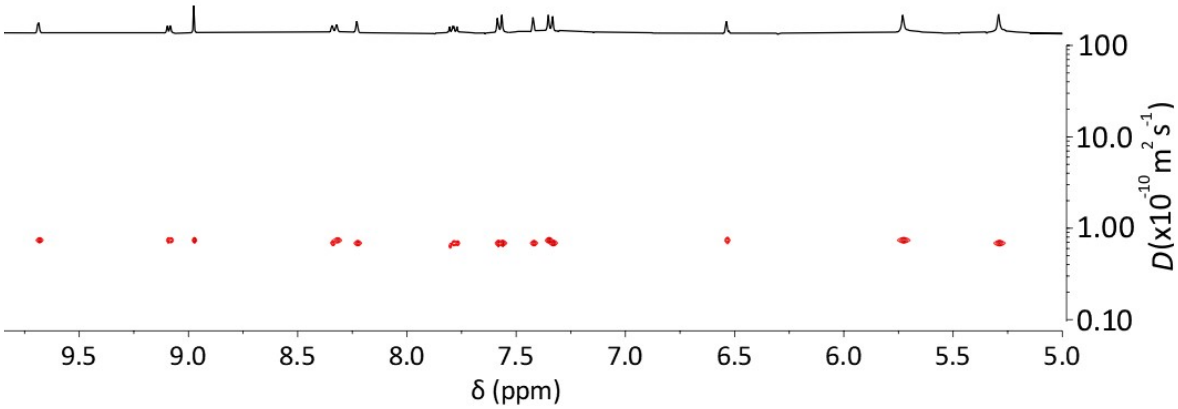

Figure S27 Partial ^{1}H NMR and corresponding DOSY NMR spectra for **C** (400 MHz, [D_6]DMSO, 298 K).

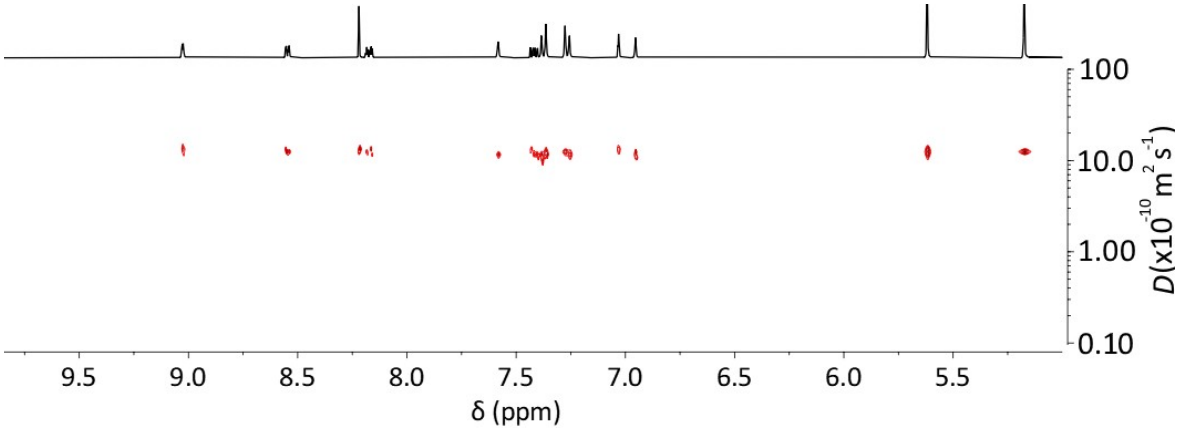

Figure S28 Partial ^{1}H NMR and corresponding DOSY NMR spectra for **L** (400 MHz, [D_3]acetonitrile, 298 K).

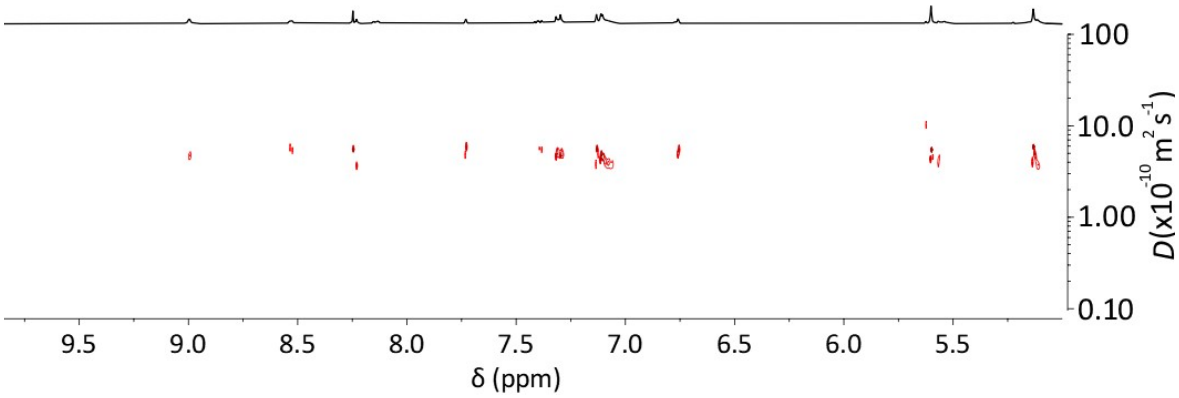

Figure S29 Partial ^{1}H NMR and corresponding DOSY NMR spectra for [Pt(**L**)$_4$](BF$_4$)$_2$ (400 MHz, [D_3]acetonitrile, 298 K).

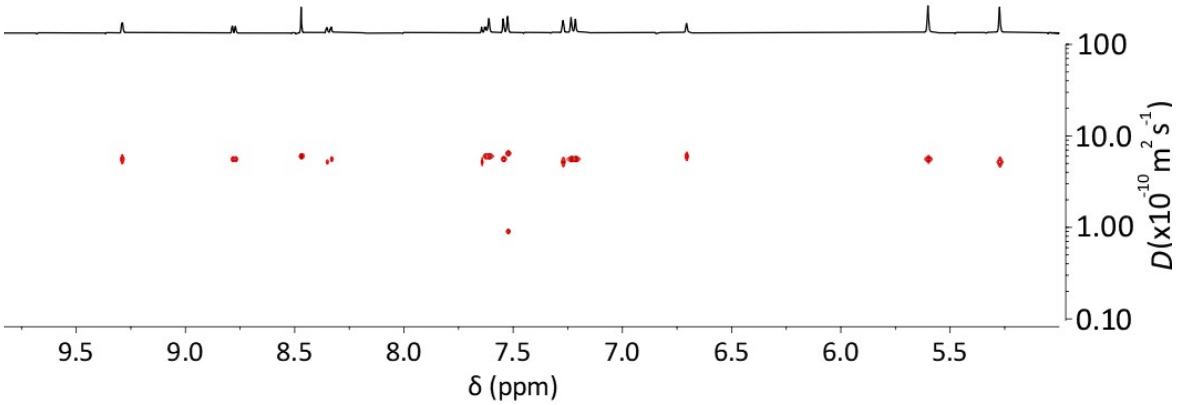

Figure S30 Partial ^{1}H NMR and corresponding DOSY NMR spectra for **C** (400 MHz, [D_3]acetonitrile, 298 K).

Table S1 Diffusion coefficients as obtained via ^{1}H DOSY NMR experiments (400 MHz, [D_3]acetonitrile or [D_6]DMSO, 298 K).

Species	Molecular Weight (g mol^{-1})	Diffusion Coefficient (x 10^{-10} m^2 s^{-1})	
		[D_6]DMSO	[D_3]Acetonitrile
L	316.368	2.07	12.0
[Pt(**L**)$_4$](BF$_4$)$_2$	1634.160	0.82	5.15
C	1914.190	0.74	5.54

5 X-ray Crystallography

5.1 L

CCDC #2175042 A concentrated solution of **L** in diethyl ether was left to stand overnight, resulting in the formation of long, colourless needles of **L**. X-ray data were collected at 100 K on an Agilent Technologies Supernova system using Mo Kα radiation with exposures over 1.0˚, and data were treated using CrysAlisPro software.[5] The structure was solved using SHELXT and weighted full-matrix refinement on F^2 was carried out using SHELXL-97[6] both running within the OLEX2-v1.2.9 package.[7] All non-hydrogen atoms were refined anisotropically. Hydrogen atoms attached to carbon atoms were placed in calculated positions and refined using a riding model. The structure was solved in the triclinic space group $P\bar{1}$ and refined to an R_1 value of 6.37%. The asymmetric unit contains one ligand **L** (Figure S31).

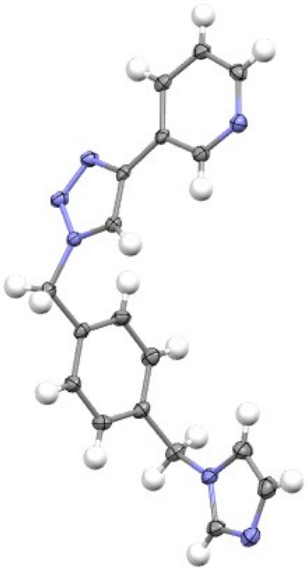

Figure S31 Mercury ellipsoid plot of the asymmetric unit of **L**. Ellipsoids are shown at the 50% probability level. Colour scheme: carbon = grey, hydrogen = white, nitrogen = periwinkle.

5.2 C

CCDC #2175045 Vapour diffusion of diethyl ether into a concentrated nitromethane solution of **C** resulted in the formation of a colourless, rectangular crystal suitable for X-ray diffraction. X-ray data were collected at 100 K on an Agilent Technologies Supernova system using Cu Kα radiation with exposures over 1.0˚, and data were treated using CrysAlisPro software.[5] The structure was solved using SHELXT and weighted full-matrix refinement on F^2 was carried out using SHELXL-97[6] both running within the OLEX2-v1.2.9 package.[7] All non-hydrogen atoms were refined anisotropically. Hydrogen atoms attached to carbon atoms were placed in calculated positions and refined using a riding model. The structure was solved in the triclinic space group $P\bar{1}$ and refined to an R_1 value of 6.93%. The asymmetric unit contains one heterometallic type cage containing four ligands **L**, one platinum(II) and one palladium(II) ion, three BF_4^- counterions, and two nitromethane molecules. The structure contained disorder at a number of atoms in the triazole and pyridine rings of one ligand, and at three of the four fluorine atoms in one of the BF_4^- anions. A solvent mask (with the OLEX2-v1.2.9 package) was applied to resolve diffuse electron density, where a void consisting of 58 electrons was

measured in the asymmetric unit, this was attributed to a molecule of nitromethane and a tetrafluoroborate (**BF_4^-**) anion (Figure S32).

CheckCIF gives an A level alert and 6 B level alerts. The A alert and five of the B alerts result from residual density observed around select atoms, deemed to be due to Fourier ripples caused by using copper X-ray source and heavy atoms present in the structure. The copper X-ray source was required in order to obtain acceptable diffraction. One B alert is due to the minor unresolved disorder of a nitrogen atom in one of the triazole rings.

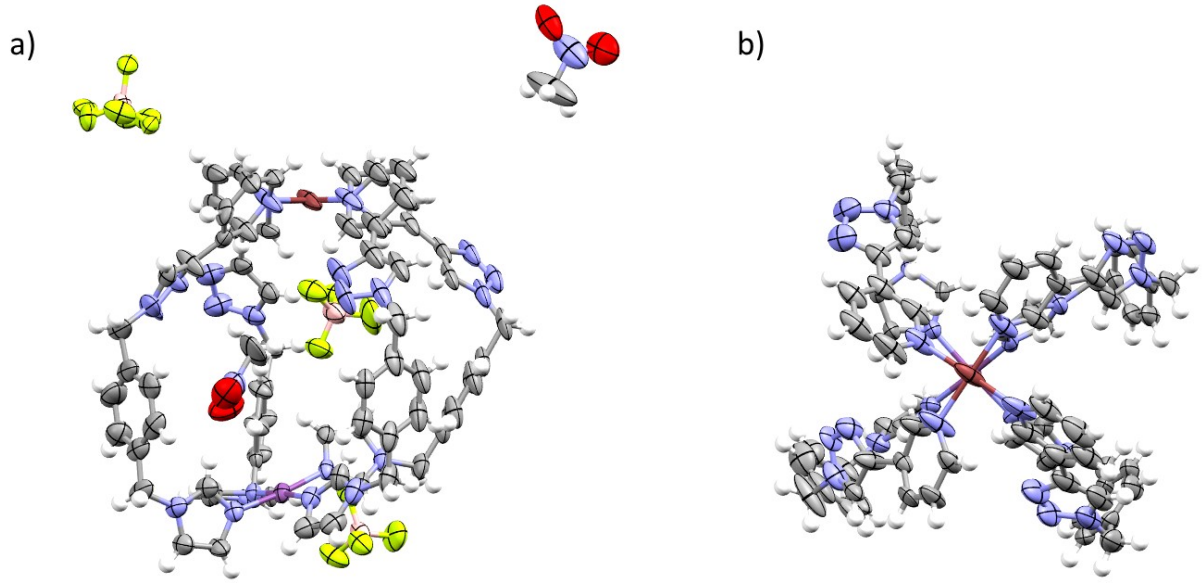

Figure S32 Mercury ellipsoid plot of the a) asymmetric unit of **C** and b) a top (palladium)-down (platinum) view of the asymmetric unit of **C** with solvent molecules and counterions omitted for clarity. Ellipsoids are shown at the 50% probability level. Colour scheme: boron = salmon, carbon = grey, fluorine = yellow, hydrogen = white, nitrogen = periwinkle, oxygen = red, palladium = brown, platinum = purple.

5.3 $[Pd(pytri)_4](BF_4)_2$

CCDC #2175043 Vapour diffusion of diethyl ether into a concentrated CH_3CN solution of $[Pd(\mathbf{pytri})_4](BF_4)_2$, resulted in the formation of a colourless, rectangular crystal suitable for X-ray diffraction. X-ray data were collected at 100 K on an Agilent Technologies Supernova system using Cu Kα radiation with exposures over 1.0˚, and data were treated using CrysAlisPro software.[5] The structure was solved using SHELXT and weighted full-matrix refinement on F^2 was carried out using SHELXL-97[6] both running within the OLEX2-v1.2.9 package.[7] All non-hydrogen atoms were refined anisotropically. Hydrogen atoms attached to carbon atoms were placed in calculated positions and refined using a riding model. The structure was solved in the triclinic space group $P\bar{1}$ and refined to an R_1 value of 9.48%. The asymmetric unit contains two **pytri** ligands coordinated to one palladium(II) ion, a BF_4^- anion and a molecule of diethyl ether. The structure contained disorder at a number of atoms in the terminal benzene rings of one of the ligands. FLAT, SIMU, RIGU and ISOR commands were used to properly model these atoms. An ISOR command was applied to a carbon atom in the diethyl ether solvent molecule to resolve disorder associated with this atom. The BF_4^- anion showed rotational disorder that was modelled using the PART command.

CheckCIF gives 1 A level alert and 2 B level alerts. These all result from residual density observed around the palladium(II) atom, deemed to be due to the large size of the crystal used to obtain the dataset and difficulties with the absorption correction.

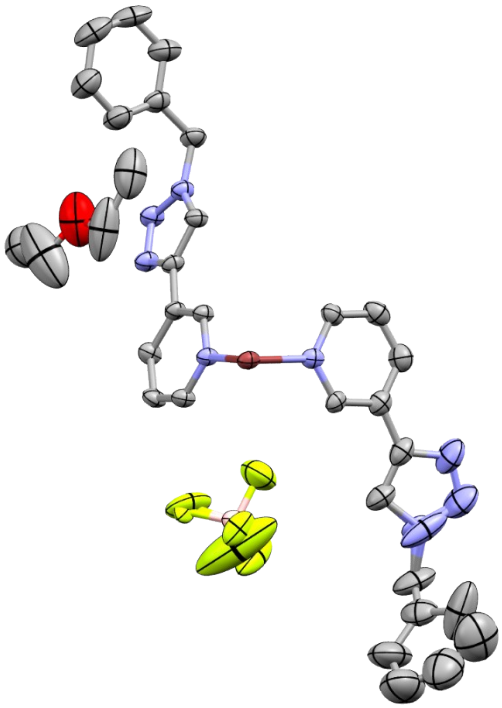

Figure S33 Mercury ellipsoid plot of the asymmetric unit of [Pd(**pytri**)$_4$](BF$_4$)$_2$. Ellipsoids are shown at the 50% probability level. Colour scheme: carbon = grey, hydrogen = white, nitrogen = periwinkle, palladium = brown, boron = salmon, fluorine = yellow, oxygen = red.

5.4 [Pd(meim)$_4$](BF$_4$)$_2$

CCDC #2175046 Vapour diffusion of diethyl ether into a concentrated CH_3CN solution of [Pd(**meim**)$_4$](BF$_4$)$_2$, resulted in the formation of a colourless, rectangular crystal suitable for X-ray diffraction. X-ray data were collected at 100 K on an Agilent Technologies Supernova system using Cu Kα radiation with exposures over 1.0˚, and data were treated using CrysAlisPro software.[5] The structure was solved using SHELXT and weighted full-matrix refinement on F^2 was carried out using SHELXL-97[6] both running within the OLEX2-v1.2.9 package.[7] All non-hydrogen atoms were refined anisotropically. Hydrogen atoms attached to carbon atoms were placed in calculated positions and refined using a riding model. The structure was solved in the triclinic space group $P2_1/n$ and refined to an R_1 value of 3.37%. The asymmetric unit contains two **meim** ligands coordinated to one palladium(II) ion, and a BF_4 anion (Figure S34).

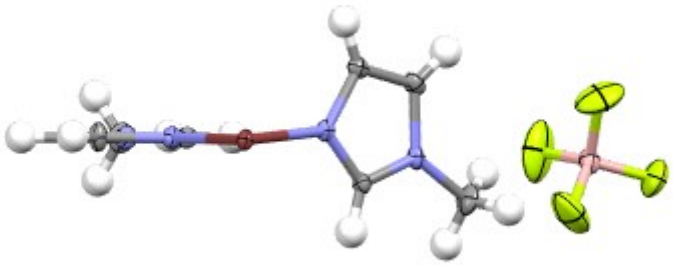

Figure S34 Mercury ellipsoid plot of the asymmetric unit of [Pd(**meim**)$_4$](BF_4)$_2$. Ellipsoids are shown at the 50% probability level. Colour scheme: carbon = grey, hydrogen = white, nitrogen = periwinkle, palladium = brown, boron = salmon, fluorine = yellow.

Table S2 Crystal data and structure refinement table for **L** and **C**.

	L	**C**
CCDC#	2175042	2175045
Empirical formula	$C_{18}H_{16}N_6$	$C_{75}H_{73}B_4F_{16}N_{27}O_6PdPt$
Formula weight	316.37	2097.358
Temperature/K	100.01(11)	100.01(10)
Crystal system	triclinic	triclinic
Space group	P-1	P-1
a/Å	5.6355(5)	11.6471(5)
b/Å	9.7050(9)	15.8160(7)
c/Å	14.0179(13)	25.1824(10)
α/°	87.811(8)	102.420(4)
β/°	79.902(8)	99.049(3)
γ/°	87.432(8)	100.243(4)
Volume/Å^3	753.68(12)	4364.9(3)
Z	2	2
ρ_{calc}g/cm^3	1.394	1.596
μ/mm^{-1}	0.089	5.499
F(000)	332.0	2096.5
Crystal size/mm^3	0.429 × 0.063 × 0.052	0.094 × 0.064 × 0.027
Radiation	MoKα (λ = 0.71073)	CuKα (λ = 1.54184)
2Θ range for data collection/°	7.146 to 58.804	7.342 to 153.144
Index ranges	-7 ≤ h ≤ 7, -12 ≤ k ≤ 13, -19 ≤ l ≤ 19	-14 ≤ h ≤ 14, -19 ≤ k ≤ 19, -31 ≤ l ≤ 28
Reflections collected	9357	43070
Independent reflections	3626 [R_{int} = 0.0798, R_{sigma} = 0.0937]	17771 [R_{int} = 0.0765, R_{sigma} = 0.0933]
Data/restraints/parameters	3626/0/217	17771/6/1173
Goodness-of-fit on F^2	1.042	1.042
Final R indexes [I>=2σ (I)]	R_1 = 0.0637, wR_2 = 0.1400	R_1 = 0.0694, wR_2 = 0.1616
Final R indexes [all data]	R_1 = 0.0975, wR_2 = 0.1621	R_1 = 0.10276, wR_2 = 0.1861
Largest diff. peak/hole / e Å^{-3}	0.28/-0.34	4.10/-4.86

Table S3 Crystal data and structure refinement table for [Pd(**pytri**)$_4$](BF$_4$)$_2$ and [Pd(**meim**)$_4$](BF$_4$)$_2$.

	[Pd(**pytri**)$_4$](BF$_4$)$_2$	[Pd(**meim**)$_4$](BF$_4$)$_2$
CCDC#	2175043	2175046
Empirical formula	$C_{63}H_{60}B_2F_8N_{16}O_2Pd$	$C_{16}H_{24}B_2F_8N_8Pd$
Formula weight	1353.29	608.45
Temperature/K	99.98(10)	100.01(10)
Crystal system	triclinic	monoclinic
Space group	P-1	$P2_1/n$
a/Å	10.1145(5)	7.98190(10)
b/Å	10.5040(6)	10.38240(10)
c/Å	17.3505(7)	14.2482(3)
α/°	74.354(4)	90
β/°	86.080(4)	94.673(2)
γ/°	61.495(6)	90
Volume/Å^3	1555.92(16)	1176.84(3)
Z	1	2
ρ_{calc}g/cm^3	1.444	1.717
μ/mm^{-1}	3.107	7.156
F(000)	694.0	608.0
Crystal size/mm^3	0.52 × 0.198 × 0.168	0.591 × 0.324 × 0.208
Radiation	CuKα (λ = 1.54184)	CuKα (λ = 1.54184)
2Θ range for data collection/°	9.934 to 154.574	12.302 to 145.628
Index ranges	-10 ≤ h ≤ 12, -11 ≤ k ≤ 13, -21 ≤ l ≤ 21	-9 ≤ h ≤ 9, -12 ≤ k ≤ 12, -17 ≤ l ≤ 13
Reflections collected	24535	9900
Independent reflections	6461 [R_{int} = 0.0960, R_{sigma} = 0.0687]	2301 [R_{int} = 0.0310, R_{sigma} = 0.0135]
Data/restraints/parameters	6460/68/468	2301/0/162
Goodness-of-fit on F^2	1.199	1.091
Final R indexes [I>=2σ (I)]	R_1 = 0.0948, wR_2 = 0.2490	R_1 = 0.0337, wR_2 = 0.0817
Final R indexes [all data]	R_1 = 0.0982, wR_2 = 0.2592	R_1 = 0.0337, wR_2 = 0.0817
Largest diff. peak/hole / e Å^{-3}	3.09/-1.04	1.33/-0.61

6 Robustness Studies

The kinetic robustness of **C** was examined in either [D_3]acetonitrile or [D_6]DMSO solutions. A [D_3]acetonitrile (0.500 mL, 1.00 mM) solution of **C** was prepared and heated at 50 °C for 96 hours (4 days, Figure S35). The same sample was then heated at 75 °C for a further 96 hours (4 days, Figure S36). These solutions were monitored via ^{1}H NMR spectroscopy (400 MHz, 298 K).

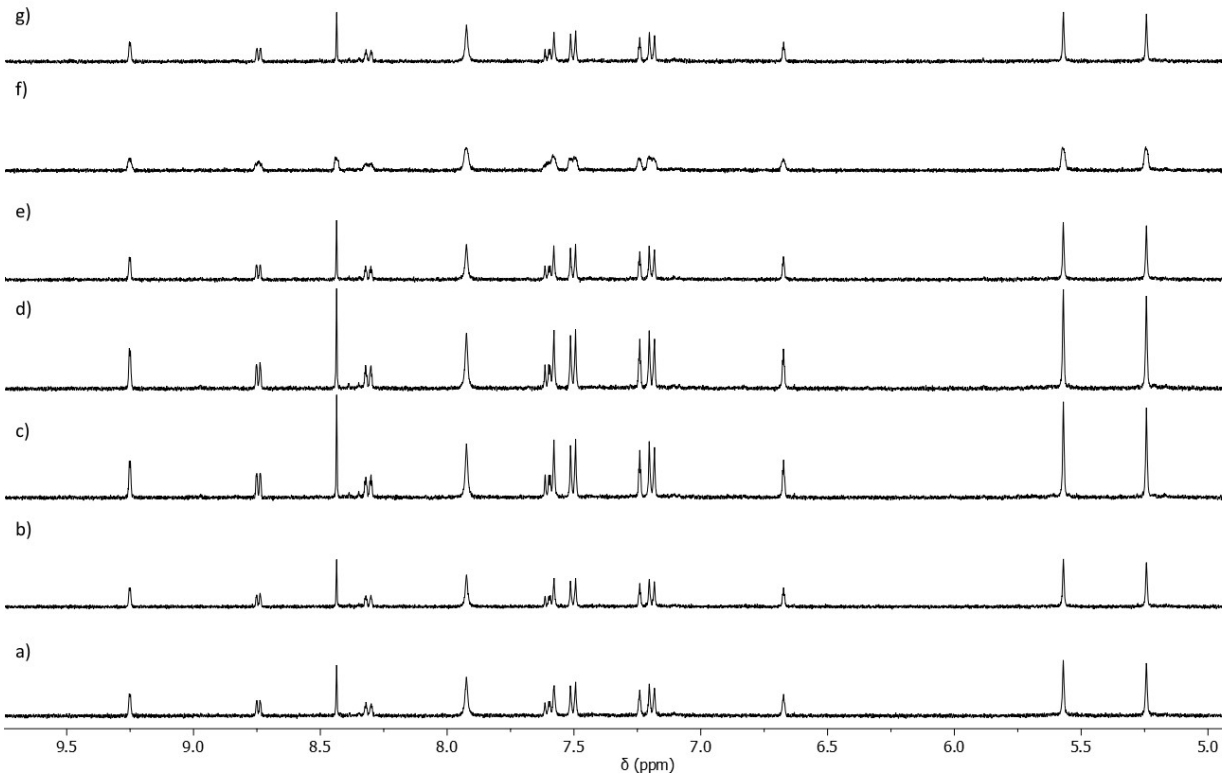

Figure S35 Stacked partial ^{1}H NMR spectra (400 MHz, [D_3]acetonitrile, 298 K) of **C** after a) 0 hours at 50 °C, b) 4 hours at 50 °C, c) 22 hours at 50 °C, d) 28 hours at 50 °C, e) 49 hours at 50 °C, f) 73 hours at 50 °C, and g) 96 hours at 50 °C. No change in the ^{1}H NMR spectrum of **C** is observed confirming that the cage is robust under these conditions.

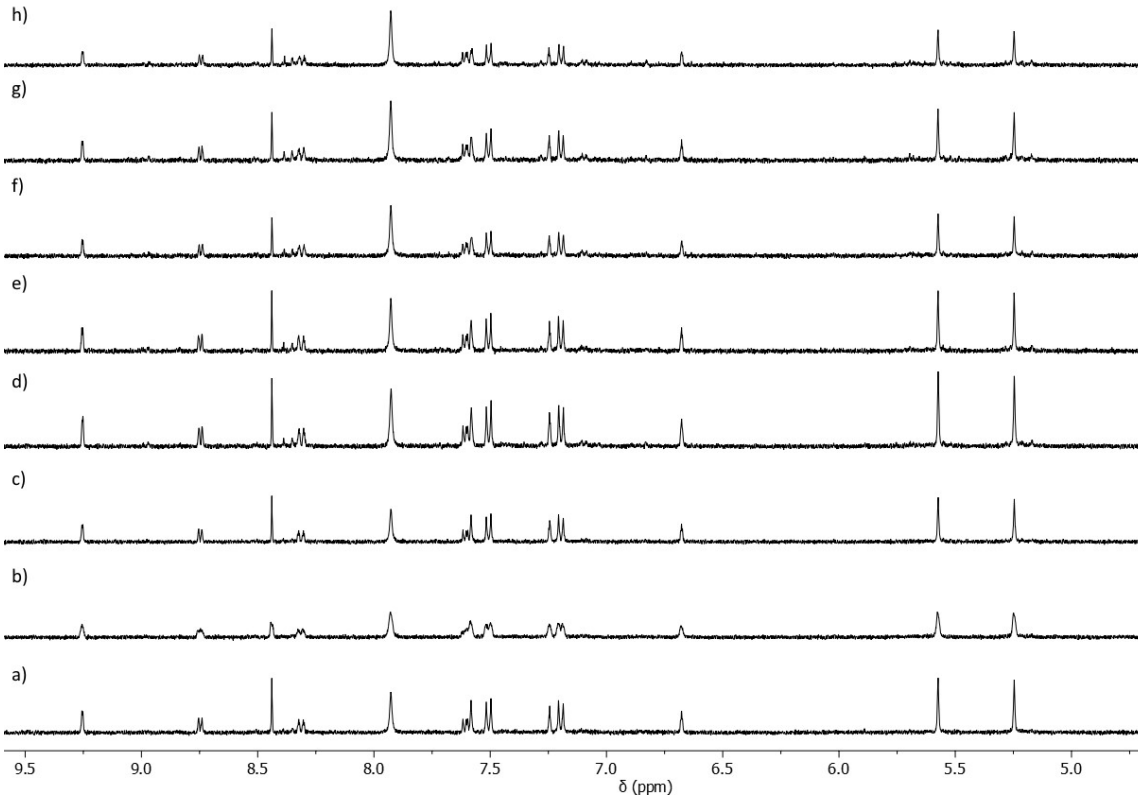

Figure S36 Stacked partial ^{1}H NMR spectra (400 MHz, [D_3]acetonitrile, 298 K) of **C** after a) 2 hours at 75 °C, b) 6 hours at 75 °C, c) 24 hours at 75 °C, d) 30 hours at 75 °C, e) 48 hours at 75 °C, f) 54 hours at 75 °C, g) 72 hours at 75 °C and h) 96 hours at 75 °C. No change in the ^{1}H NMR spectrum of **C** is observed confirming that the cage is robust under these conditions.

Similar experiments were then carried out with a [D_6]DMSO solution of **C** (0.6 mL, 0.870 mM). The [D_6]DMSO solution was initially heated at 50 °C for 96 hours (4 days, Figure S37). Then the temperature was raised to 75 °C and maintained at that level for a further 96 hours (4 days, Figure S38). Finally, the solution was heated to 100 °C and maintained at that level for a further 96 hours (Figure S38) The solution was monitored using ^{1}H NMR spectroscopy (400 MHz, 298 K).

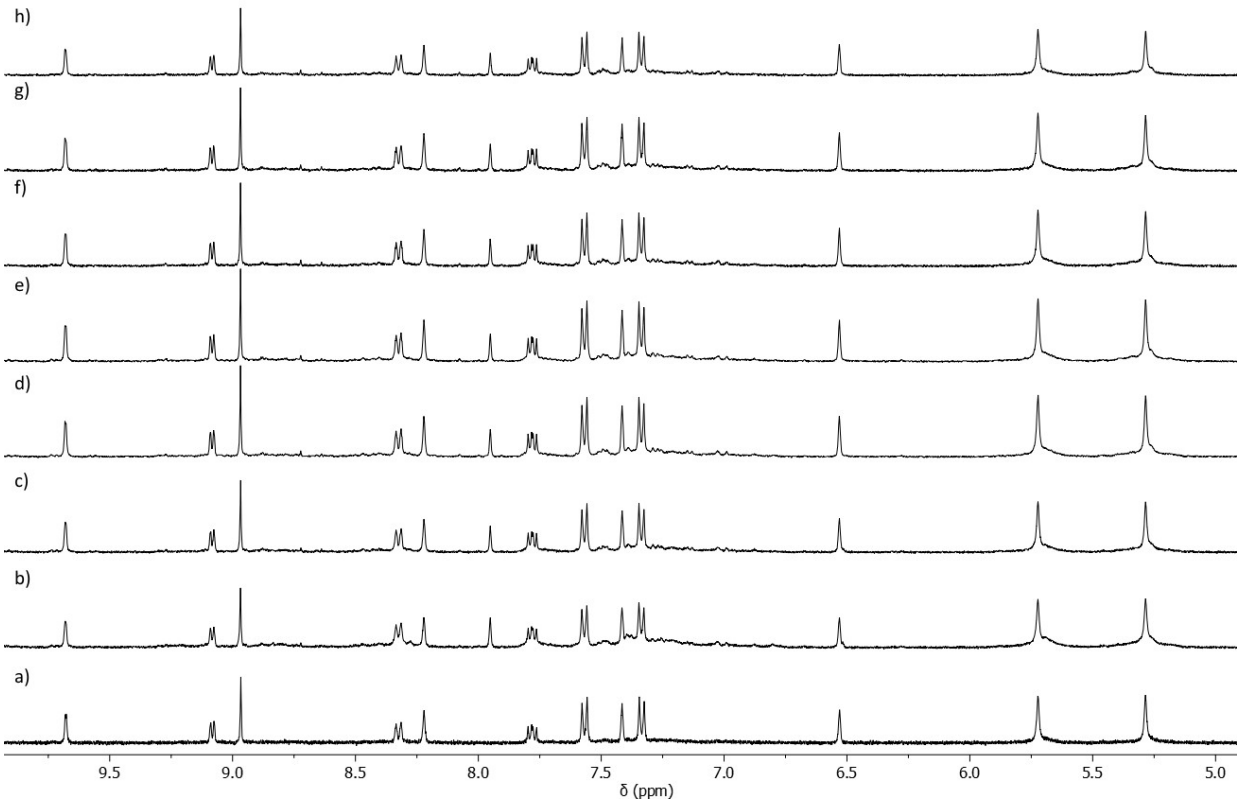

Figure S37 Stacked partial ^{1}H NMR spectra (400 MHz, [D_6]DMSO, 298 K) of **C** a) isolated pure **C**, b) 2 hours at 50 °C, c) 4 hours at 50 °C, d) 22 hours at 50 °C, e) 28 hours at 50 °C, f) 49 hours at 50 °C, g) 73 hours at 50 °C, and h) 96 hours at 50 °C. No change in the ^{1}H NMR spectrum of **C** is observed confirming that the cage is robust under these conditions.

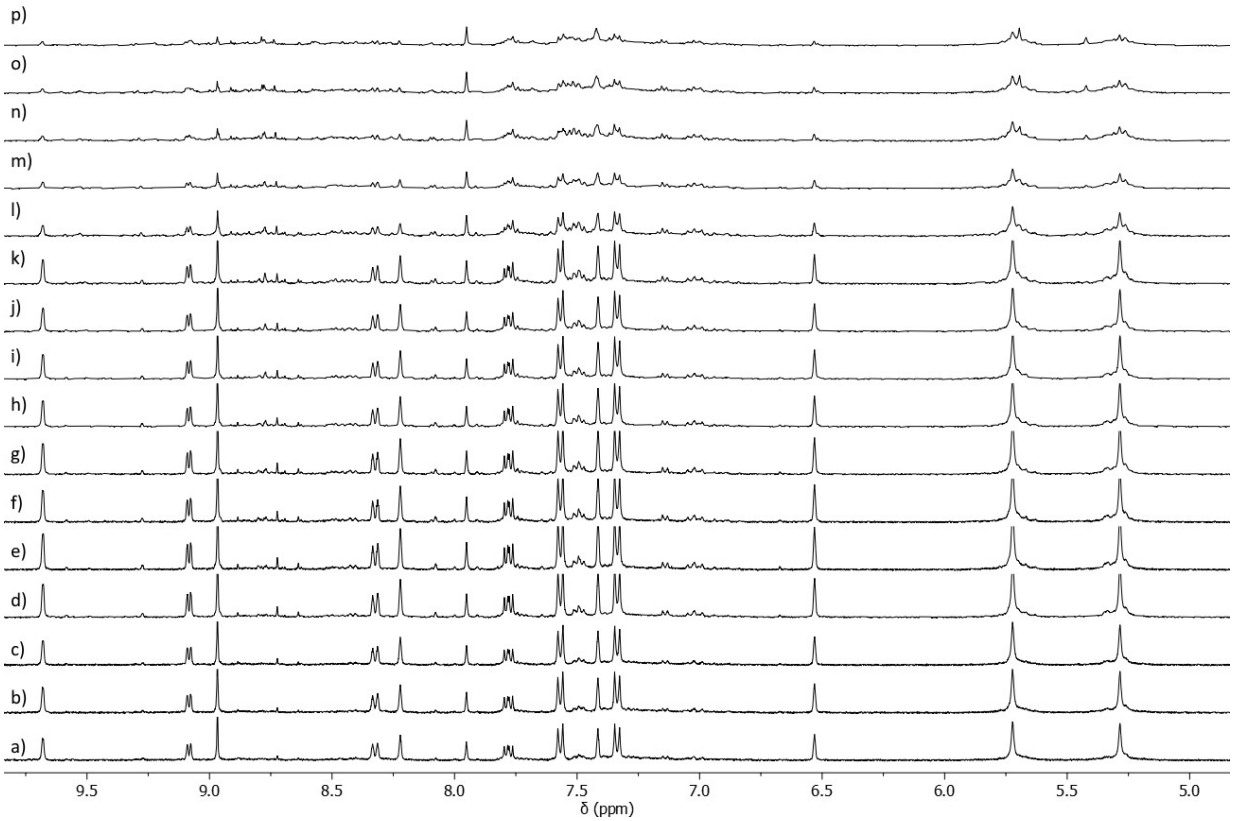

Figure S38 Stacked partial ^{1}H NMR spectra (400 MHz, [D_6]DMSO, 298 K) of **C** a) after 2 hours at 75 °C, b) 6 hours at 75 °C, c) 24 hours at 75 °C, d) 30 hours at 75 °C, e) 48 hours at 75 °C, f) 54 hours at 75 °C, g) 73 hours at 75 °C, h) after 96 hours at 75 °C, i) after 1 hour at 100 °C, j) after 2 hours at 100 °C, k) after 4 hours at 100 °C, i) after 24 hours at 100 °C, m) after 30 hours at 100 °C, n) after 53 hours at 100 °C, n) after 76 hours at 100 °C, and n) after 100 hours at 100 °C. After 4 days at 75 °C some new small peaks are observed indicating that some of the cage **C** has isomerised. However, even after 4 days at 75 °C **C** is the major (>90%) species in solution, indicating that it is reasonably robust under these conditions. Raising the temperature of the solution to 100 °C leads to faster isomerisation. After 24 hours at 100 °C the amount of **C** has reduced by half and several new peaks from other cage isomers are observed. The intensity of the resonances due to **C** continue to decrease and other species grow as the [D_6]DMSO solution is heated at 100 °C. Therefore, **C** is not isomerically robust if it is kept at 100 °C in [D_6]DMSO for an extended period.

7 Host-Guest Chemistry

7.1 ^{19}F NMR Spectroscopy

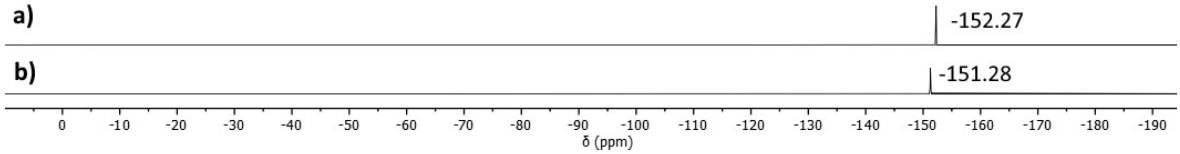

Figure S39 Partial ^{19}F NMR spectra (376 MHz, [D_3]acetonitrile, 298 K) of a) $NaBF_4$ and b) **C** indicating association of the BF_4^- counterion with the cage.

7.2 Host-Guest Models

Before experimental screening of guests, some potential host-guest complexes were modelled with SPARTAN'18[8] using the Merck Molecular Force Field (MMFF).

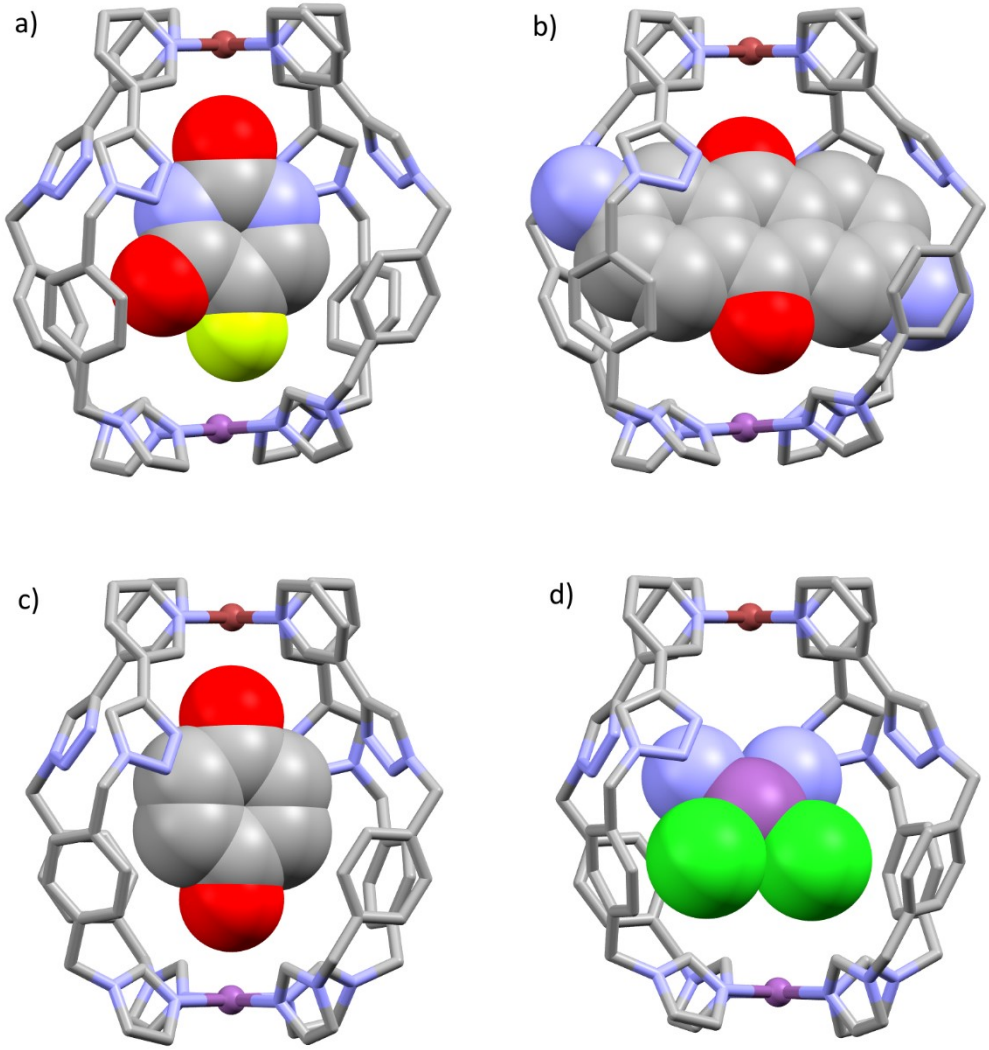

Figure S40 SPARTAN'18 Merck Molecular Force Field (MMFF) models of potential host-guest complexes. a) **C**⊂5-Fluorouracil, b) **C**⊂2,6-Diaminoanthraquinone, c) **C**⊂Benzoquinone, d) **C**⊂Cisplatin. Hydrogen atoms omitted for clarity. Colour scheme: carbon = grey, nitrogen = periwinkle, oxygen = red, palladium = brown, platinum = purple, fluorine = yellow, chloride = green.

7.3 Guest Molecules used in the Screening for Host-Guest Interactions

A variety of molecules were screened for potential guest binding affinity with **C** (Figure S41). In these initial screenings, 2 eq. of solid **G** were added to a solution of **C** (0.60 mL, 1.3 mM) in [D_3]acetonitrile or [D_6]DMSO, and shifts in resonances of protons on the host or guest molecules were examined using ^{1}H NMR spectroscopy (400 MHz, 298 K, Figure S42, Figure S43).

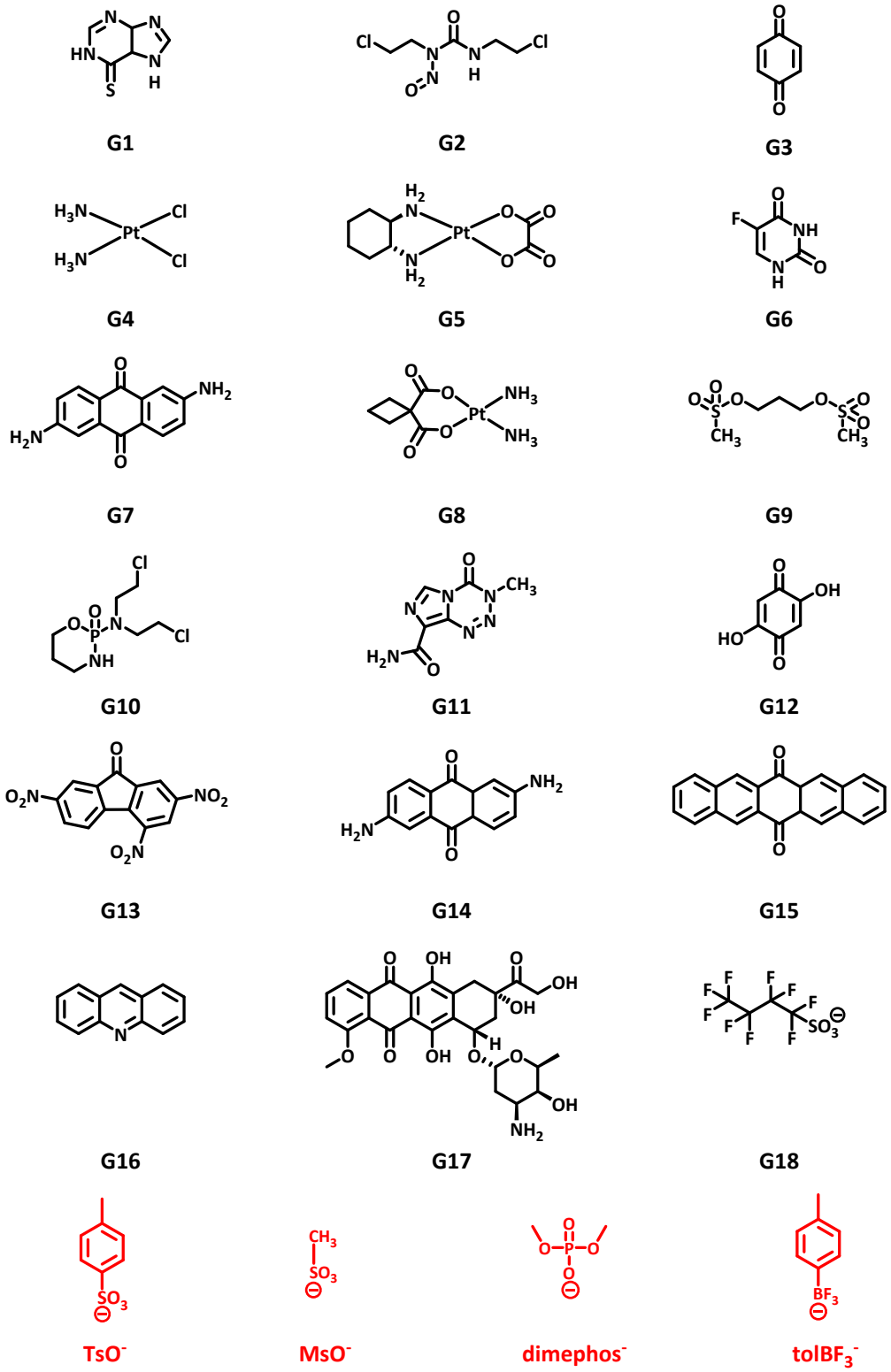

Figure S41 Chemical structures of guests screened. Labels: **G1** = 6-Mercaptopurine, **G2** = Carmustine, **G3** = Benzoquinone, **G4** = Cisplatin, **G5** = Oxaliplatin, **G6** = 5-Fluorouracil, **G7** = 2,6-Diaminoanthraquinone, **G8** =

Carboplatin, **G9** = Busulfan, **G10** = Cyclophosphamide, **G11** = Temozolomide, **G12** = 2,5-Dihydroxy-1,4-benzoquinone, **G13** = 2,4,7-Trinitrofluoren-9-one, **G14** = 2,6-Diaminoanthraquinone, **G15** = 6,13-Pentacenequinone, **G16** = Acridine, **G17** = Doxorubicin, **G18** = Nonafluoro-1-butanesulfonate, **TsO**$^-$ = *p*-Toluenesulfonate, **MsO**$^-$ = Methanesulfonate, **dimephos**$^-$ = dimethylphosphate, **tolBF$_3$**$^-$ = *p*-tolyltrifluoroborate. Guest coloured in red showed affinity for **C**.

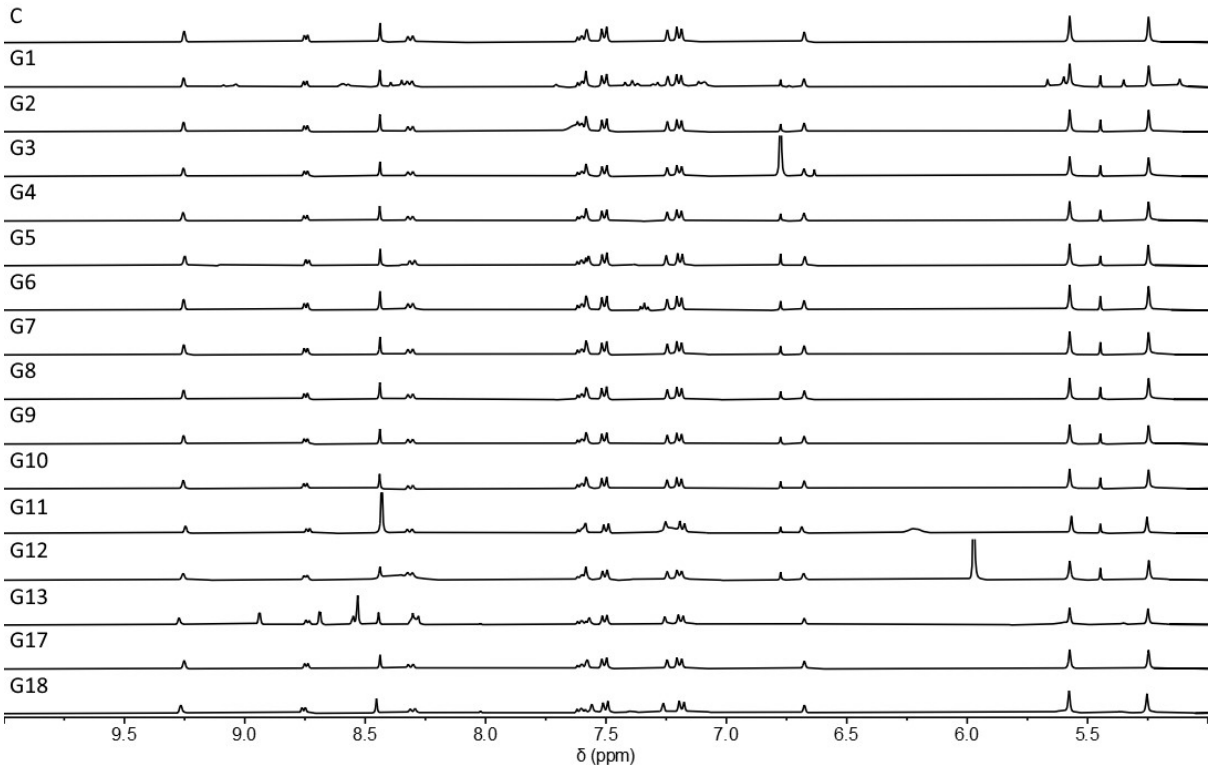

Figure S42 Stacked partial ^{1}H NMR spectra (400 MHz, [D$_3$]acetonitrile, 298 K) of 2 eq. of various guests with **C**.

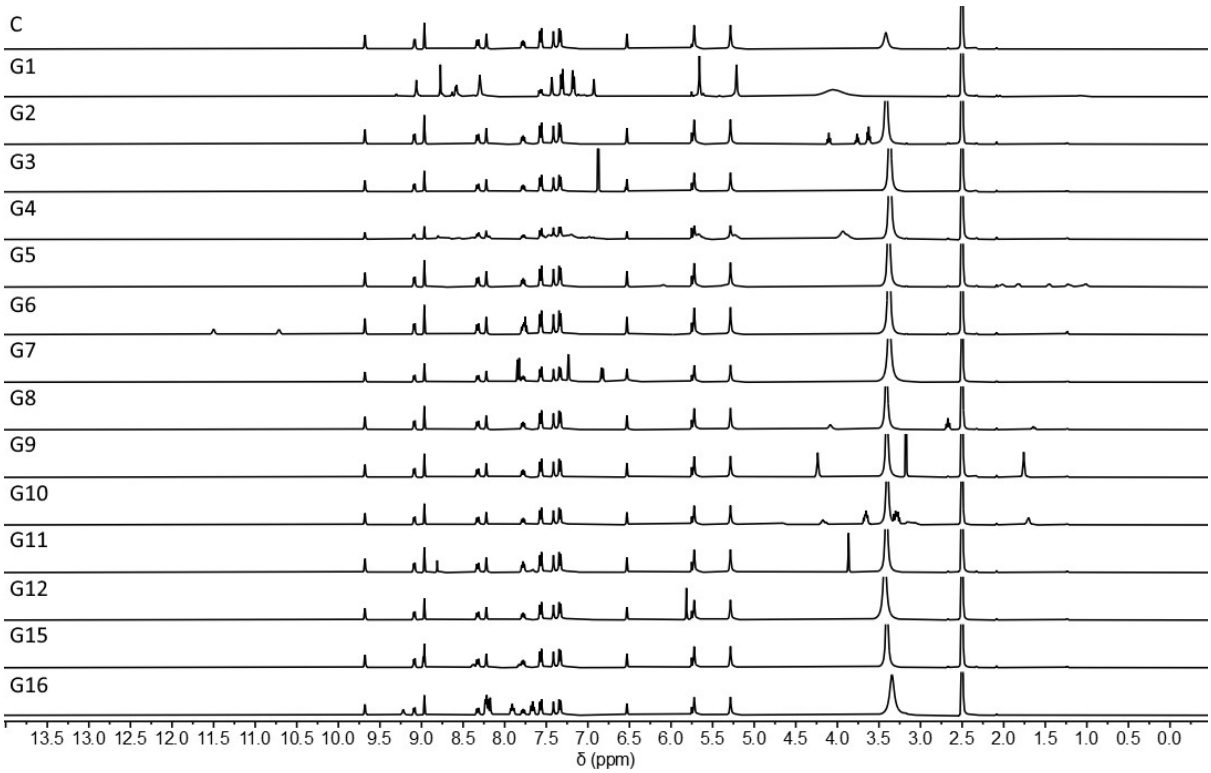

Figure S43 Stacked partial ^{1}H NMR spectra (400 MHz, [D$_6$]DMSO, 298 K) of 2 eq. of various guests with **C**.

The ^{1}H NMR spectrum when screening **G1** in both [D_3]acetonitrile and [D_6]DMSO differed from that of free **C**. This was due to the decomplexation of the Pd(II) ion from **C** and the formation of, presumably, a [Pd(**G1**)$_2$](BF$_4$)$_2$ complex through the chelation of a purine nitrogen and the thiol present in **G1**, and the [Pt(**L**)$_4$](BF$_4$)$_2$ complex (Figure S44).

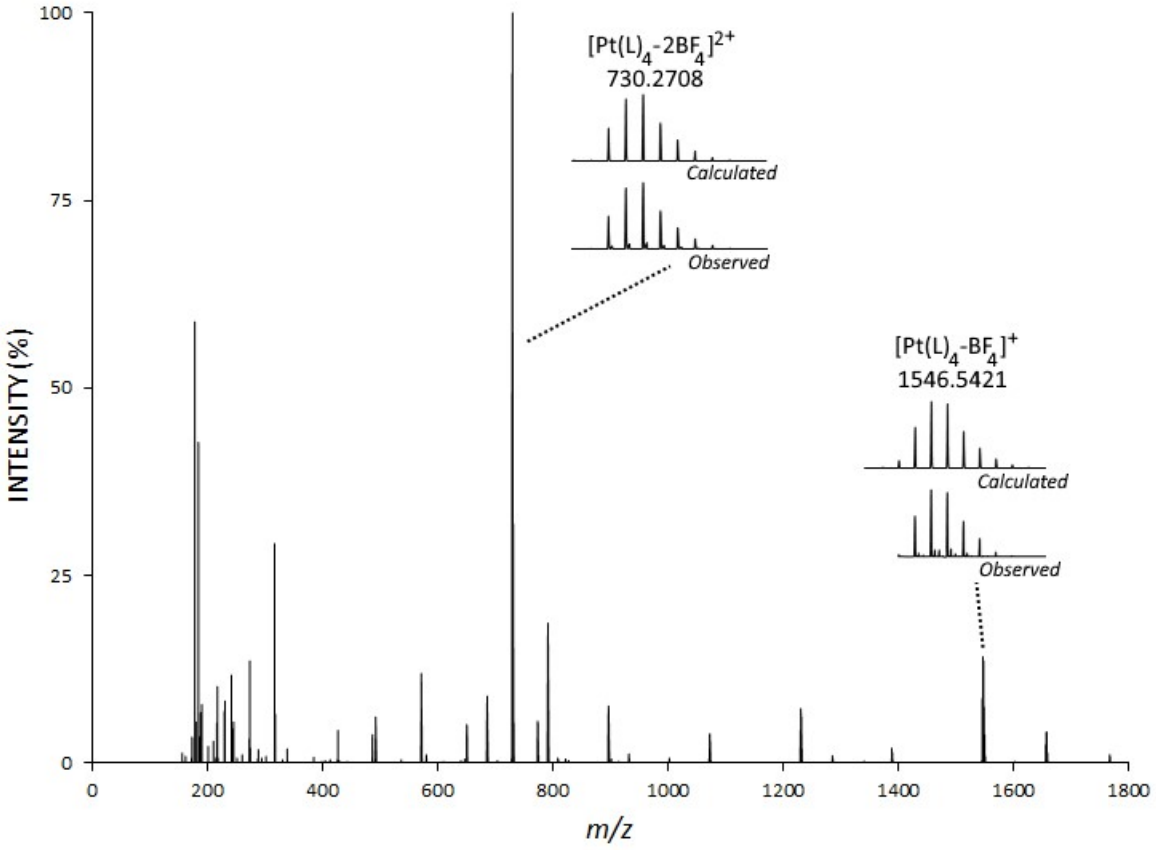

Figure S44 High-resolution electrospray ionisation mass spectrum (CH_3CN) of **C**:**G1** at 1:2 ratio, performed under pseudo-cryospray conditions.

7.4 Titration of Tetrabutylammonium *p*-Toluenesulfonate with C in CD_3CN

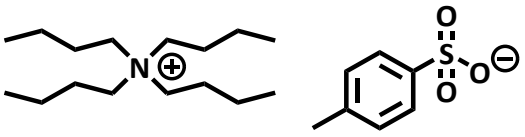

Tetrabutylammonium *p*-toluenesulfonate (**TsO**$^-$)

Guest binding studies were carried out in [D_3]acetonitrile, using a tetrakis(trimethylsilyl)silane internal standard. A stock solution of **C** (1.00 mL, 0.5 mM) in [D_3]acetonitrile was prepared. Half of the **C** stock solution (0.50 mL, 0.5 mM) was added to solid [NBu_4]$^+$(**TsO**$^-$) (0.731 µmol) giving a theoretical 1:5 host-guest stock solution. Then, varying amounts of the host-guest stock solution (either 10, 20 or 50 µL) were titrated into the **C** stock solution (0.50 mL, 0.5 mM) to give a series of different host-guest stoichiometries (0.21 – 9.45 equivalents) that were examined using ^{1}H NMR spectroscopy (500 MHz, 298 K, Figure S46 and Figure S47). Resonances attributable to [Pt(**L**)$_4$](BF$_4$)$_2$ were seen growing in size during the titration. Due

to this observation, the concentration of the host and guest species was then calculated from a known amount of the tetrakis(trimethylsilyl)silane (0.037 μmol, 0.25 eq.) internal standard that was used in the titration experiment, and integration of this standard signal relative to host and guest signals. Data was processed using Microsoft Excel 2016. Association constants were obtained by analysis of the resulting titration using a 1:1 host:guest stoichiometry with Bindfit (supramolecular.org).[9] An average of three binding constants was calculated to give K_a = 17200 ± 1600.

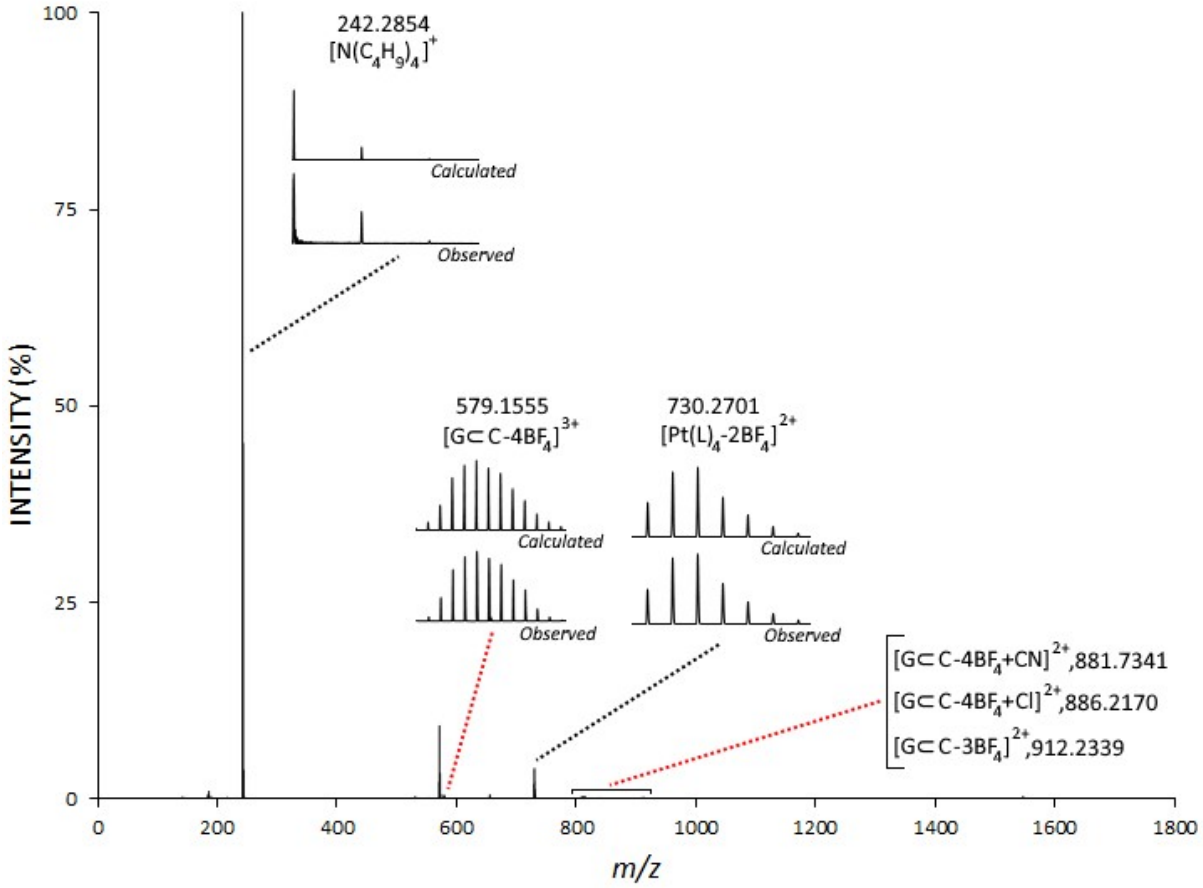

Figure S45 High-resolution electrospray ionisation mass spectrum (CH_3CN) of **C⊂TsO**$^-$ at 1:1 ratio, performed under cryospray conditions. G = **TsO**$^-$.

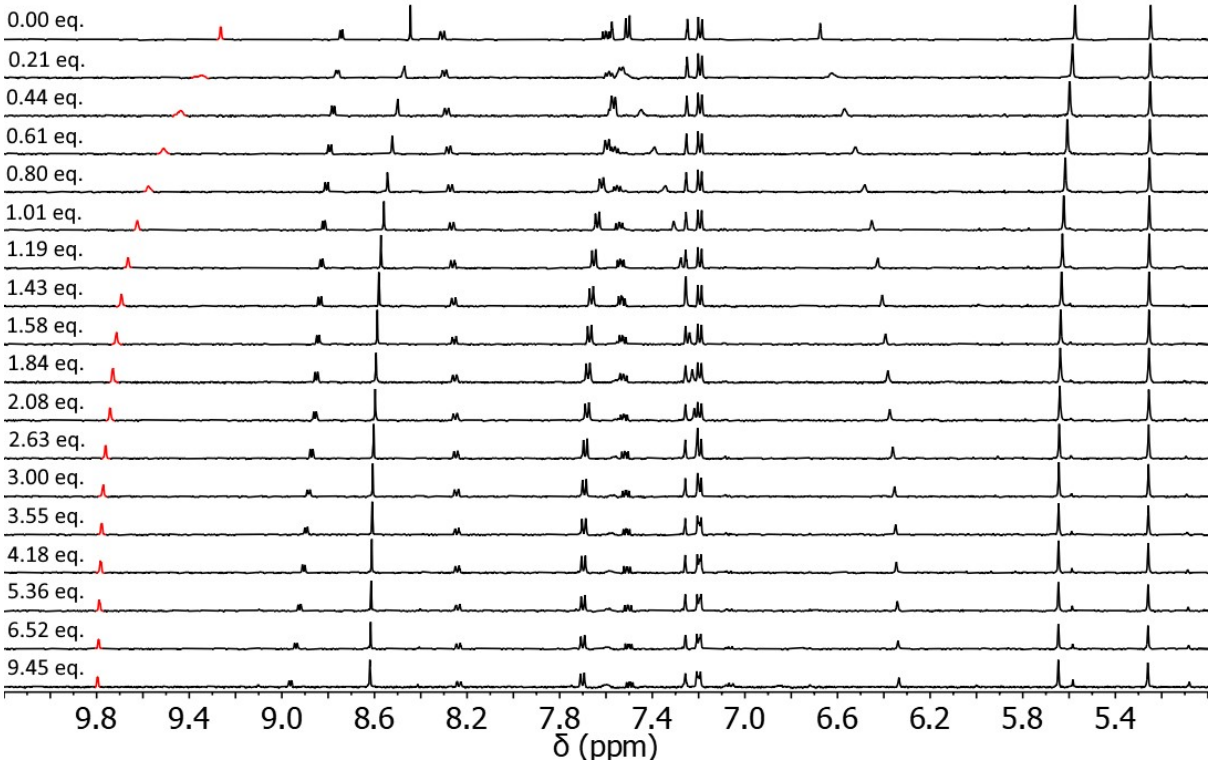

Figure S46 Stacked partial ^{1}H NMR spectra (500 MHz, [D_3]acetonitrile, 298 K) of the titration of tetrabutylammonium *p*-toluenesulfonate (**TsO**$^{-}$) into **C**. Red peaks correspond to resonances of the *ortho* pyridyl proton.

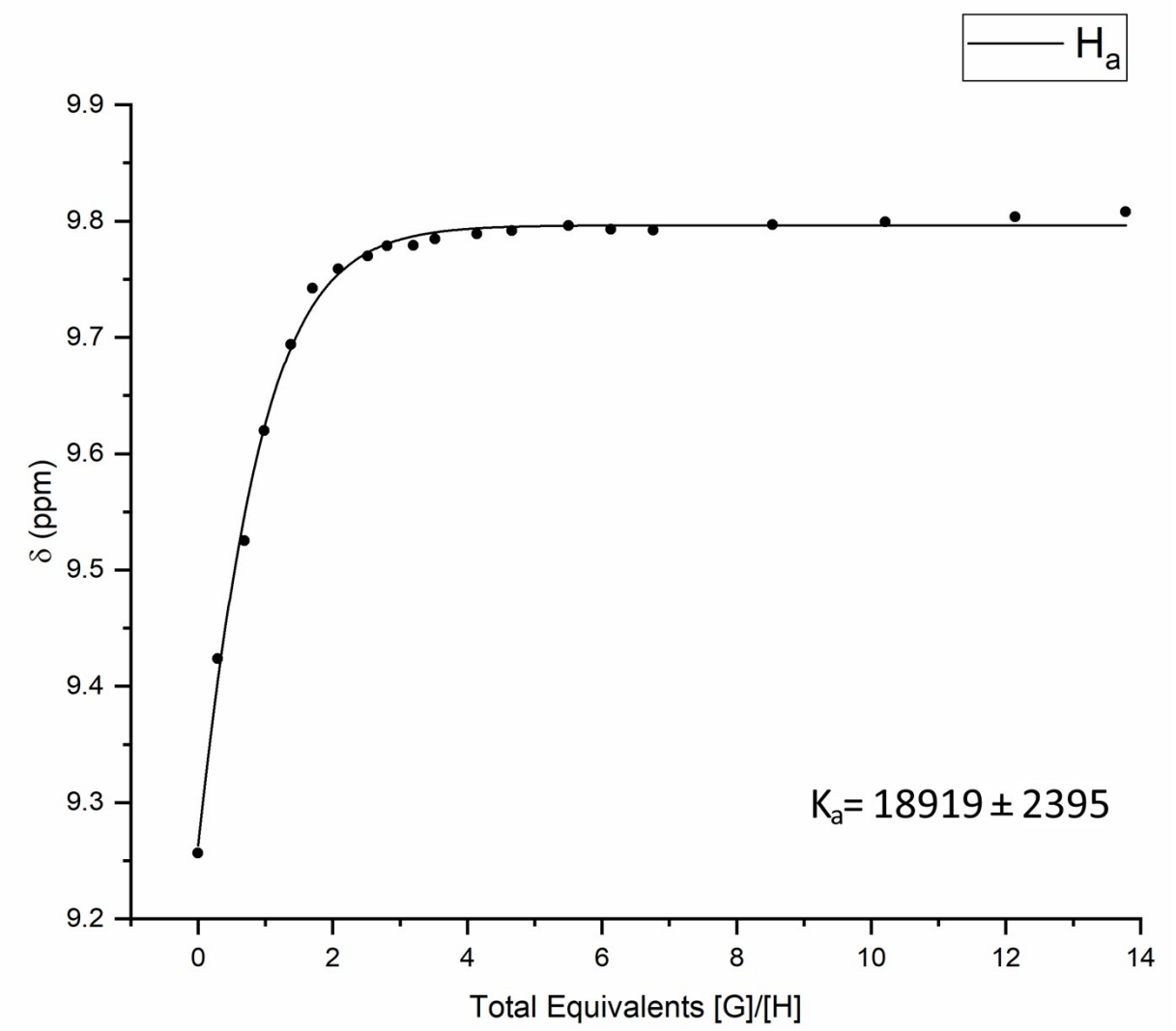

Figure S47 ^{1}H NMR (500 MHz, [D_3]acetonitrile, 298 K) titration curve of **C** with tetrabutylammonium *p*-toluenesulfonate (**TsO**$^-$). Curve monitored by the shift of proton signal H_a. Data shown is from one of the three titrations used to generate the average binding constant.

7.4.1 Variable-temperature ^{1}H NMR spectroscopy of Tetrabutylammonium *p*-Toluenesulfonate with C in CD_3CN

Variable-temperature ^{1}H NMR spectroscopy experiments were conducted on an [D_3]acetonitrile solution containing **C**:**TsO**$^-$ in a 1:0.19 ratio.^{1}H NMR spectroscopy (500 MHz, Variable, Figure S48) was then performed at 298 K (Figure S48a), 323 K (Figure S48b) and 343 K (Figure S48c).

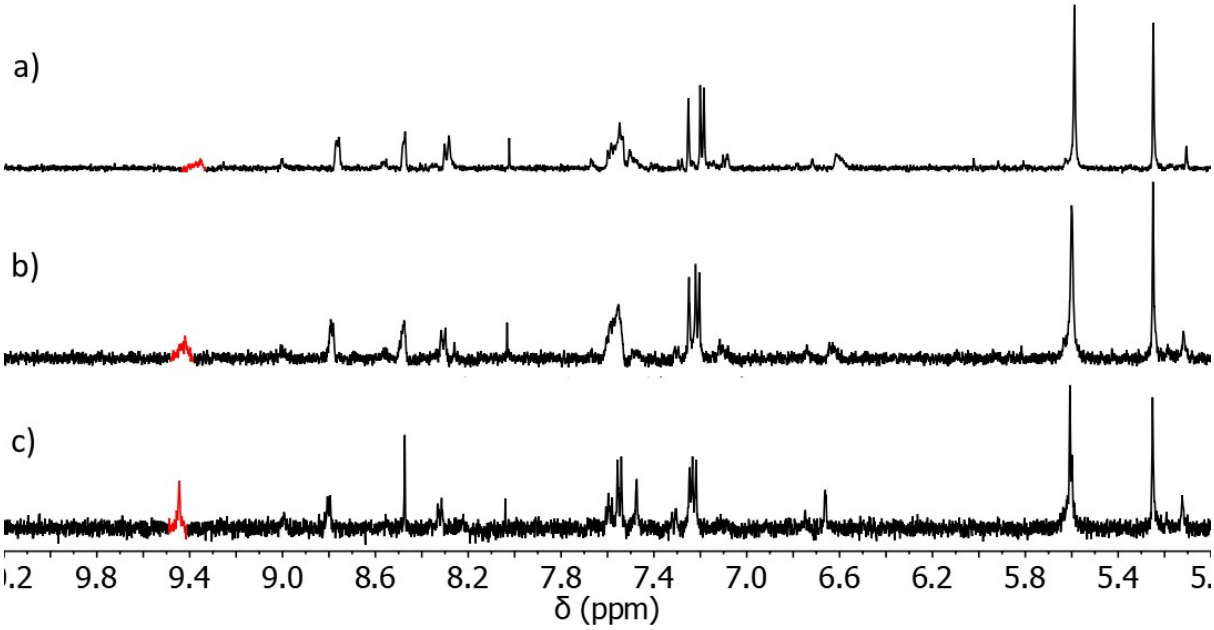

Figure S48 Stacked partial variable-temperature ^{1}H NMR spectra (500 MHz, [D_3]acetonitrile) of **C⊂TsO**$^-$ at a 1:1 ratio. A) ^{1}H NMR spectrum obtained at 298 K, b) ^{1}H NMR spectrum obtained at 323 K, c) ^{1}H NMR spectrum obtained at 343 K. Samples equilibrated at temperature for 5 minutes prior to obtaining ^{1}H NMR spectrum.

7.5 Titration of Tetrabutylammonium Methanesulfonate with C in CD_3CN

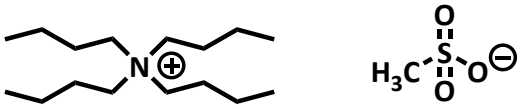

Tetrabutylammonium methanesulfonate (**MsO**$^-$)

Guest binding studies were carried out in [D_3]acetonitrile, using a tetrakis(trimethylsilyl)silane standard. A stock solution of **C** (1.00 mL, 0.5 mM) in [D_3]acetonitrile was prepared. Half of the **C** stock solution (0.50 mL, 0.5 mM) was added to solid $[NBu_4]^+$(**MsO**$^-$) (0.731 µmol) giving a theoretical 1:5 host-guest stock solution. Then, varying amounts of the host-guest stock solution (either 10, 20 or 50 µL) were titrated into the **C** stock solution (0.50 mL, 0.5 mM) to give a series of different host-guest stoichiometries (0.23 – 5.92 equivalents) that were examined using ^{1}H NMR spectroscopy (500 MHz, 298 K, Figure S50, Figure S51). Using this procedure the concentration of **C** was kept at 0.5 mM through the duration of the titration. Data was processed using Microsoft Excel 2016. Association constants were obtained by analysis of the resulting titration using a 1:1 host:guest stoichiometry with Bindfit (supramolecular.org).[9] An average of three binding constants was calculated to give K_a = 29400 ± 2700.

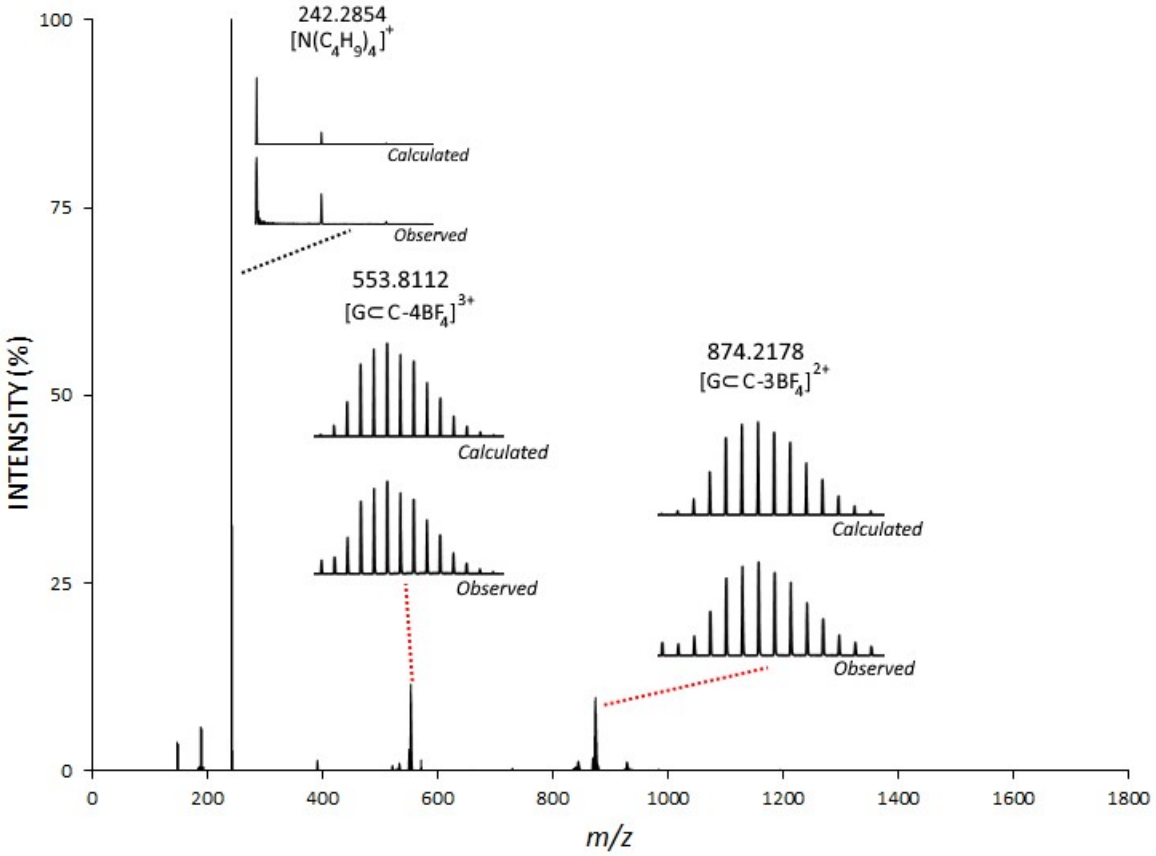

Figure S49 High-resolution electrospray ionisation mass spectrum (CH_3CN) of **C**⊂**MsO**$^-$ at 1:1 ratio, performed under cryospray conditions. G = **MsO**$^-$.

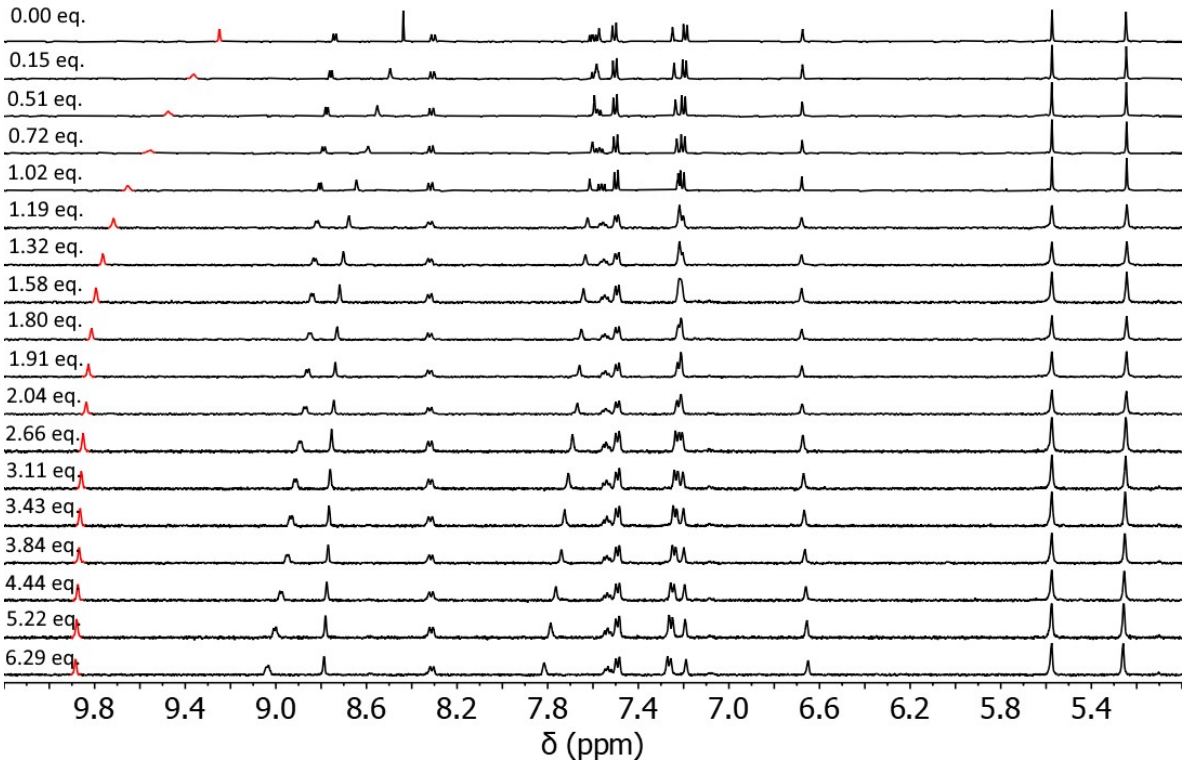

Figure S50 Stacked partial ^{1}H NMR spectra (500 MHz, [D_3]acetonitrile, 298 K) of the titration of tetrabutylammonium methanesulfonate (**MsO**$^{-}$) into **C**. Red peaks correspond to resonances of the *ortho* pyridyl proton.

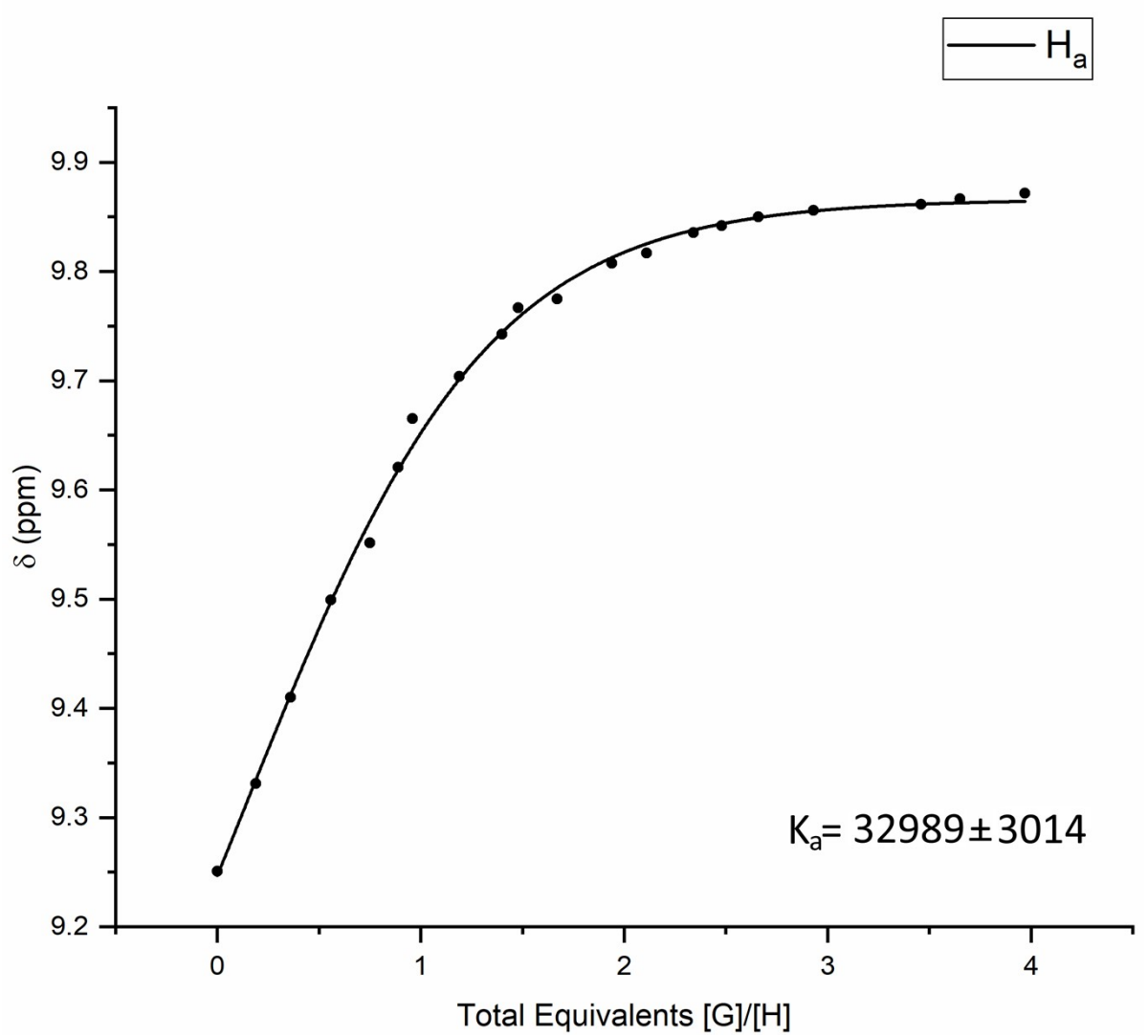

Figure S51 ^{1}H NMR (500 MHz, [D_3]acetonitrile, 298 K) titration curve of **C** with tetrabutylammonium methanesulfonate (**MsO**$^-$). Curve monitored by the shift of proton signal H_a. Data shown is from one of the three titrations used to generate the average binding constant.

7.5.1 Variable-temperature ^{1}H NMR spectroscopy of Tetrabutylammonium methanesulfonate with C in CD_3CN

Variable-temperature ^{1}H NMR spectroscopy experiments were conducted on an [D_3]acetonitrile solution containing **C**:**MsO**$^-$ in a 1:0.23 ratio. ^{1}H NMR spectroscopy (500 MHz, Variable, Figure S52) was performed at 298 K (Figure S52a), 323 K (Figure S52b) and 343 K (Figure S52c).

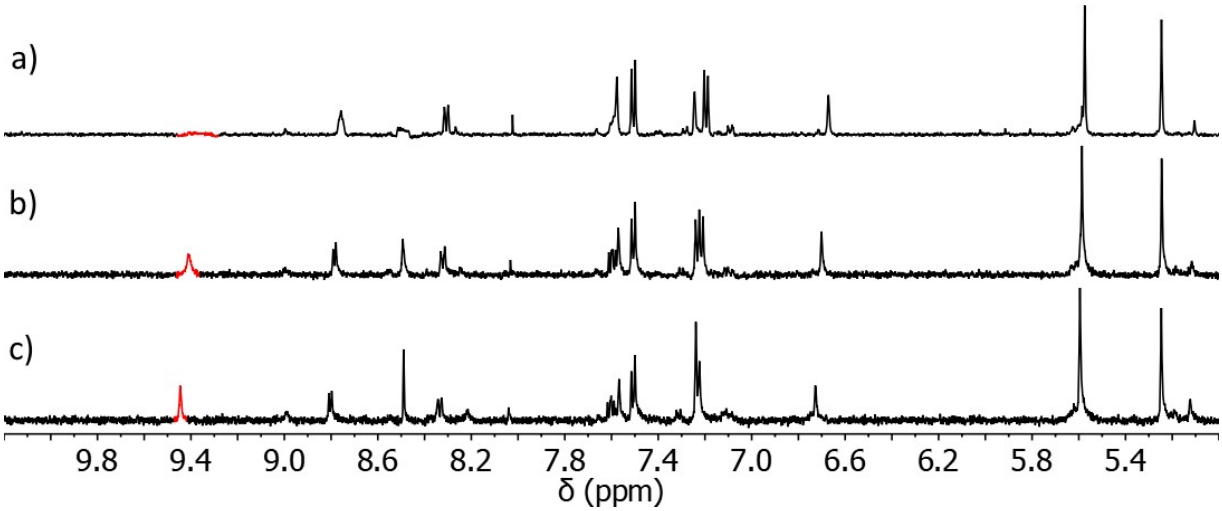

Figure S52 Stacked partial variable-temperature ^{1}H NMR spectra (500 MHz, [D_3]acetonitrile) of **C⊂MsO**$^-$ at a 1:0.23 ratio. A) ^{1}H NMR spectrum obtained at 298 K, b) ^{1}H NMR spectrum obtained at 323 K, c) ^{1}H NMR spectrum obtained at 343 K. Samples equilibrated at temperature for 5 minutes prior to obtaining ^{1}H NMR spectrum.

7.6 Molecular Structure of the C⊂MsO$^-$ Host-Guest Adduct

CCDC #2175044 Vapour diffusion of diethyl ether into a concentrated CH_3CN solution of **C⊂MsO**$^-$ at 277 K resulted in the formation of a colourless, plate-like crystal of **C⊂MsO**$^-$. X-ray data were collected at 100 K on an Agilent Technologies Supernova system using Cu Kα radiation with exposures over 1.0˚, and data were treated using CrysAlisPro software.[5] The structure was solved using SHELXT and weighted full-matrix refinement on F^2 was carried out using SHELXL-97,[6] both running within the OLEX2-v1.2.9 package.[7] All non-hydrogen atoms were refined anisotropically. Hydrogen atoms attached to carbon atoms were placed in calculated positions and refined using a riding model. The structure was solved in the triclinic space group $P\bar{1}$ and refined to an R_1 value of 7.25%. The asymmetric unit contains one heterometallic type cage containing four ligands **L**, one platinum(II) and one palladium(II) ion, two BF_4 counterions, three CH_3CN solvent molecules, and one **MsO**$^-$ anion. The structure contained disorder at a select few fluorine atoms in the two BF_4^- counteranions, this was addressed by using the PART command and assigning the correct chemical occupancy. The oxygen atoms on the encapsulated **MsO**$^-$ guest ion were also disordered, a chemical occupancy of ¾ was assigned to these atoms to account for this and the ISOR and SIMU commands deployed to model these atoms. The ISOR command was used on a carbon atom in one of the pyridine rings to account for disorder (C01C). The DFIX command was used to properly model the sulfur-oxygen bond of a rotationally disordered oxygen atom (O6 – S01Q, 1.7 Å), and the DANG command was used to correct the C-S-O angles of the **MsO**$^-$ guest ion. A solvent mask (with the OLEX2-v1.2.9 package) was applied to resolve diffuse electron density, where a void consisting of 122 electrons was measured in the asymmetric unit, this was attributed to two tetrafluoroborate (BF_4^-) anions and two molecules of acetonitrile (Figure S53).

CheckCIF gives 3 B level alerts. Two are a result of residual density observed around the palladium(II) atom, deemed to be due to Fourier ripples caused by using copper X-ray source with the heavy atoms present in the structure. One is due to two reflections with (Iobs-Icalc)/Sigma(W) > 10. As this only pertained to two reflections these were not omitted.

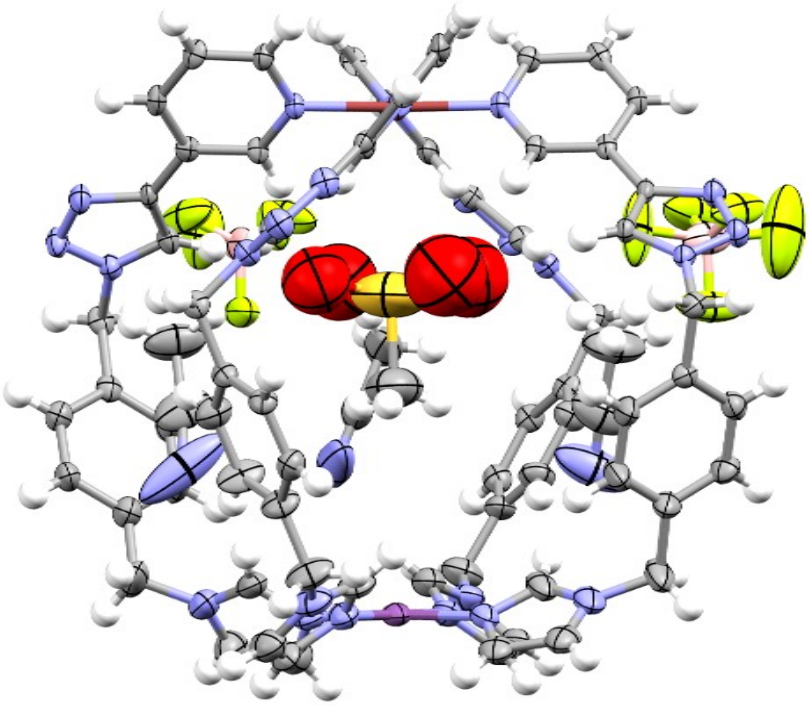

Figure S53 Mercury ellipsoid plot of the **C⊂MsO**$^{-}$ host-guest adduct. Ellipsoids are shown at the 50% probability level. Colour scheme: boron = salmon, sulphur = gold, carbon = grey, fluorine = yellow, hydrogen = white, nitrogen = periwinkle, oxygen = red, palladium = brown, platinum = purple.

Table S4 Crystal data and structure refinement table for **C⊂MsO**$^-$.

	C⊂MsO$^-$
CCDC#	2175044
Empirical formula	$C_{83}H_{82}B_4F_{16}N_{29}O_3PdPtS$
Formula weight	2214.60
Temperature/K	100.01(10)
Crystal system	triclinic
Space group	P-1
a/Å	13.8621(2)
b/Å	14.0385(3)
c/Å	27.2264(6)
α/°	79.615(2)
β/°	75.366(2)
γ/°	89.377(2)
Volume/Å^3	5039.14(18)
Z	2
ρ_{calc}g/cm^3	1.460
μ/mm^{-1}	4.967
F(000)	2223.3
Crystal size/mm^3	0.169 × 0.114 × 0.098
Radiation	CuKα (λ = 1.54184)
2Θ range for data collection/°	7.792 to 153.152
Index ranges	-17 ≤ h ≤ 16, -17 ≤ k ≤ 17, -34 ≤ l ≤ 34
Reflections collected	55561
Independent reflections	20488 [R_{int} = 0.0423, R_{sigma} = 0.0396]
Data/restraints/parameters	20488/35/1130
Goodness-of-fit on F^2	1.029
Final R indexes [I>=2σ (I)]	R_1 = 0.0710, wR_2 = 0.1775
Final R indexes [all data]	R_1 = 0.0787, wR_2 = 0.1804
Largest diff. peak/hole / e Å^{-3}	2.88/-2.10

7.7 Titration of 1,3-Dimethylimidazolium Dimethylphosphate with C in CD_3CN

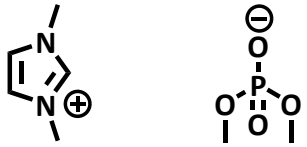

1,3-Dimethylimidazolium Dimethylphosphate (**dimephos**$^-$)

Guest binding studies were carried out in [D_3]acetonitrile, using a tetrakis(trimethylsilyl)silane standard. A stock solution of **C** (1.00 mL, 0.5 mM) in [D_3]acetonitrile was prepared. Half of the **C** stock solution (0.50 mL, 0.5 mM) was added to solid [Im(Me)$_2$]$^+$(**dimephos**$^-$) (3.65 μmol) giving a theoretical 1:25 host-guest stock solution. Then, varying amounts of the host-guest stock solution (either 5, 10, 20 or 40 μL) were titrated into the **C** stock solution (0.50 mL, 0.5 mM) to give a series of different host-guest stoichiometries (0.11 – 42.0 equivalents) that were examined using ^{1}H NMR spectroscopy (500 MHz, 298 K, Figure S54, Figure S55). Resonances attributable to [Pt(**L**)$_4$](BF$_4$)$_2$ were seen growing in size during the titration. Due to this observation, the concentration of the host and guest species was then calculated from

a known amount of the tetrakis(trimethylsilyl)silane (0.037 μmol, 0.25 eq.) internal standard that was used in the titration experiment, and integration of this standard signal relative to host and guest signals. Data was processed using Microsoft Excel 2016. Association constants were obtained by analysis of the resulting titration using a 1:2 host:guest stoichiometry with Bindfit (supramolecular.org).[9] Binding constants were calculated to give K_1 = 5870 ± 320 and K_2 = 1540 ± 70.

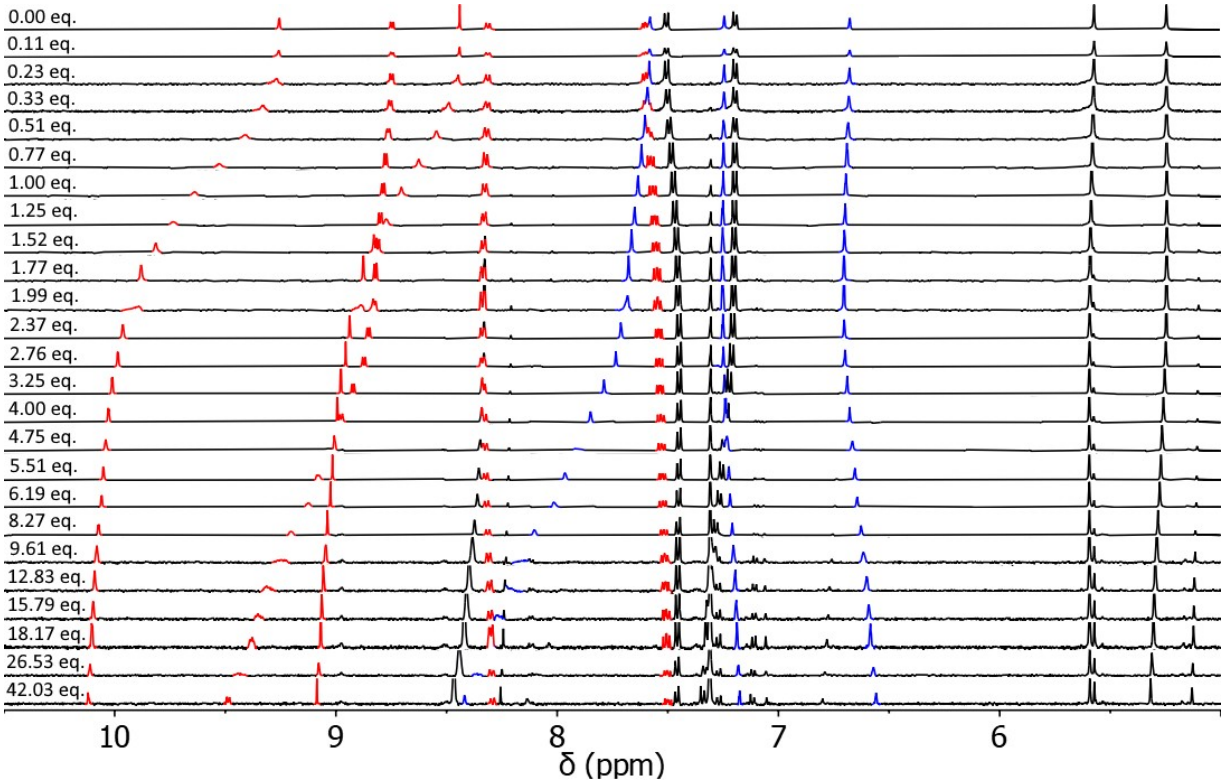

Figure S54 Stacked partial ^{1}H NMR spectra (500 MHz, [D_3]acetonitrile, 298 K) of the titration of 1,3-dimethylimidazolium dimethylphosphate (**dimephos**$^-$) into **C**. Red peaks correspond to resonances of the pyridyl and triazole protons, while blue peaks correspond to resonances of the imidazole protons. At high equivalents of guest (~10 eq.) we observe formation of the $[Pt(\mathbf{L})_4]^{2+}$ complex which we attribute to decomposition caused by the $[Im(Me)_2]^+$ countercation.

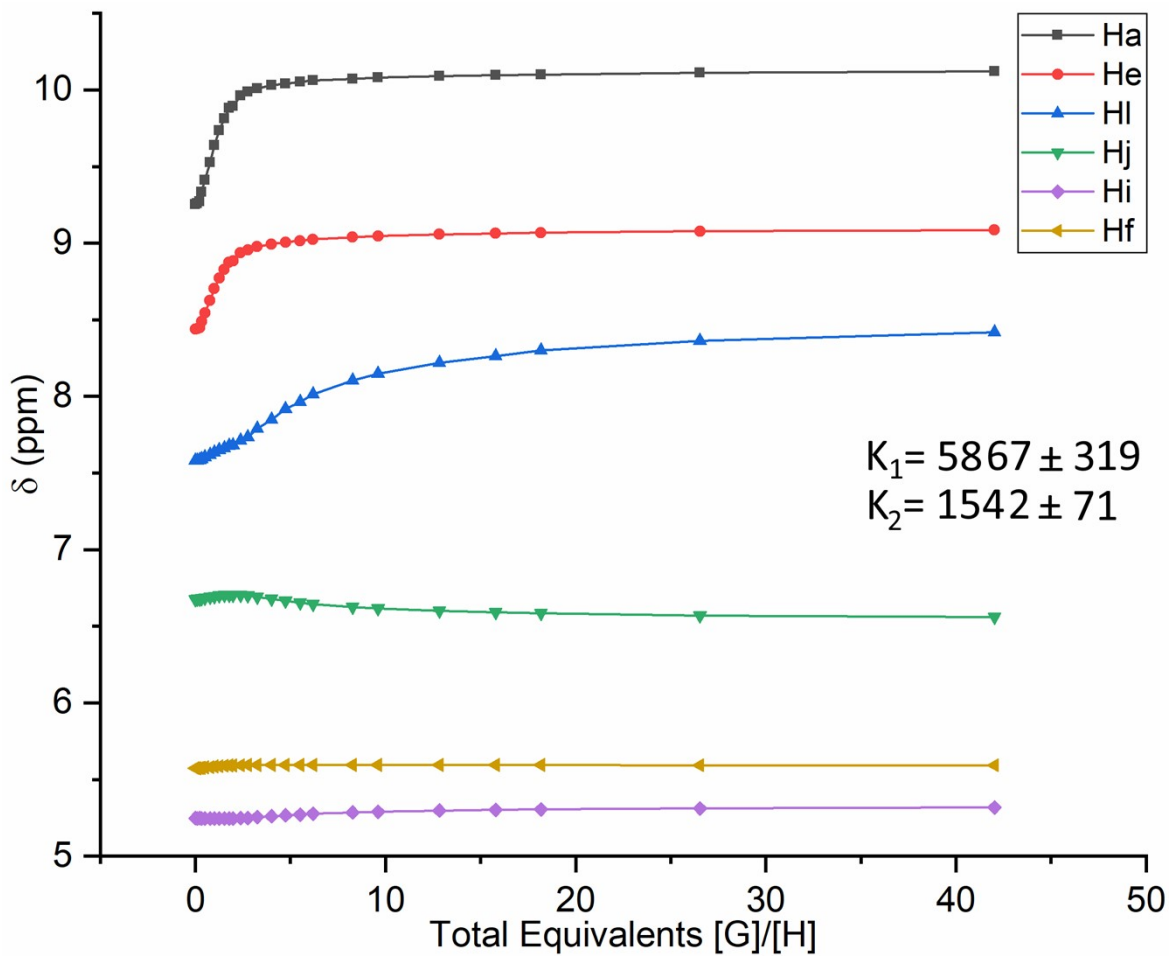

Figure S55 ^{1}H NMR (500 MHz, [D_3]acetonitrile, 298 K) titration curve of **C** with dimethylphosphate (**dimephos**$^{-}$). Curve monitored by the shift of multiple different proton signals.

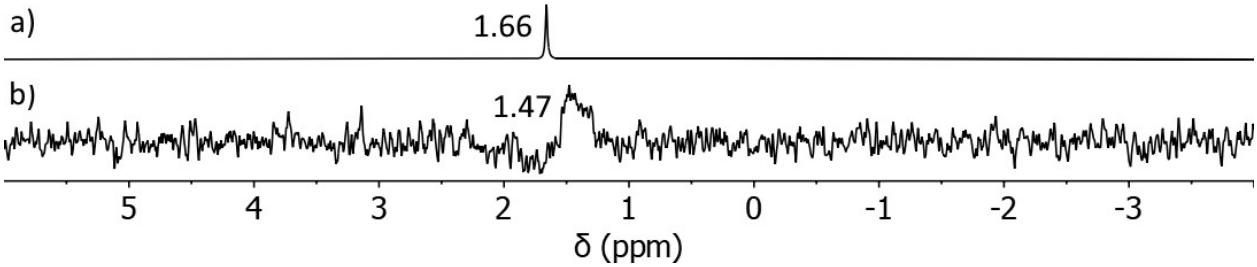

Figure S56 Partial ^{31}P NMR spectra (162 MHz, [D_3]acetonitrile, 298 K) of a) free **dimephos**$^{-}$, b) **C** + 8 eq. **dimephos**$^{-}$.

7.8 MMFF Model of 1:2 Host:Guest Complex with Dimethylphosphate

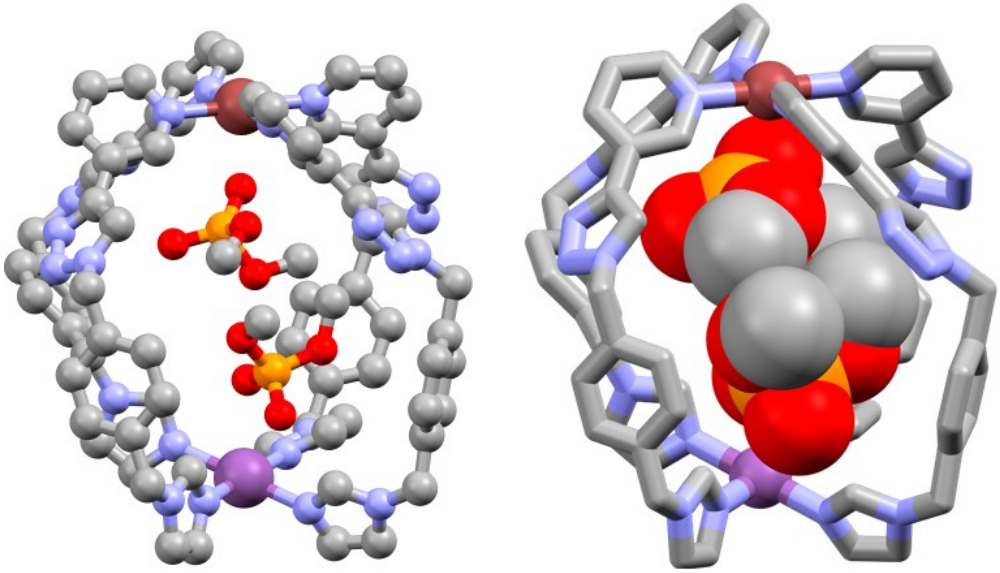

Figure S57 SPARTAN'18 Merck Molecular Force Field (MMFF) models of potential 1:2 host:guest complex shown all in ball and stick (left), and cage in capped stick with the guests in spacefill (right). Hydrogen atoms omitted for clarity. Colour scheme: carbon = grey, nitrogen = periwinkle, oxygen = red, palladium = brown, platinum = purple, phosphorus = gold.

7.9 Titration of Potassium *p*-Tolyltrifluoroborate with C in CD_3CN

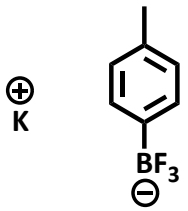

Potassium *p*-tolyltrifluoroborate (**tolBF$_3^-$**)

Guest binding studies were carried out in [D_3]acetonitrile, using a tetrakis(trimethylsilyl)silane standard. A stock solution of **C** (1.00 mL, 0.5 mM) in [D_3]acetonitrile was prepared. Half of the **C** stock solution (0.50 mL, 0.5 mM) was added to solid K^+(**tolBF$_3^-$**) (1.462 µmol) giving a theoretical 1:10 host-guest stock solution. Then, varying amounts of the host-guest stock solution (either 10, 20 or 50 µL) were titrated into the **C** stock solution (0.50 mL, 0.5 mM) to give a series of different host-guest stoichiometries (0.12 – 10.5 equivalents) that were examined using ^{1}H NMR spectroscopy (500 MHz, 298 K, Figure S58, Figure S59). Using this procedure, the concentration of **C** was maintained at 0.5 mM throughout the titration experiment. Data was processed using Microsoft Excel 2016. Association constants were obtained by analysis of the resulting titration using a 1:1 host:guest stoichiometry with Bindfit (supramolecular.org).[9] An average of three binding constants was calculated to give K_a = 2190 ± 40.

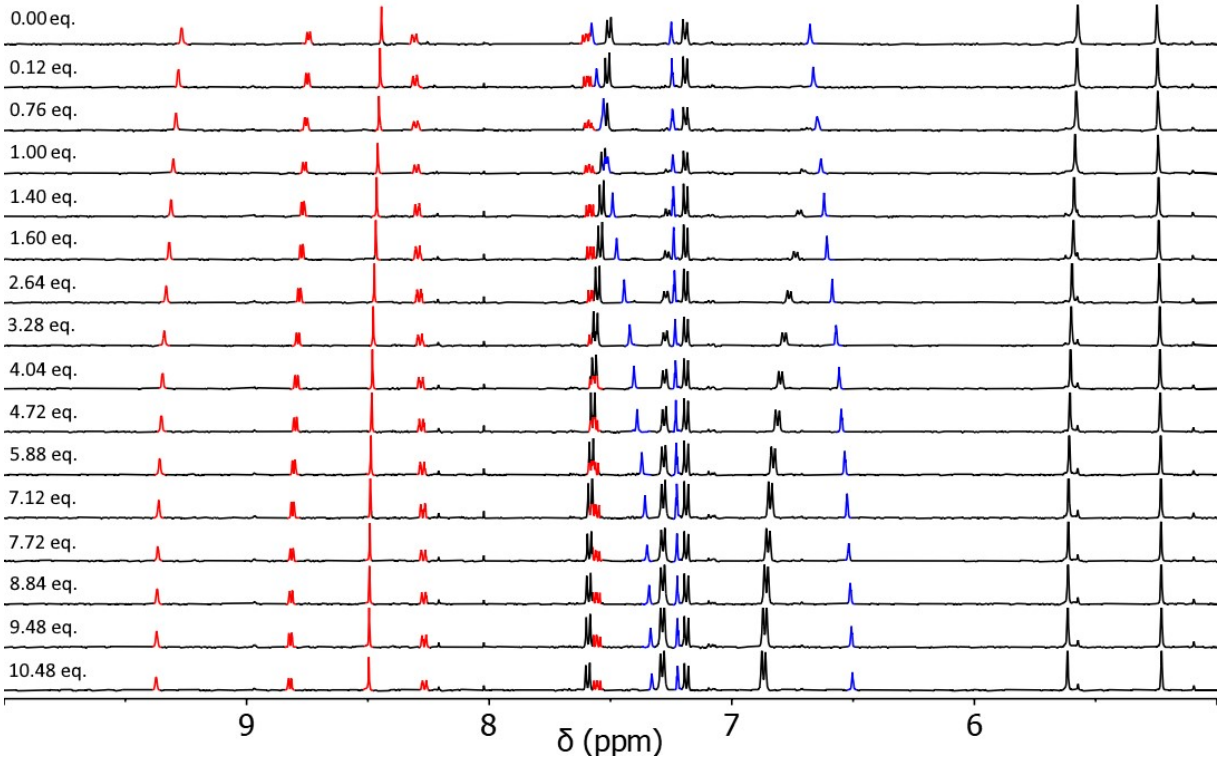

Figure S58 Stacked partial ^{1}H NMR spectra (500 MHz, [D_3]acetonitrile, 298 K) of the titration of potassium *p*-tolyltrifluoroborate (**tolBF$_3^-$**) into **C**. Red peaks correspond to resonances of the pyridyl and triazole protons, while blue peaks correspond to resonances of the imidazole protons.

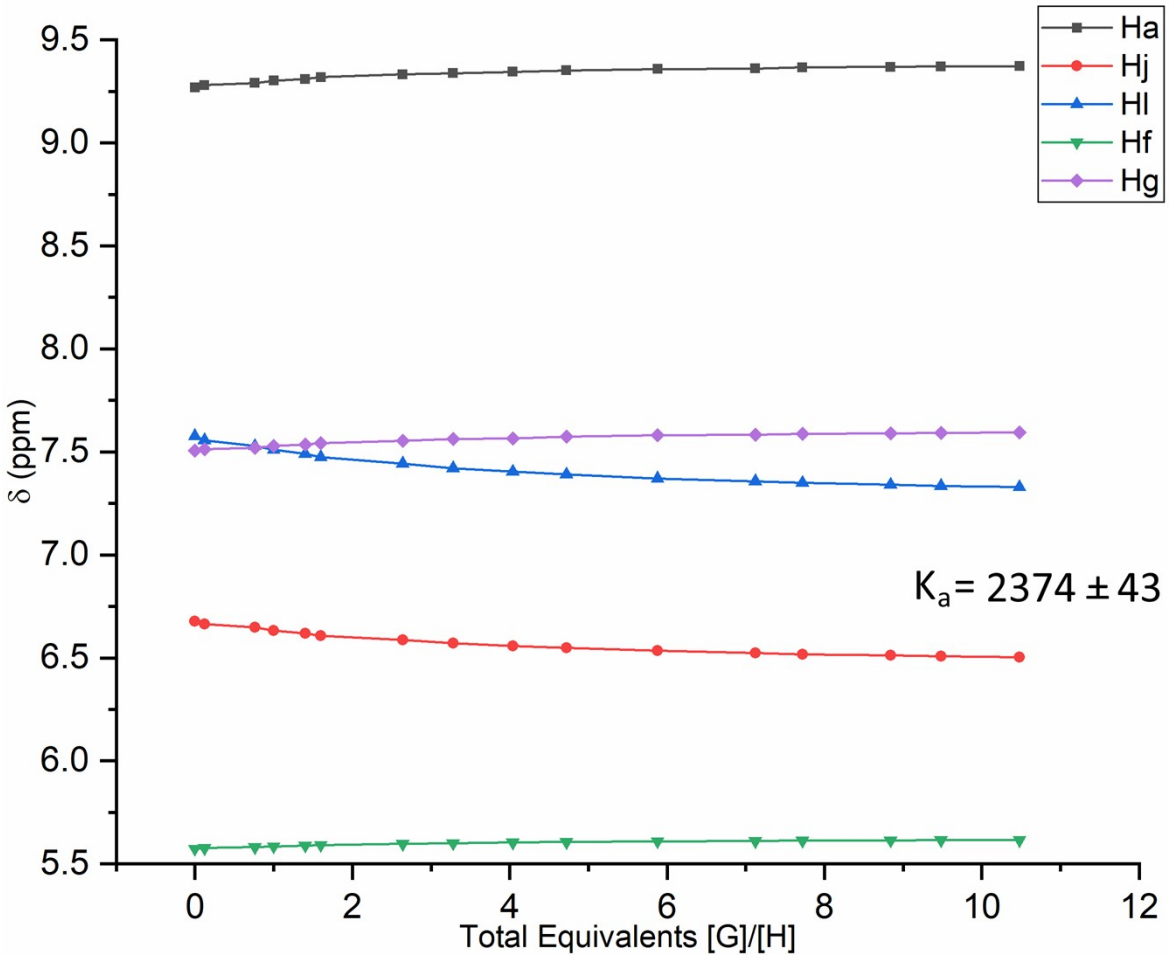

Figure S59 ^{1}H NMR (500 MHz, [D_3]acetonitrile, 298 K) titration curve of **C** with *p*-tolyltrifluoroborate (**tolBF$_3^-$**). Curve monitored by the shift of multiple different proton signals. Data shown is from one of the three titrations used to generate the average binding constant.

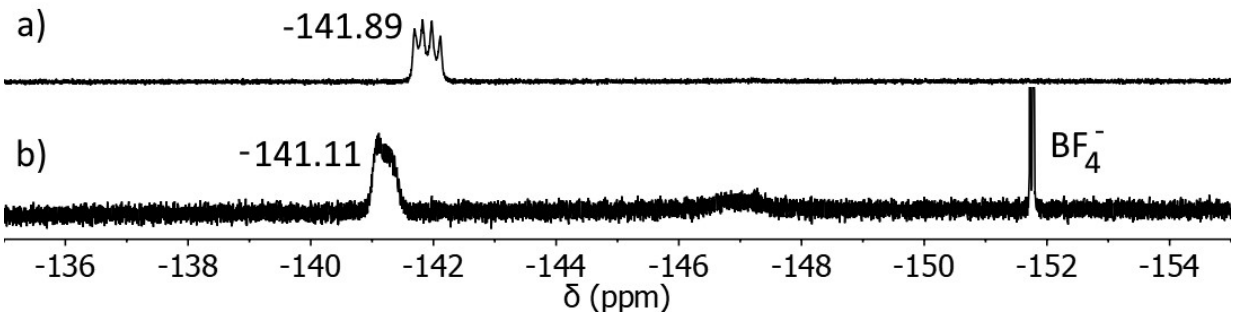

Figure S60 Partial ^{19}F NMR spectra (376 MHz, [D_3]acetonitrile, 298 K) of a) free **tolBF$_3^-$**, b) **C** + 1 eq. **tolBF$_3^-$**.

7.10 Summary of Binding Constants

Table S5 Binding constants of titrated guests.

Guest	K_1	K_2
MsO$^-$	29400 ± 2700	-
TsO$^-$	17200 ± 1600	-
dimephos$^-$	5870 ± 320	1540 ± 70
tolBF$_3^-$	2190 ± 40	-

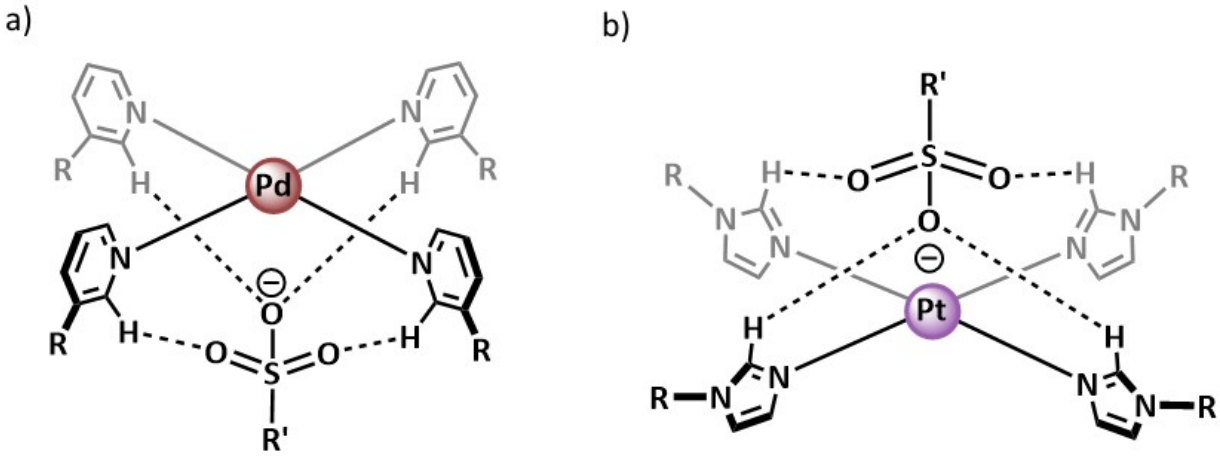

Figure S61 Chemdraw diagrams of two possible binding modes: a) the anionic sulfonate group located in the pyridyl pocket of the host, b) the anionic sulfonate group located in the imidazole pocket of the host. R = ligand scaffold, R' = CH_3 for **MsO$^-$**, *p*-tolyl for **TsO$^-$**.

8 Switchability

8.1 Opening and Closing of Cage C

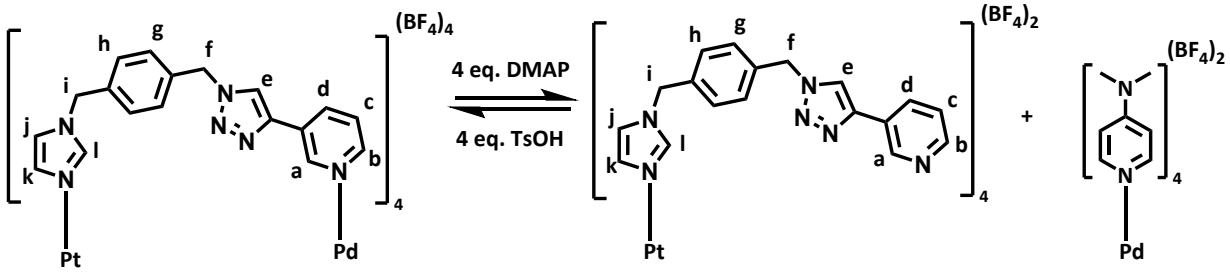

Scheme S2 The reversible transformation between **C** and the open $[Pt(\mathbf{L})_4](BF_4)_2$ complex using DMAP and TsOH (DMAP and TsOH side products excluded).

As a preliminary test to assess the opening of **C** to form $[Pt(\mathbf{L})_4](BF_4)_2$, 4 equivalents of 4-dimethylaminopyridine (DMAP) were added to a solution of the cage in $[D_6]$DMSO. Figure S62 shows the upfield shift in peaks of the α-protons (H_a, H_b) of the pyridine coordinated to Pd(II), suggesting decomplexation. The formation of a $[Pd(DMAP)_4](BF_4)_2$ complex (Figure S62a) also suggests decomplexation from the pyridyl units of L, as it indicates that DMAP has successfully removed the Pd(II) ion from the cage assembly. The ^{1}H NMR spectrum of the cage solution with 4 eq. DMAP added (Figure S62c) largely resembles the ^{1}H NMR spectrum of $[Pt(\mathbf{L})_4](BF_4)_2$ (Figure S62d), with the additional signals corresponding to the $[Pd(DMAP)_4](BF_4)_2$ complex.

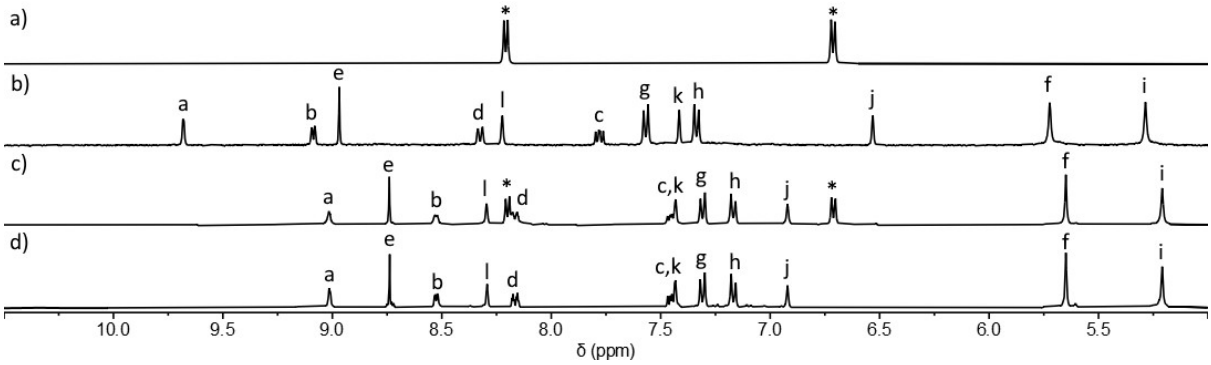

Figure S62 Stacked partial ^{1}H NMR spectra (400 MHz, $[D_6]$DMSO, 298 K) of a) $[Pd(DMAP)_4](BF_4)_2$, b) **C**, c) a mixture of $[Pt(\mathbf{L})_4](BF_4)_2$ and $[Pd(DMAP)_4](BF_4)_2$ formed by the addition of 4 eq. DMAP to **C**, d) $[Pt(\mathbf{L})_4](BF_4)_2$. Asterisks mark signals due to $[Pd(DMAP)_4](BF_4)_2$.

To test the closing of the $[Pt(\mathbf{L})_4](BF_4)_2$ complex to form **C**, 4 equivalents of *p*-toluenesulfonic acid (TsOH) were added to a solution containing a mixture of $[Pt(\mathbf{L})_4](BF_4)_2$ and $[Pd(DMAP)_4](BF_4)_2$ (Figure S63b). Downfield shifts of the ortho-protons on the pyridine ring (H_a, H_b) indicate coordination to a metal ion. The ^{1}H NMR spectrum of $[Pt(\mathbf{L})_4](BF_4)_2$ and $[Pd(DMAP)_4](BF_4)_2$ mixture after the addition of 4 eq. of TsOH (Figure S63c) is almost identical to that of **C** (Figure S63d). These observations coupled with the loss of signals corresponding to $[Pd(DMAP)_4](BF_4)_2$ suggest the reformation of **C**, after Pd(II) ions have been released back into the system from protonation of the DMAP ligands in the $[Pd(DMAP)_4](BF_4)_2$ complex. Signals marked with a pink circle correspond to protonated DMAP. These signals are also seen in the ^{1}H NMR spectrum after addition of 4 eq. of TsOH, adding further evidence that TsOH has protonated the DMAP ligands, releasing free Pd(II) ions back into the system to reform **C**.

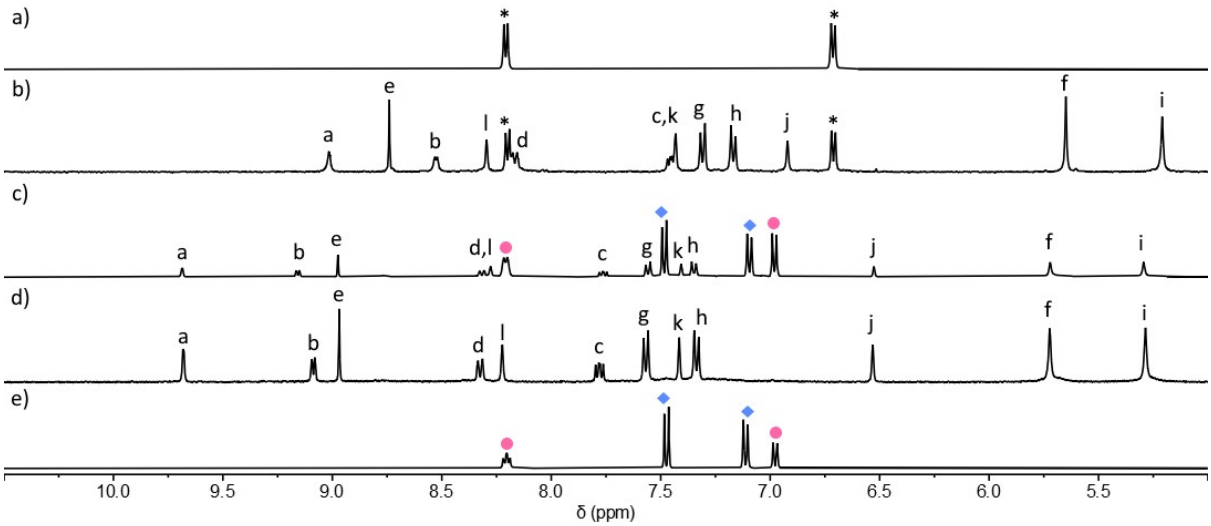

Figure S63 Stacked partial ^{1}H NMR spectra (400 MHz, [D_6]DMSO, 298 K) spectra of a) $[Pd(DMAP)_4](BF_4)_2$, b) a mixture of $[Pt(\mathbf{L})_4](BF_4)_2$ and $[Pd(DMAP)_4](BF_4)_2$ formed by the addition of 4 eq. DMAP to **C**, c) the reformation of **C** after the addition of 4 eq. TsOH to the $[Pt(\mathbf{L})_4](BF_4)_2$ and $[Pd(DMAP)_4](BF_4)_2$ mixture d) **C**, e) a combination of DMAP and TsOH. Pink circles mark signals due to protonated DMAP, blue diamonds mark signals due to TsOH, asterisks mark signals due to $[Pd(DMAP)_4](BF_4)_2$.

8.2 DMAP and TsOH Titrations

The conversion of **C** into the $[Pt(\mathbf{L})_4](BF_4)_2$ complex was investigated further via ^{1}H NMR spectroscopy (400 MHz, 298 K, Figure S64) titration experiments were conducted in which a stock solution of DMAP (0.104 M) was added 1 eq. at a time to a solution of **C** (1.741 mM, 0.6 mL) in [D_6]DMSO. A steady increase in the $[Pt(\mathbf{L})_4](BF_4)_2$ peaks was observed with no intermediate products seen in the timeframe of this experiment. At 5 eq. DMAP, no new signals were seen, suggesting that an excess of DMAP under the conditions of this experiment was insufficient to extract the platinum(II) ion from the $[Pt(\mathbf{L})_4](BF_4)_2$ complex.

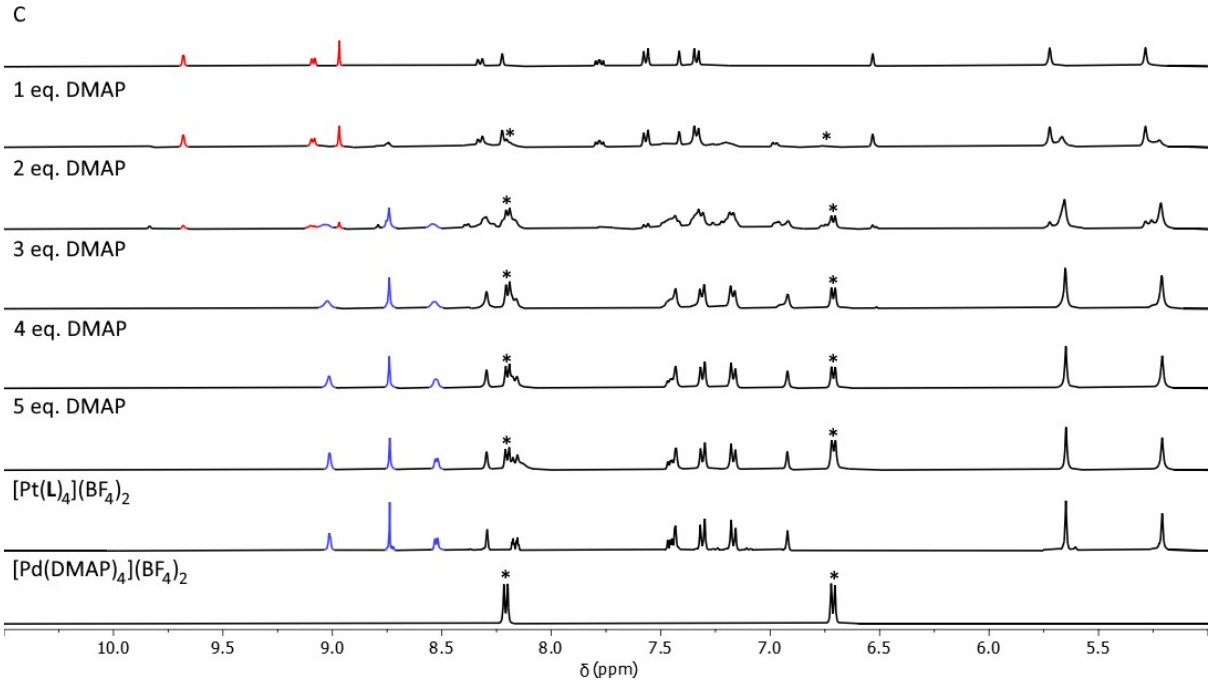

Figure S64 Stacked partial ^{1}H NMR spectra (400 MHz, [D_6]DMSO, 298 K) of the titration of DMAP into **C**. Peaks highlighted in red indicate pyridine-palladium coordination, peaks highlighted in blue indicate uncoordinated pyridine sites. Asterisks mark peaks that are due to $[Pd(DMAP)_4](BF_4)_2$.

Single equivalents of TsOH were sequentially added to the sample of **C** treated with 5 eq. DMAP resulting in the formation of $[Pt(\mathbf{L})_4](BF_4)_2$ (1.668 mM, 0.6 mL). The reaction was monitored via ^{1}H NMR spectroscopy (400 MHz, 298 K, Figure S65) and a stock solution of TsOH (0.100 M) was used. A decrease in peaks assigned to $[Pt(\mathbf{L})_4](BF_4)_2$ was observed, and a new set of signals steadily grew in intensity. These new signals matched those of **C**.

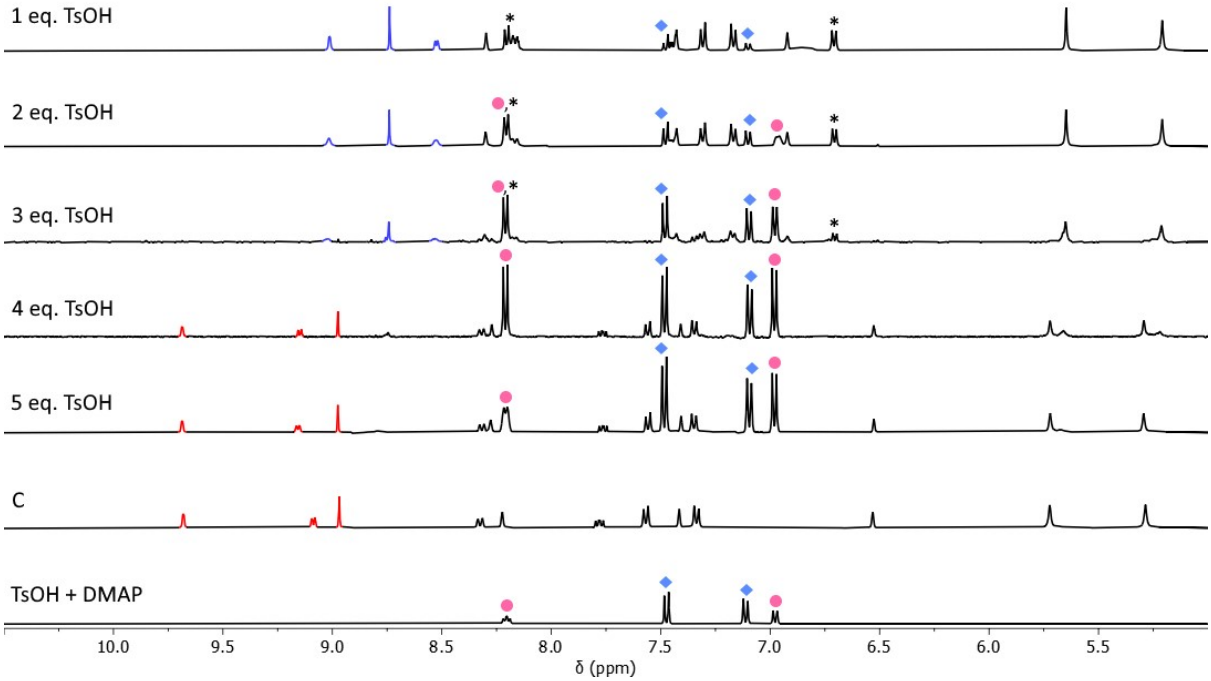

Figure S65 Stacked partial ^{1}H NMR spectra (400 MHz, [D$_6$]DMSO, 298 K) of the titration of TsOH into **C** + 5 eq. DMAP. Peaks highlighted in red indicate pyridine-palladium coordination, peaks highlighted in blue indicate uncoordinated pyridine sites. Pink circles mark signals due to protonated DMAP, blue diamonds mark signals due to TsOH, asterisks mark signals due to $[Pd(DMAP)_4](BF_4)_2$.

8.3 Switching on a Host-Guest Adduct

8.3.1 Using Methanesulfonic acid

The switchability of a 1:1 host:guest adduct was investigated using a **C**⊂**MsO**$^-$ host guest complex and the reaction was monitored via ^{1}H NMR spectroscopy (400 MHz, 298 K, Figure S66). A tetrakis(trimethylsilyl)silane standard was added and the relative integration of the standard to resonances from the cage and complex were used to determine the amounts of reagents to add. A 1:1 **C**⊂**MsO**$^-$ host guest complex was formed in [D$_3$]acetonitrile (0.500 mL, 1.00 mM, Figure S66b), then DMAP (2.00 µmol, 4 eq.) was added (Figure S66c). Peaks pertaining to $[Pt(\mathbf{L})_4](BF_4)_2$ were seen growing in, while peaks corresponding to **C** vanished. Methanesulfonic acid (MsOH, 2.00 µmol, 4 eq.) was then added (Figure S66d). Peaks consistent with the reformation of the host-guest adduct were now seen, while peaks for $[Pt(\mathbf{L})_4](BF_4)_2$ disappeared. The resonance pertaining to the methyl peaks on the guest reflects this behaviour. In the host-guest adduct (Figure S66b) it is shifted upfield from free **MsO**$^-$ (Figure S66e). Once DMAP is added the resonance shifts to where it is in free **MsO**$^-$ (Figure S66c). After the addition of MsOH the peak shifts upfield, but not as much as in the original host-guest adduct, due to the greater equivalents of **MsO**$^-$ now present after the deprotonation of MsOH (Figure S66d).

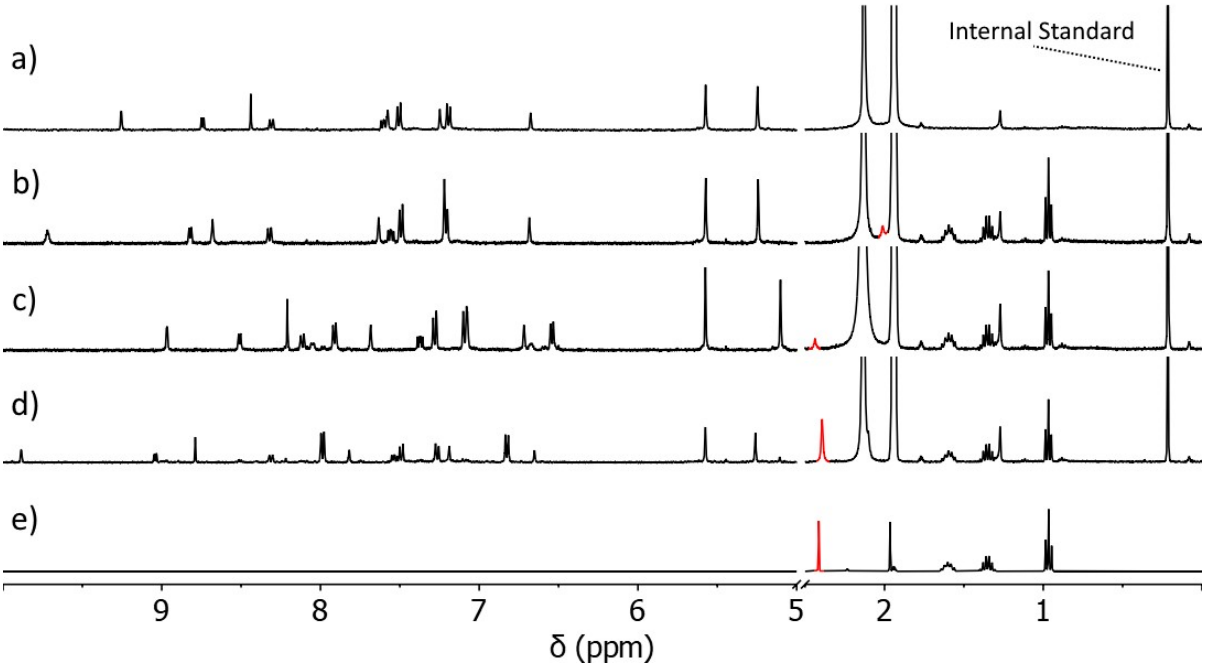

Figure S66 Stacked partial ^{1}H NMR spectra (400 MHz, [D_3]acetonitrile, 298 K) of the switching of the **C⊂MsO**$^{-}$ host-guest adduct. a) Free **C**, b) **C⊂MsO**$^{-}$ host-guest adduct ([**C**] = 1.00 mM), c) [Pt(**L**)$_4$](BF$_4$)$_2$ open complex after the addition of DMAP, d) restored **C⊂MsO**$^{-}$ host-guest adduct after addition of MsOH, e) free **MsO**$^{-}$. Red peaks denote the methyl groups on the **MsO**$^{-}$ guest molecule.

8.3.2 Using *p*-toluenesulfonic acid

As we have previously used DMAP and TsOH together to switch open and closed a host guest adduct[10] we chose to employ them in this new heterobimetallic system. The switchability of this 1:1 **C⊂MsO**$^{-}$ host guest adduct was then investigated using TsOH and the reaction was monitored via ^{1}H NMR spectroscopy (400 MHz, 298 K, Figure S67). A 1:1 **C⊂MsO**$^{-}$ host guest complex was formed in [D_3]acetonitrile (0.500 mL, 1.00 mM, Figure S67a), then DMAP (2.00 mM, 4 eq.) was added (Figure S67b). Peaks pertaining to [Pt(**L**)$_4$](BF$_4$)$_2$ were seen growing in, while peaks corresponding to **C** vanished. TsOH (2.00 mM, 4 eq.) was then added (Figure S67c). Peaks consistent with the reformation of the host-guest adduct were now seen, while peaks for [Pt(**L**)$_4$](BF$_4$)$_2$ disappeared. The ^{1}H NMR spectrum of the reformed host-guest adduct displays shifts of key resonances due to the solution now containing a mixture of both the **C⊂MsO**$^{-}$ host-guest adduct, and a newly formed **C⊂TsO**$^{-}$ host-guest adduct. The latter results from the deprotonation of the added TsOH, and the fast exchange between the two host-guest adducts causing averaging of the two sets of resonances on the NMR timescale.

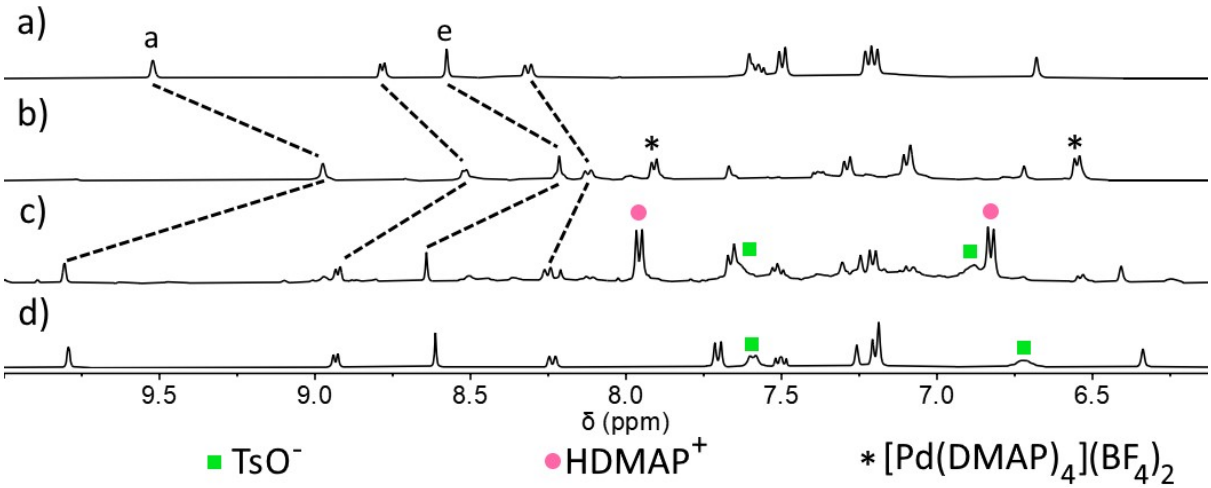

Figure S67 Stacked partial ^{1}H NMR spectra (400 MHz, [D_3]acetonitrile, 298 K) of a) **C**⊂**MsO**$^-$ at a 1:1 ratio ([**C**] = 1.00 mM), b) [Pt(**L**)$_4$](BF$_4$)$_2$ open complex after the addition of DMAP, c) mixture of restored **C**⊂**MsO**$^-$ and new **C**⊂**TsO**$^-$ host-guest adducts after addition of TsOH, d) **C**⊂**TsO**$^-$ host-guest adduct made independently at a 1:1 ratio.

9 Water Stability Studies

Water stability studies were conducted to compare the robustness of the second generation heterobimetallic cage to the imine-based cage.[10] Solutions of **C** (0.6 mL, 0.870 mM) was prepared in 1:19 D_2O:[D_6]DMSO and 1:1 D_2O:[D_6]DMSO. These solutions were monitored via ^{1}H NMR spectroscopy (400 MHz, 298 K, Figure S68 and Figure S69) over a period of 21 days.

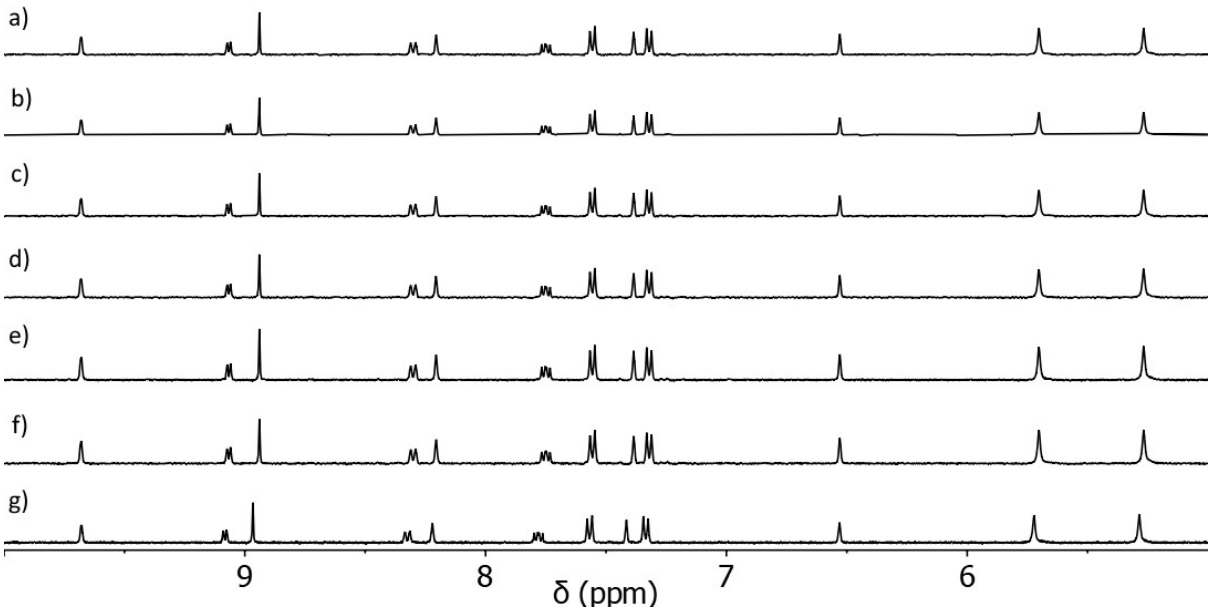

Figure S68 Stacked partial ^{1}H NMR spectra (400 MHz, 1:19 [D_2]H_2O:[D_6]DMSO, 298 K) of **C** at t = a) 0 days, b) 1 day, c) 3 days, d) 7 days, e) 14 days, f) 21 days, and g) **C** in 100% [D_6]DMSO.

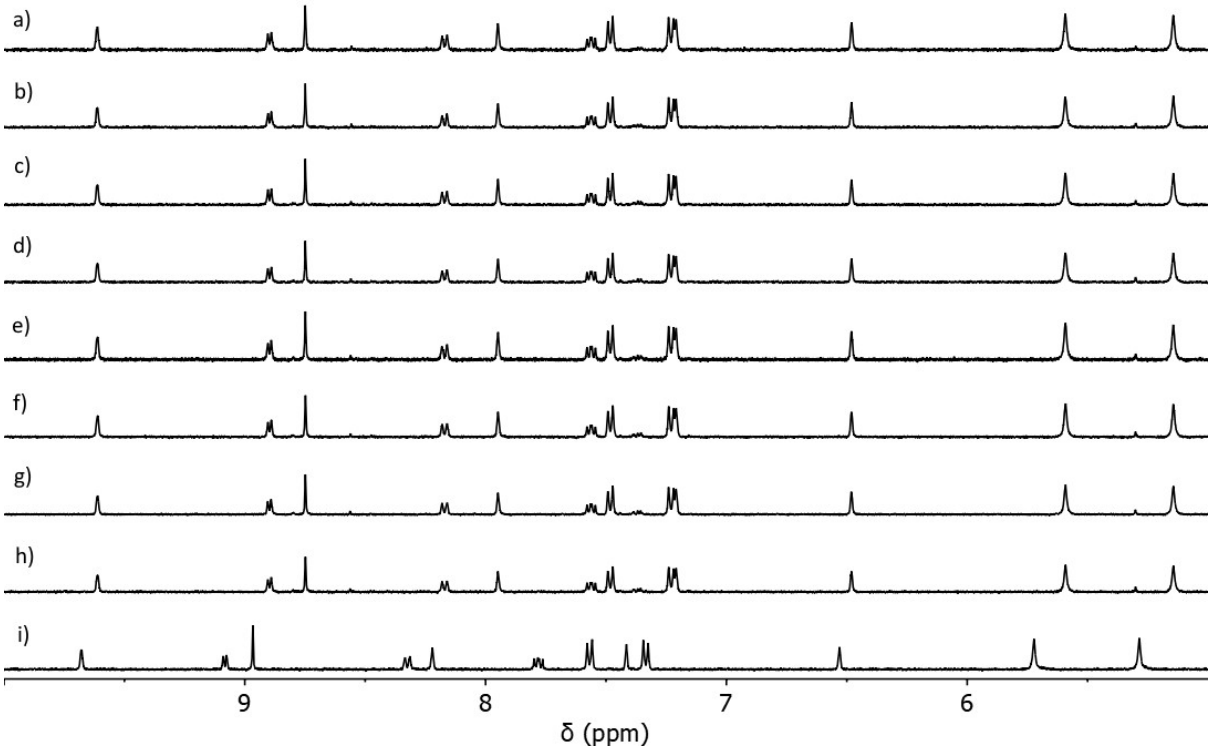

Figure S69 Stacked partial ^{1}H NMR spectra (400 MHz, 1:1 [D_2]H_2O:[D_6]DMSO, 298 K) of **C** at t = a) 0 days, b) 1 day, c) 2 days, d) 3 days, e) 5 days, f) 7 days, g) 14 days, h) 21 days, and i) **C** in 100% [D_6]DMSO.

10 UV-Visible Spectra

UV-Vis absorption spectroscopy studies were carried out at a concentration of 1 x 10^{-5} mol L^{-1} in CH_3CN using quartz cuvettes.

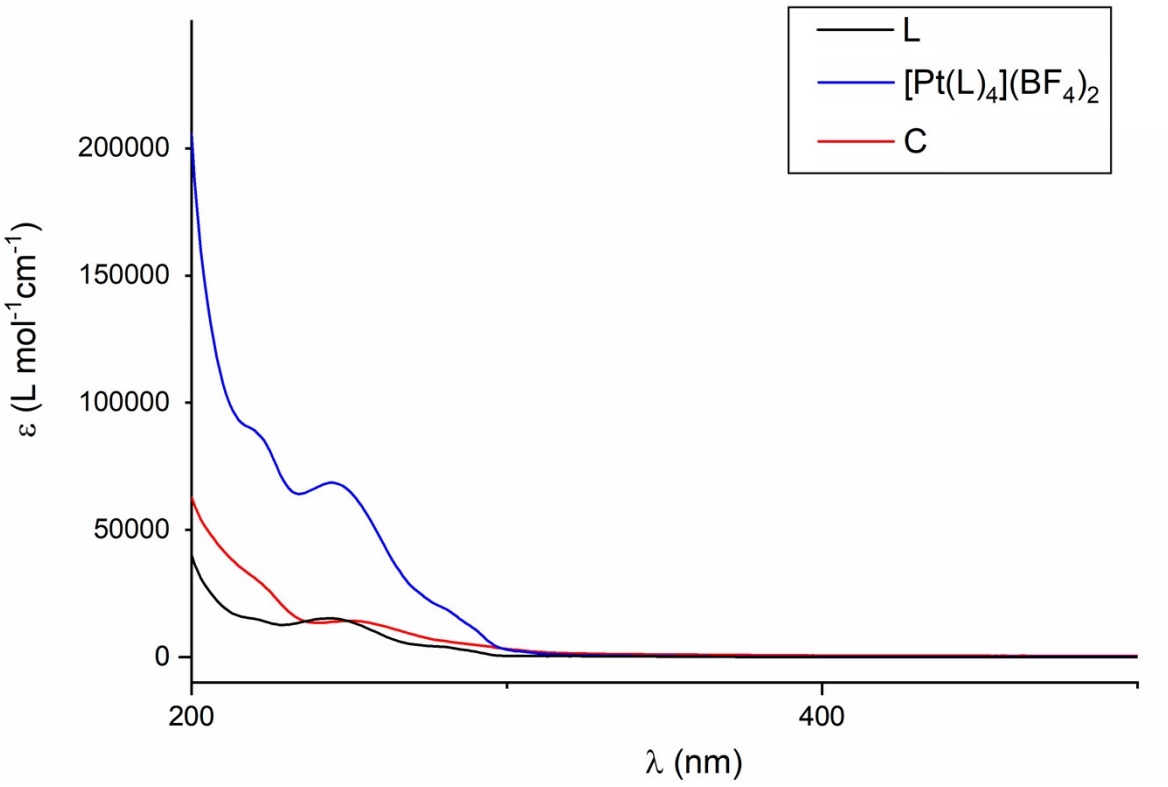

Figure S70 UV-visible absorption spectra of **L**, $[Pt(\mathbf{L})_4](BF_4)_2$, and **C** ($CH_3CN$, 1 x 10^{-5} M).

11 References

[1] J. E. M. Lewis, E. L. Gavey, S. A. Cameron, J. D. Crowley, *Chem. Sci.* **2012**, *3*, 778-784.

[2] T. R. Chan, V. V. Fokin, *QSAR & Combinatorial Science* **2007**, *26*, 1274-1279.

[3] I. Abdelhedi-Miladi, D. Montarnal, M. M. Obadia, H. Ben Romdhane, E. Drockenmuller, *ACS Macro Lett.* **2014**, *3*, 1187-1190.

[4] a) A. Jerschow, N. Müller, *Journal of Magnetic Resonance, Series A* **1996**, *123*, 222-225; b) A. Jerschow, N. Müller, *Journal of Magnetic Resonance* **1997**, *125*, 372-375.

[5] CrysAlisPro, *Agilent Technologies* **2012**.

[6] G. Sheldrick, *Acta Crystallographica Section A* **2008**, *64*, 112-122.

[7] O. Dolomanov, L. Bourhis, R. Gildea, J. Howard, H. Puschmann, *J. Appl. Cryst. J. Appl. Cryst* **2009**, *42*, 339-341.

[8] SARTAN'18, **Wavefunction, Inc.**

[9] J. E. M. Lewis, J. D. Crowley, *Supramol. Chem.* **2014**, *26*, 173-181.

[10] L. S. Lisboa, J. A. Findlay, L. J. Wright, C. G. Hartinger, J. D. Crowley, *Angew. Chem. Int. Ed.* **2020**, *59*, 11101-11107.